THESIS

INTERRUPTION OF NEURON-MICROGLIA BIDIRECTIONAL COMMUNICATION TO

MODULATE COFILIN:ACTIN ROD FORMATION

Submitted by

Maia Zoller

Department of Biochemistry & Molecular Biology

In partial fulfillment of the requirements

For the Degree of Master of Science

Colorado State University

Fort Collins, Colorado

Spring 2022

Master's Committee:

   Advisor: James Bamburg

   Soham Chanda
   Mark Zabel

ABSTRACT

INTERRUPTION OF NEURON-MICROGLIA BIDIRECTIONAL COMMUNICATION TO

MODULATE COFILIN:ACTIN ROD FORMATION

Immune responses in the central nervous system are mediated by microglia, whose responses to CNS threats can be replicated *in vitro* to study the role of microglia in the onset, progression, and treatment of neurodegenerative diseases. Previous work has identified a pathway common to neurodegenerative diseases such as Alzheimer's Disease, Parkinson's Disease, and HIV-Associated Neurocognitive Dementia in which the actin-severing protein, cofilin, forms a 1:1 bundle with actin making rod-shaped inclusions (rods) that can be found in the dendrites and axons of neuronal cells. This thesis focuses on developing methods for examining the role of primary microglia, activated by different factors, to secrete rod-inducing chemokines/cytokines or directly attacking neurons leading to neuronal death. Understanding both of these mechanisms is important in study of neuroinflammation and disease progression. Hemin, a hemoglobin metabolite, and alarmin, S100B, a astrocyte secreted, calcium binding protein, protein, were used to model the environment of intracerebral hemorrhage and general neuroinflammation respectively. Preliminary experimental results suggest blockage of actin-rod inducing signaling pathways via CXCR4/CCR5 receptor antagonist improves neuronal survival to both microglia conditioned medium and direct exposure the microglia-activating hemin or S100B. Further studies are in progress to obtain sufficient statistical data to verify these results.

ACKNOWLEDGMENTS

So many people have made the work completed in my time in graduate school possible, and it is not without anyone of the lovely humans listed here that I would be able to finish such a task as a master's degree.

First, I'd like to acknowledge my support network, without such a caring group of family, friends, and colleagues I never would have been able to complete the work contained in this thesis. My father, who not only taught me how to be a curious, independent thinker, also served as a shoulder to cry on, a cheerleader, and even a guinea pig. The remainder of the Zollers, Mom, Nolan, Kira, Piper, and El Martinez also helped me survive countless long nights, holidays, and weekends spent in the lab.

I would not be the scientist I am today without the Bamburg lab, especially, Jim Bamburg. Thank you for the incredible guidance, wisdom, encouragement, and support. The Bamburg Lab environment has pushed me to be not only the best scientist, but also the best friend, teacher, student, and person possible. Thank you to Laurie Minamide who navigated the majority of my silly questions -with a kind smile might I add- and Lubna Tahtamouni who provided much needed encouragement, laughs, mentorship, and insight. Additionally, thank you to Tom Kuhn, and Sydney Alderfer for making the lab feel like a family.

I would like to thank Joni Triantis-Van Sickle for encouraging me during my first days in the lab. Thank you to Julie McFarland for teaching me that discipline and self-love are two parts that make a whole human. Lastly, thank you Meghan Stettler for making the long hours of writing, imaging, and culturing tolerable, if not fun. Your encouragement and kindness have not gone unnoticed.

TABLE OF CONTENTS

LIST OF TABLES

LIST OF FIGURES

CHAPTER 1: BACKGROUND

The central nervous system (CNS) is believed to be an immune privileged area with limited defensive ability mediated by the resident immune cells, microglia. Microglia were first characterized in the 1930s (Rio-Hortega, 1932). Since the turn of the 21st century, interest and research in microglia have spiked drastically. Today microglia are studied intensively in the neuropathology of Alzheimer's disease (AD) and other neurodegenerative diseases, as well as more generally during instances of chronic or severe acute neuroinflammation. Often, neuroinflammation is found co-morbidly with neurodegenerative diseases and disorders, such as Parkinson's disease (PD), hemorrhagic stroke, multiple sclerosis, and HIV-associated neurodegenerative disorder (HAND). Given their relatively uncharacterized state and role in plethora diseases, microglia present an interesting and novel perspective on neurodegeneration. Thus, microglia are a possible common target for therapeutic intervention.

Microglia Origin & Role in Development

Microglia originate from the embryonic yolk sac among haemopoietic precursor cells (Alliot et al., 1999). Progenitors can be detected in murine models at embryonic day 8-9.5 in the neural folds (Ginhoux et al., 2010; Marinelli et al., 2019). In the 22 years since the discovery of microglia's yolk sac origin, fate mapping has shown that microglia differentiate in the yolk sac and prior to the formation of the blood brain barrier, migrate to the brain via pial surfaces within the area that gives rise to the fourth ventricle (Ginhoux et al., 2010).

Studies of microglia in early embryonic brain development has led to the conclusion that microglia aid in the clearance of apoptotic cells, and promote both angiogenesis, and

neurogenesis (Ginhoux et al., 2010; Marinelli et al., 2019). Postnatally and during the first few

years of life s, microglia greatly aid with synaptic pruning in murine models via engulfment and

phagocytosis of immature and aberrant synapses in response to "eat me" signals(Marinelli et al.,

2019; Stevens et al., 2007; Wu et al., 2015). The two weeks following birth in mice synaptic

plasticity and pruning activities peak. In the post-development stage, microglia shift from

mediators of synaptic pruning to primarily phagocytic immune cells.

In the human adult brain, microglia maintain a distribution of approximately 6.5 x 10^3 per

mm^3 irrespective of cell layer or blood vessel proximity (Nimmerjahn et al., 2005). Most

microglia have large thick microtubule-dependent ramifications that extend over 100 μm or more

and which can extend and retract slowly (Bernier et al., 2019). Much more rapid surveillance of

the brain parenchyma for pathogenic threats, apoptotic cells, and other abnormalities is

accomplished by very thin, actin-dependent filopodia which extend from along these ramified

processes (Bernier et al., 2019). The ramifications and filopodial extensions have distinct

sensitivity to signals. For example, filopodia increase in elongation in response to elevated

cAMP, which causes the retraction of the larger ramifications and major shape alterations

(Bernier et al., 2019). They can rapidly proliferate in response to injury or pathogenic threat

unlike many other brain cell types such as neurons which are post-mitotic (Block et al., 2007;

Lee & Landreth, 2010). Additionally, microglia can migrate following chemokine signals to

distant sites of injury. Cultured healthy microglia have a phenotype that is very different from

microglia *in situ* but still easily identifiable.

A decade ago, the CNS was believed to be immune privileged and incapable of resolving

pathogenic threats by only mediating inflammation and possessing a limited defensive ability.

However, it has been determined that microglia are responsive to inflammatory mediators such

as pro-inflammatory cytokines, prostaglandins, free radicals, and complement (Lucas et al., 2006). After encountering a molecule of threat, microglia *in situ* shift to an activated morphology. Interestingly, activated microglia that still bear processes (microglia which do not occupy the amoeboid or spherical morphology common to phagocytic microglia) have been observed during periods of synaptic refinement in areas such as the thalamus, hippocampus, cerebellum, and others (reviewed in Tremblay et al., 2011).

Microglia in a healthy brain are highly mobile and reactive. They can migrate, proliferate, and extend processes to promote innate immunity. Most populations of microglia can be classified as quiescent, but they can be activated to anti-inflammatory or pro-inflammatory phenotypes. Classification into only these two activation states is considered reductive by the field but remains useful in generally referring to the expression profile, type of secretions, and morphology of the microglia (Shi & Holtzman, 2018). Unfortunately, much of the nuance of microglia activation states remain to be determined (Ransohoff, 2016). Often, the observable changes in morphology are conflated with disease indicators; however, due to the lack of research in this area this may be an inaccurate conclusion (Bernier et al., 2019). To circumvent much of the inaccuracy, many researchers choose to use sub-categories, such as those used for macrophages. For example, the sub-categorization, M2b, indicates an anti-inflammatory phenotype which clears away reactive oxygen and nitrogen species and expresses CCL1 and IL-10 (Varnum & Ikezu, 2012). The concentration of microglia differs from brain region to region, with dense populations in the hippocampus, substantia nigra, and basal ganglia; however, no area in the human brain is devoid of immune protection. Mice have microglia predominately in grey matter with distinctly higher relative numbers in the hippocampus, basal nuclei, and substantia nigra (Block et al., 2007).

Pro-inflammatory, classically activated, or M1-microglia activation occurs when exposed to Th1 cell-derived cytokines such as IFN-γ, TNF-α, and IL-1β and causes a release of pro-inflammatory cytokines, reactive oxygen and nitrogen species, and other cytotoxic components (Chhor et al., 2013; Ransohoff, 2016; Varnum & Ikezu, 2012). A neuroprotective, anti-inflammatory, or M2 phenotype secretes cytokines such as IL-10, and IL-4 (Alsegiani & Shah, 2020). M1 microglia promote neuronal apoptosis, phagocytic clearance of cellular debris, and inhibit oligodendrocyte precursors from differentiating into mature oligodendrocytes, whereas M2 microglia promote angiogenesis, neuronal survival, tissue repair (Shi & Holtzman, 2018; W. Y. Wang et al., 2015). Importantly, microglia can be activated to either state in a reversible manner, and M1 and M2 microglia are not different cell subtypes (Figure 1).

Different systems of the CNS are believed to employ different mechanisms for synaptic removal. For example, the reticulo-geniculate system, which oversees arousal and consciousness, is dependent on complement cascade components to provide "eat me" signals, whereas the hippocampus, involved in memory and learning, relies on chemokines, small chemotactic cytokines, and possibly TREM2, a receptor on myeloid cells to be discussed later (Filipello et al., 2018; Marinelli et al., 2019). Additionally, mice missing the microglia-specific chemokine receptor, CX3CR1, demonstrate a significant reduction in microglia density as well as synaptic plasticity during postnatal development; generally implicating CX3CR1 in these functions (Paolicelli et al., 2011). Contrasting the phagocytic microglia in an adult neurodegenerative brain, the microglia which phagocytose synapses during inflammation or enriched environment-induced adult neurogenesis are ramified and unchallenged, or inactivated (Sierra et al., 2010).

Myriad of inflammatory factors activate microglia to protect against antigens. However, excess activation and removal of non-damaged neurons during an immune response can lead to

neurodegeneration and thus accelerate some CNS-specific diseases such as PD, AD, Multiple Sclerosis and others (Xu et al., 2016). In neurodegenerative disease states, typically microglia switch from a predominately M2 phenotype to a M1 phenotype with the progression of chronic neuroinflammation into disease (W. Y. Wang et al., 2015). Commonly, reactive oxygen species (ROS) are present and contribute to neurodegeneration. Primarily ROS generated by NADPH oxidase (NOX) are involved in immune disease processes, but in the murine immortalized cell line, BV-2, mitochondrial ROS is involved in microglial activation (Park et al., 2015). NOX generated ROS is important for phagocytosis and MAPK activation. (Park et al., 2015), and ROS are secondary messenger molecules that activate transcription factors for pro-inflammatory molecules (Park et al., 2015).

Stroke and Intracerebral Hemorrhage

Strokes are the second most common cause of death globally. Although ischemic stroke accounts for >80% of all stroke cases, intracerebral hemorrhage (ICH) is the most severe form. ICH accounts for only ~15% of all cases, but 34% of ICH cases result in death within 30 days (Sayeed et al., 2017; M. Wang et al., 2020; Weinstein et al., 2010). Often the primary physical insult of ICH is less severe than the secondary effects of innate immunity-mediated inflammation
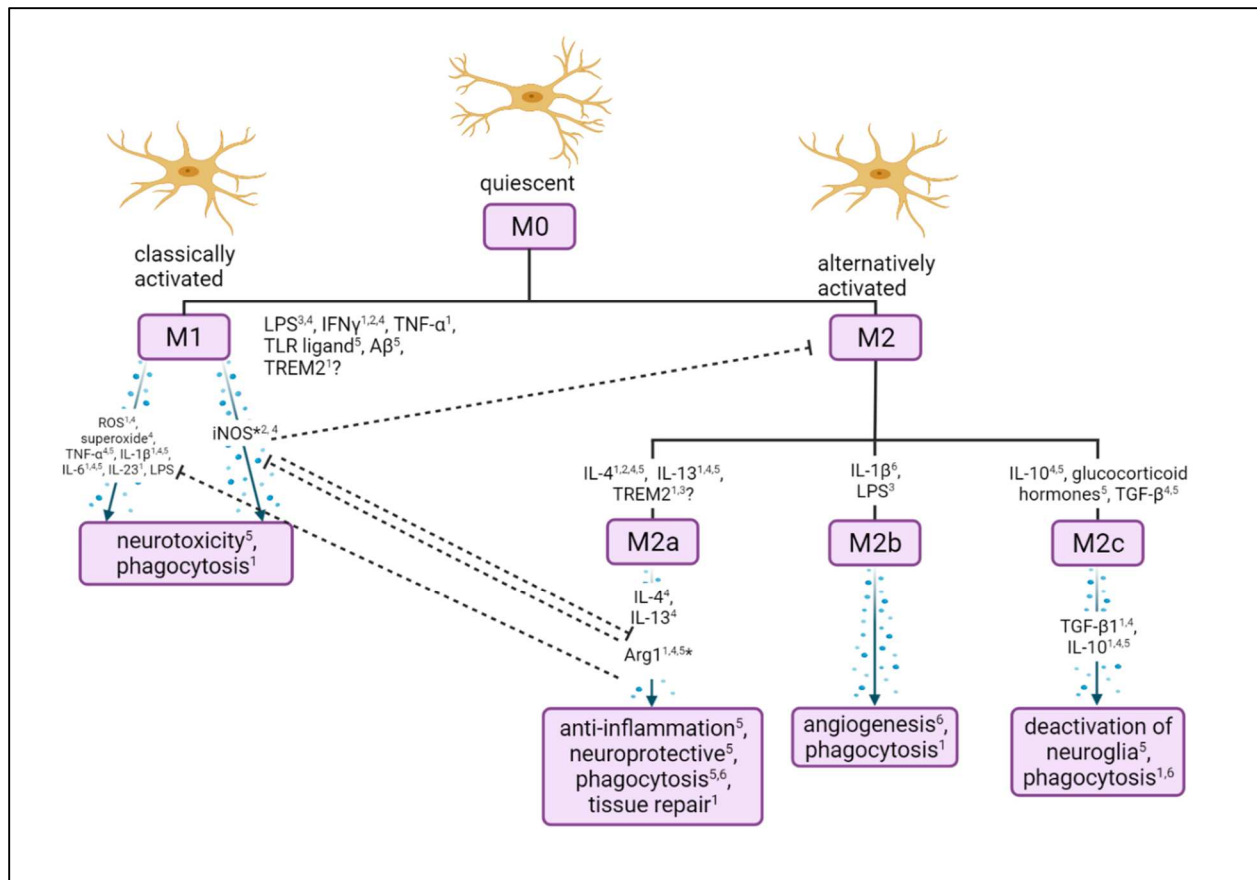
Figure 1: Microglia Activation Spectrum

Microglia follow the macrophage phenotype classifications. M0 microglia can be activated to classically or alternatively activated states depending on the soluble signaling factors available. Classically activated microglia mediate neurotoxicity and phagocytosis via several secreted factors and are inhibited via Arginase 1 expression. Alternatively activated microglia occupy 3 widely recognized sub-states and mediate typically neuroprotective actions. *: expressed proteins, ?: evidence suggests an expression-dependent variable function (Guerreiro et al., 2013). LPS is pro-inflammatory activator, but is found on gram-negative bacteria outer membranes, rather than endogenously in the CNS. Graphic created with BioRender.

over the weeks following the stroke (M. Wang et al., 2020). Oxidative stress is the primary damaging component of the secondary effects, as many of the hemoglobin metabolites from the hemorrhage accumulate to toxic levels and continue to produce ROS (Sayeed et al., 2017). Secondary inflammation mediators recruit peripheral leukocytes which further contribute to the damage (Sayeed et al., 2017; Taylor & Sansing, 2013).

After ICH, hemin is released from methemoglobin from red blood cells (Chen-Roetling et al., 2014) and cleared along with serum proteins and cellular debris over the following weeks (Robinson et al., 2009). Intracellular levels of hemin can accumulate to 10 mM and can quickly become cytotoxic (Tan et al., 2018). Hemin is taken up by astrocytes and neurons and degraded by cleavage of the porphyrin ring by heme oxygenase-1 (HO1) which is expressed on microglia after ICH (Sayeed et al., 2017). Iron-handling proteins have also been found intracellularly, indicating microglia are responsible for iron clearance (Taylor & Sansing, 2013). In early post-ICH phases, limiting HO1 effect prevented hemoglobin-induced edema in rats. But in later stages HO1 inhibition interfered with phagocytosis, demonstrating the duality of HO1 after ICH (Sayeed et al., 2017). How hemin facilitates the second wave of insult after ICH is multi-faceted; but the increase of HO1 may mediate toxicity or hemin may react with inflammation associated peroxides to produce free radicals (Chen-Roetling et al., 2014; Robinson et al., 2009). Studies have shown a hemin concentration-dependent release of NO (Sayeed et al., 2017). It is also thought that loss of cellular export of hemin contributes to toxicity (Chen-Roetling et al., 2014). Additionally, it is known that hemin induces a response via the NLRP3 inflammasome (Tan et al., 2018) comprised of NLRp3, ASC, and pro-caspase 1, which downstream culminate in the production of additional pro-inflammatory factors via activation hydrolases (Tan et al., 2018). Predominately, the NLRP3 inflammasome functions to mature IL-1β, but studies have

found that the increased concentration of active caspase-1, the target of the NLRP3 inflammasome, is correlated with neurodegenerative disease, especially AD (Heneka et al., 2013).

Another M1 activating protein of import is the astrocyte or Schwann cell secreted, S100B. S100 proteins are ubiquitous, with various, tissue-specific expression profiles (Heizmann, 2003). CSF S100B concentrations increase readily physiologically in response to intense physical exercise, or more commonly, in pathological conditions (Donato & Heizmann, 2010). Increased levels of S100B in CSF are observed following TBI. Intracellularly, S100B regulates the assembly of intermediate filaments, stimulates cell proliferation and migration, activates astrocytes to a proliferative state, and stimulates microglia to produce pro-inflammatory cytokines (Donato & Heizmann, 2010; Hayakata et al., 2004; Kabadi et al., 2015). The exact mechanism for these functions remains to be elucidated, but S100B exists as a soluble, acidic, calcium binding agent in the cytoplasm (Zhang et al., 2021). Receptor for advanced glycation end products (RAGE) has been identified as a potential co-receptor for S100B-mediated activation of microglia (Donato & Heizmann, 2010). In neurons and microglia, high concentrations of S100B (micromolar) signal via RAGE for production of reactive oxygen and nitrogen species respectively, as well as signaling through the MAPK, AKT/NF-κB pathways to mediate cell proliferation and survival (Bongarzone et al, 2012; Donato & Heizmann, 2010; Zhang et al., 2021).

Microglia Intercellular Signaling

Because microglia avoid direct contact with each other they rely on signaling molecules to communicate with other microglia and neighboring cells. To effectively respond to a range of signaling molecules, microglia express a variety of receptors and in return secrete numerous

signaling molecules. Intercellular communication is especially important for processes during growth and development such as angiogenesis, neurogenesis, axonal growth, pruning, and neuronal circuit remodeling (Chamera et al., 2019).

For simplicity, the neuron-microglia interaction will only be discussed, although other cell types influence the function of these cells *in situ*. Chemokines present a major form of communication in the CNS. Various chemokines mediate blood brain barrier (BBB) permeability, synaptic plasticity, and transmission, as well as neurogenesis (Chamera et al., 2019). CXCL12, and its receptor, CXCR4, promote microglia migration such as after amyloid plaque formation (Süß & Schlachetzki, 2020).

The chemokine receptor CX3CR1 is specifically expressed on microglia and responds to fractalkine (CX3CL1) which is secreted by neurons to promote microglial adhesions to the endothelium and in soluble form acts as a chemoattractant (Marinelli et al., 2019). The CX3CR1-CX3CL1 axis further promotes neurogenesis, microglia activation, synaptic pruning, plasticity, and foraging neural networks and synaptic connections (reviewed in Chamera et al., 2019) (Figure 2). CX3CR1/CX3CL1 is the only identified chemokine receptor/ligand pair that is binding specific in the CNS, while the other chemokines and chemokine receptors have myriad binding combinations (Chamera et al., 2019). CX3CL1 has two distinct forms, one full-length, membrane-bound form and a N-terminal, secreted, signaling molecule that can selectively bind to CX3CR1 after cleavage from its membrane-bound stalk domain (Bolós et al., 2017; Sellner et al., 2016). The signaling pathway of CX3CR1 is variable, and includes the PI3K, AkT and NF-κB-mediated pathways (Marinelli et al., 2019; Sellner et al., 2016). A study in *CX3CR1* knockout mice, showed increased microglia activation in the dentate gyrus and increased IL-1β levels indicating that CX3CR1 is responsible in some manner for the homeostatic maintenance

of NF-κB activation (Sellner et al., 2016). Deficiency or variants of the CX3CR1 are related to an increase in neurodegeneration progression and risk (Marinelli et al., 2019). CX3CR1 loss of function mutations and knockout studies show a decrease in neurogenesis in young and adult mice respectively; with no such effect seen with a lack of CX3CL1 (Bachstetter et al., 2011; Sellner et al., 2016). Bachstetter *et al.* found that CX3CL1 expression was restricted to mature neurons and exogenous addition of CX3CL1 reversed the decrease in neurogenesis seen in the CX3CR1 KO, potentially implicating CX3CL1 as a factor that protects mature neurons from phagocytic or chronically active microglia. Additionally, CX3CR1 KO mice showed a decrease in ability to effectively clear tau, a microtubule-binding protein that aids with microtubule stability (Tudorica et al., 2017). Additionally, CX3CR1 KO demonstrated a reduction tau binding to microglia *in vitro* (Bolós et al., 2017).

Clusters of differentiation (CD) factors are instrumental in the function of healthy microglia. Studies have relied on categorizing by immunotyping the activation status of microglia based on the expressed membrane-bound CD molecules on a given cell (Chamera et al., 2019). The neuronal CD-200 glycoproteins and the receptor that is only found on myeloid cells, CD-200R, is important for the regulation of phagocytic activity (Marinelli et al., 2019) and maintains microglia in a quiescent phenotype (Chamera et al., 2019). Dysregulation of CD-200R-CD-200 such as that which occurs in aging brains causes microglia to become activated to a M1 or M2 state (Marinelli et al., 2019). In aged brains, CD200 expression decreases, coinciding with an increase in microglia activation (Varnum & Ikezu, 2012). Such reduction in CD200 levels has been observed in AD patients and the brains of Aβ-treated mice (Varnum & Ikezu, 2012). The axis is also involved in BBB permeability and protections of dopaminergic neurons (Chamera et al., 2019). Because of their specificity to neuron-microglia signaling, and the process that are

regulated are vital, CX3CR1 CX3CL1 and CD-200R-CD-200 are the most pivotal in maintenance of CNS homeostasis (Chamera et al., 2019). Complement proteins, toll- like receptors (TLRs), as well as purinergic and adrenergic signaling are employed by microglia to survey and respond to the microenvironment (Chamera et al., 2019). Complement membrane proteins are expressed in both microglia and neurons. Complement receptors C1q, C3, and C5 are expressed in microglia and control a range of functions such as motility, phagocytosis, and cytokine secretion. Bidirectional communication between microglia and neurons is important for maintenance of homeostasis in the brain, and evidence indicates that alterations or degeneration in this communication can cause disease making this an area worthy of further exploration (Marinelli et al., 2019).
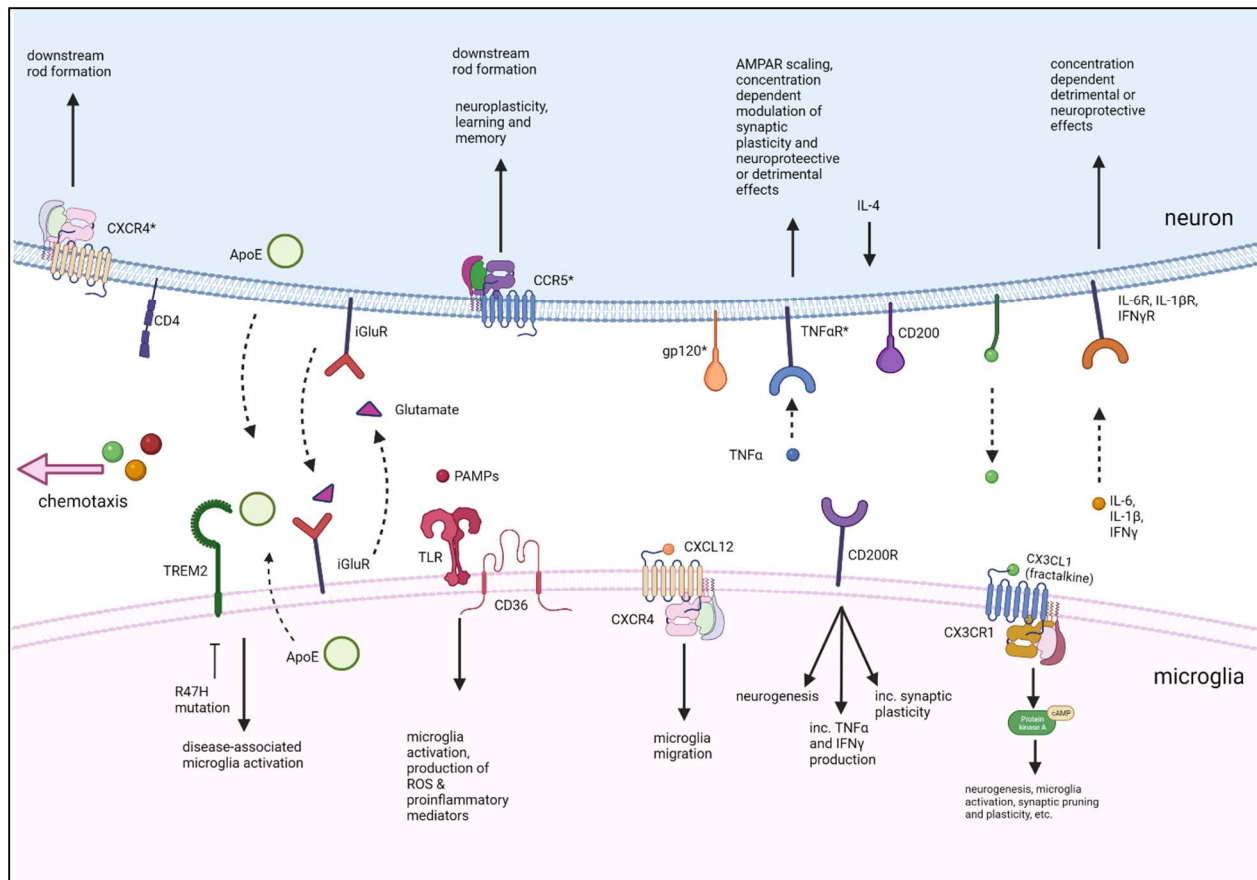
Figure 2: Microglia-Neuron Chemokine and Cytokine Axes

Outlined are some of important signaling pathways employed for bidirectional communication between neurons and microglia. Of particular interest are the effects that mediate cofilin:actin rod formation (indicated by the label being followed by *). Recent evidence indicates that many of the signaling components required for cofilin:actin rod formation are co-localized to lipid rafts, regions of cholesterol dense, thick membrane (J. R. Bamburg et al., 2021; Smith et al., 2018). Microglia activation along the established spectrum (see Fig. 1) is mediated via several signaling pathways including TREM2 signaling via ApoE (Süß & Schlachetzki, 2020), TLR activation by PAMPs (Marinelli et al., 2019), and CX3CR1 activation via fractalkine (Chamera et al., 2019; Marinelli et al., 2019). CD36 acts with TLR4 or TLR6 to signal for microglia activation, and production of neurotoxic factors such as ROS (Marinelli et al., 2019; Süß & Schlachetzki, 2020; Varnum & Ikezu, 2012). Additionally, the CD200-CD200R axis modulates the function of microglia greatly (Marinelli et al., 2019; Süß & Schlachetzki, 2020; Varnum & Ikezu, 2012). PAMPs: pathogen associated molecular patterns; *: established signaling molecules for rod formation; R47H: TREM2 loss of function mutation. Graphic created with BioRender

11

Microglia in Alzheimer's Disease

As the world's population grows older, the number of individuals affected by neurologic disease also increases. Primarily the individuals affected by AD are expected to increase drastically due to the strong correlation of age with AD onset. The Amyloid Hypothesis, which has driven therapeutic strategies for treatment of AD for decades, states that AD is driven by the accumulation of pathogenic extracellular amyloid-β (Aβ), which can deposit into plaques, but which can promote the formation of intracellular neurofibrillary tangles, ending with neurodegeneration, cognitive impairment, and dementia (Süß & Schlachetzki, 2020). Extensive imaging studies have verified that Aβ aggregation is the earliest pathological event that can be non-invasively detected in patients with familial AD and can precede clinical symptoms by decades (Shi & Holtzman, 2018).

AD is hallmarked by the formation of extracellular Aβ plaques, intracellular neurofibrillary tangles composed of tau paired helical filaments, and dementia that culminates from the loss of synapses and ultimately neurons. Senile plaques are formed by Aβ, which is cleaved from a larger amyloid precursor protein (APP) into 39-42 amino acid peptides (Wirths et al., 2010). Cleavages can also be made to form non-amyloidogenic peptides (reviewed in Varnum & Ikezu, 2012). The Amyloid Hypothesis states that processing of Aβ by BACE 1/2 or the γ-secretase complex prevent the clearance of Aβ oligomers which accumulate and create a toxic environment for neurons (Schlachetzki & Hüll, 2009; Varnum & Ikezu, 2012). Aβ accumulation can promote phosphorylation of tau, which enhances its release from microtubules, causing microtubule instability, as well as tau hyperphosphorylation by many kinases leading to neurofibrillary tangle formation, an hallmark of AD. Synapse loss is another prominent feature that causes the cognitive decline (Gireud et al., 2014).

Studies have shown that inflammatory processes involving microglia and astrocytes occur early in AD pathogenesis (Wirths et al., 2010). Neurotoxicity mediated by microglia typically is progressive and adds to the advancement of neurodegeneration (Block et al., 2007). Although microglia were once determined to be bystanders in AD pathology, by the late 1980s microglia had been observed surrounding senile plaques in human AD brains (McGgeer et al., 1989) and later at the onset of Aβ plaque formation in AD, APP/PS1 mouse models (Wirths et al., 2010). It remains unknown if the accumulation of microglia around a senile plaque is the result of recruitment and migration of local clonal expansion. There is a possibility that microglia react during initial stages of AD pathogenesis and lose their ability to clear plaques in later disease stages (Parhizkar et al., 2019). Genome-wide association studies (GWAS) have revealed several AD variant risk genes are preferentially expressed in microglia, including TREM2, CD33, CLEF1, and PTK2B (Süß & Schlachetzki, 2020). TREM2 (triggering receptor found on myeloid cells) is necessary for survival and proliferation, chemotaxis, phagocytosis of Aβ, energy metabolism, and engulfment of dead cells and debris (Parhizkar et al., 2019).

TREM2 has been found in the neocortex, hippocampus, and white matter as well as low levels in the cerebellum (Boutajangout & Wisniewski, 2013). Studies show that functional TRM2 helps microglia cluster around plaques and may possibly aid in their clearance. TREM2 loss-of-function mice exhibit less microglia clustering around plaques and less phagocytosis of Aβ (Parhizkar et al., 2019). The loss-of-function variant, R47H, of TREM2 correlates with a 3-fold increase in an individual's risk for AD (Boutajangout & Wisniewski, 2013; Shi & Holtzman, 2018; Süß & Schlachetzki, 2020). A potential ligand for TREM2 is ApoE which, presents the largest risk factor for sporadic AD, other than age (Parhizkar et al., 2019). ApoE is a major cholesterol carrier produced by astrocytes. It is found in amyloid plaques and may

promote their deposition and aggregation (Liu et al., 2014; Süß & Schlachetzki, 2020). It is highly upregulated in microglia in neurodegenerative disease states (Süß & Schlachetzki, 2020). If homozygously expressed, the ApoE ε4 allele can dramatically increase the risk for AD by nearly 12-fold (Süß & Schlachetzki, 2020). Of the three Apo isoforms that are associated with a risk of AD, ApoE ε4 forms neurotoxic Aβ aggregates most readily (Liu et al., 2017).

Neuronal circuits in the basal nuclei are primarily affected in neurodegenerative diseases such as PD. Degradation of the circuitry which connects the basal ganglia in behavior loops cause many of the hallmark symptoms of PD. The loss of dopaminergic neurons of the substantia nigra of the midbrain which synapse on the striatum is responsible for the tell-tale PD sign of movement-associated tremor (Chinta & Andersen, 2005). The hippocampus is the main area for physiological and pathological changes in AD (Chamera et al., 2019) and is understood to comprise the dentate gyrus, the CA1, CA2, and CA3 fields of the hippocampus proper, and the subiculum (Mu & Gage, 2011). Interestingly, dysfunction of the CX3CL1-CX3CR1 or the CD200-CD200R axis result increased CX3CL1 and progressive development of AD and increased CD200 which correlates with lower levels of phosphorylated tau in Aβ plaques and neurofibrillary tangles respectively (Chamera et al., 2019).

Cytoskeletal Regulation

Irregular regulation of the neuronal cytoskeleton can lead to transport deficiencies, loss of dendritic spines, and cell death. Cytoskeletal abnormalities, specifically pathologies that contain the actin binding and assembly regulatory protein, cofilin, have been observed *in situ* and *in vitro* in postmortem AD patients and AD animal models respectively (Minamide et al., 2000). Actin and its dynamics are important for necessary cell functions such as maintenance of cell shape, endocytosis, molecular trafficking, and cellular motility. With regard to neurons and their

function in memory and learning, actin is critical for synaptic plasticity and trafficking of AMPA receptors to synapses as well as for vesicle delivery (Gu et al., 2010; J. R. Bamburg & Bernstein, 2016; Rust et al., 2010).

Monomeric, globular actin (G-actin) polymerizes spontaneously under intracellular ionic conditions to form filamentous actin (F-actin) and its dynamics are tightly regulated by monomer sequestering, polymerization enhancing, and filament severing, capping, and branching proteins. F-actin is comprised of two parallel helical strands of actin, associated side-to-side but in a uniform direction to give rise to a head to tail polarity. The Actin Depolymerizing Factor (ADF)/cofilin protein family is ubiquitous among all eukaryotes. In mammals it is comprised of three separately encoded isoforms: cofilin-1, cofilin-2, and actin depolymerizing factor (ADF) (Alsegiani & Shah, 2020; Tahtamouni et al., 2013). Although the ubiquitous cofilin-1 (referred to cofilin hereafter) and ADF have many redundant functions, they possess some unique roles in cell migration and adhesion (Tahtamouni et al., 2013). Essential cellular processes such as proliferation, migration, and synaptic plasticity preferentially require cofilin to recycle actin monomers and regulate actin filament elongation (Alsegiani & Shah, 2020; Rust et al., 2010). However, ADF has a role in presynaptic function and neurotransmitter release (Rust et al, 2019).

Cofilin binding to F-actin is regulated by phosphorylation on a single serine residue, ser3, by several kinases but primarily by LIMK1/2. Phosphorylation inhibits actin binding and recruits the scaffolding protein 14-3-3 (reviewed in: Alhadidi & Shah, 2018; Bamburg et al., 2021; Bamburg & Bernstein, 2016; Kang & Woo, 2019). The kinases that regulate cofilin function, LIM, and TES kinase families, are also subject to phospho-regulation by members of the Rho kinase and p21-activated protein kinase (Pak) families. Dephosphorylation by phosphatases in the Slingshot Homolog-1 (SSH-1) family or chronophin (CIN, aka pyridoxal-5-phosphate

15

phosphatases) activate cofilin allowing its binding to actin (Niwa et al., 2002; Gohla and Bokoch, 2002).

The efficiency of cofilin as an F-actin severing protein is highest at low cofilin/F-actin ratios. At low cofilin/actin ratios, cofilin does not bind to F-actin in a quick and cooperative manner to saturate the filament. The slight rotation of the filament induced by cofilin binding leads to severing (Chan et al., 2009). Unbound actin filaments favor a helix with 167° twist with only a small region of subunits with a rotation of 162° (McGough et al., 1997; Galkin et al., 2001); however, cofilin-bound actin requires the 162° twist. At higher cofilin-actin ratios F-actin becomes saturated with cofilin and all subunits have the 162° rotation. (Chan et al., 2009).

Severing leads to more filament ends and if there is an assembly competent pool of ATP-actin, can cause nucleated filament growth. If the local pool of actin is sequestered by monomer binding proteins, filament disassembly will ensue. However, within a range of ATP-actin monomer concentration, filaments can elongate from their plus end (also called barbed end based upon the arrowhead decoration observed in electron micrographs of F-actin with myosin fragments) and shorten from their pointed end, a process called treadmilling that can be maintained at steady-state (van Troys et al., 2008). Alternatively, at high cofilin/actin ratios, cofilin binds cooperatively to filaments in which all actin subunits have the 162° rotation causing a conformational change that propagates over hundreds of actin subunits (Chan et al., 2009; van Troys et al., 2008). Sporadic binding leads to increased regions of torsional strain between cofilin-saturated and unsaturated regions which leads to severing (van Troys et al., 2008). This function is not seen with highly cofilin-decorated segments due to the stability induced by bound-cofilin. It is believed that cofilin may lower the dissociation rate of cofilin:actin dimers, thus causing some stability for the F-actin (Andrianantoandro & Pollard, 2006). Two proteins

physically interact with cofilin to regulate actin filament dynamics. Severing and depolymerization of cofilin-actin filaments is enhanced by actin-interacting proteins (Aip1, aka WDR1), and cyclase-activated proteins (CAP1/2). Aip1, which when phosphorylated by a constitutively activated serine/threonine kinase, STK16 (Lopez-Coral et al., 2018), caps the barbed end of actin to cause fragmentation by preventing the elongation and reannealing of filaments. Severing ability of Aip1 recognizes cofilin-bound actin filaments, and thus cofilin is required for Aip1-mediated fragmentation. (Ono, 2003), Cyclase-activated proteins (CAP1/2) which recycle released cofilin helps free ADP-actin monomers for nucleotide exchange to cause filament severing/depolymerization (Balcer, 2010).

Cofilin in Neurological Pathologies

Hyperactivation of cofilin, overexpression of cofilin, initiators of energetic or oxidative stress, proinflammatory cytokines such as TNFα, and pathologic substrate exposure can initiate the formation of rod-shaped inclusions containing 1:1 cofilin:actin (rods) which have been correlated with neurodegeneration (reviewed in Alhadidi & Shah, 2018, Minamide et al., reviewed in Bamburg & Bernstein, 2016). Cofilin-actin rods have been identified as hallmarks in many neurodegenerative diseases including Huntington's disease (HD), AD, PD, and HAND (Minamide et al., 2000; Munsie et al., 2011; Rahman et al., 2014; Smith et al., 2018; Walsh, Minamide, et al., 2014; Smith et al., 2021). In HD, rods are found in nuclei of white blood cells and in α-huntingtin expressed neurons, rods form in the soma. But in other diseases listed, rods are found in neurites where they can disrupt vesicular transport and cause synaptic loss (Munsie et al., 2011). Studies in which the huntingtin protein has been mutated, showed an increased persistence of heat shock induced, nuclear rods over WT (non-mutated huntingtin). These data could implicate a role for nuclear cofilin-actin rods in huntingtin disease (Munsie et al., 2011).

There are at least two identified pathways leading to rod formation. One pathway is activated in neurons by ATP-depletion or glutamate-induced excitotoxicity and is independent of PrPC and NOX, while the other pathway depends on both (Walsh, Kuhn, et al., 2014). Initially, formation of rods might be a protective mechanism in which cofilin is sequestered to slow the turnover of actin (Bernstein et al., 2006), a major consumer of ATP in neurons (Bernstein & Bamburg, 2002). However, prolonged rod inclusions can impair intracellular trafficking (Maloney & Bamburg, 2007; Mi et al., 2013) and inhibit synaptic functions to further impair neuronal function (Cichon et al., 2012). It is worth noting that rods form in neurites rather than soma, and their blockage of trafficking can bring about synaptic loss (Cichon et al., 2012). Therefore, mitigating rod formation in the neurites may be a method for protecting the synapses from damage. Additionally, rods were found in the brains of old but not young rats indicating there may be a temporal variable in which cofilin accumulation or its oxidation causes rod formation (Cichon et al., 2012; reviewed in Alhadidi & Shah, 2019). It remains to be determined whether rods are a transient protective mechanism, a reporter of stress, or a direct mediator of synapse loss (Bamburg & Bernstein, 2016).

Cofilin may accumulate in regions of membrane enriched in cellular prion protein (PrP^C), called lipid rafts, through its binding to phosphatidylinositol-bis-phosphate (Yonezawa et al., 1990) which accumulates on the cytoplasmic leaflet of lipid rafts. After PrP^C synthesis begins, the N-terminal signal peptide is inserted into the endoplasmic reticulum (ER), and as synthesis ends, the PrP^C becomes linked via an internal lipid-transfer sequence to the membrane lipid, glycosylphosphatidylinositol (GPI). PrP^C thus appears only on the outer leaflet of the plasma membrane following its vesicular transport and membrane fusion (Haigh et al., 2005). PrP^C and the sphingolipid-enriched membrane raft domains in which it occurs serve as receptor platforms

for signaling rod formation in AD, PD, and HAND (Smith et al., 2018; Walsh, Minamide, et al., 2014; Bamburg et al., 2021). The role of PrP^C is likely unrelated to its folding into the pathogenic form (PrP^{SC}) that occurs in prion diseases such as scrapie (Schmitz et al., 2014).

In AD and PD mouse models, knockout of PrP^C protects against development of disease-associated dementia (Brody & Strittmatter, 2018; Ferreira et al., 2017). The disease signaling often requires additional co-receptors that seem to be enriched in the PrP^C raft domains, such as mGluR5 and α7NACHR for entry of oligomeric amyloid-beta (Aβo) or α-synuclein (αSyn) and monomeric Aβ$_{42}$ respectively (Brody & Strittmatter, 2018; Ferreira et al., 2017; Oliveira da Silva et al., 2021). Recent data also implicate the CCR5 and CXCR4 receptors (Smith et al., 2021). Additionally, an isoform of NAPDH oxidase (NOX) to generate ROS, is required for dementia development (Walsh, Minamide, et al., 2014). The generation of reactive oxygen species is certainly one commonality between the pathways for cofilin:actin rod formation. Additionally, it is likely that pathological Aβo and αSyn signaling through PrP^C may both involve Fyn and PYK2 (Brody & Strittmatter, 2018; Ferreira et al., 2017).

Lipid Rafts & HIV Co-Receptors as Drug Targets

The membrane lipid raft domains also mediate interactions between the HIV spike protein, gp120, and chemokine receptors such as CXCR4 (X4) and CCR5 (R5) (Smith et al., 2018, 2021). In microglia, X4 mediates cellular recruitment, neural stem cell proliferation, and more (Bonham et al., 2018). Bioinformatic studies predicted interaction between X4, and other microglia genes such as TLR2, CXCL12, and R5 (Bonham et al., 2018). R5 and X4 are both co-receptors that associate with CD4-gp120 (active) to mediate viral HIV entry via interaction with the V3 loop of gp120 and the chemokine receptor (Alkhatib, 2009; Smith et al., 2018). HIV strains can be categorized by their preference for R5 or X4 to mediate cellular entry. CD4, X4,

and R5 have been identified on astrocytes, microglia, and neurons with data showing R5 being less convincing (Boche et al., 2013; Chamera et al., 2019; Smith et al., 2018). It is proposed that lipid raft domains containing elements described above such as PrP^C, X4, and R5, mediate neurodegeneration in myriad disease states including AD, PD, HAND, and cerebral hemorrhagic stroke (Bamburg et al., 2021). Studies of pharmacological blockage of R5 on microglia with Maraviroc, a allosteric R5 inhibitor, in glioma pathology showed a decrease in microglia exhibiting the M2 phenotype. Prior to pharmacological intervention, microglia were seen predominately in the proinflammatory, M1, phenotype, suggesting that R5 plays a role in combating pathogenesis and activation of microglia (Laudati et al., 2017). Similarly, mice modeling stroke that were treated with the X4 inhibitor, AMD3100, presented with anti-inflammatory microglia phenotypes. The mice treated with AMD3100 scored better in neurological tests post-stroke, when compared to untreated stroke mice (Walter et al., 2015).

Modulation of chemokine receptors has proven to be effective in mitigating astrocyte and microglia mediated neurotoxicity, and protection of synapses and neuronal damage. Chemokine receptor-active peptides (RAPs) specifically block the receptors that participate in neuroinflammation, epilepsy, ischemic stroke, traumatic brain injury, and HAND. Early studies showed treatment with the RAP, D-Ala-peptide T-amide (DAPTA), reduced microglia and astrocyte activation in rat AD models by specifically blocking R5 in hippocampal slice cultures (Rosi et al., 2005). In clinical trials DAPTA has been met with marked success in immunomodulation of serum cytokine production making it a possible treatment for HIV-positive individuals (Ruff et al., 2003). A shorter, stable analog of DAPTA, RAP103, has shown to effectively block either or both R5 and CCR2 receptors in rodent nerve pain models and prevent R5 and CCR2 mediated monocyte chemotaxis (Padi et al., 2012). RAP103, also

prevented the activation of microglia in the spinal cord in response to nerve injury (Padi et al., 2012). Given its ability to protect against microglia-mediated damaging inflammation, the effects RAP103 could be beneficial and protect against neuronal spine loss and death via R5 receptor binding on either microglia or neurons.

The following study seeks to determine the molecular mechanism by which pro-inflammatory cytokines mediate rod induction in neurons. Chemokine receptor antagonists for X4 and R5, RAP103 and R103, will be used to disrupt bidirectional communication between neurons and microglia via the X4 and R5 receptor and/or signal molecule secretion elicited by the binding of these receptors. The function of the RAPs will be determined in response to the M1 microglia-activating molecules, hemin, and S100B . Rod formation in hippocampal rat neurons will be quantified as an endpoint for actin dynamic response to X4 or R5 signaling. Using rod formation and viability assays as indicators of neuronal stress, and hemin and S100B as models for neurodegenerative disease, we seek to determine if acute microgliosis and signaling via X4 and R5 receptors are a mechanism for rod formation and a potential target for therapeutic intervention in the common pathologies facilitated by cofilin:actin rods.

CHAPTER 2: CULTURING, AND ACTIVATION OF MICROGLIA IN SEPARATE AND
CO-CULTURE SYSTEMS AND THE ROLE OF RAPs ON NEURONAL HEALTH

Introduction

The central nervous system (CNS) is an environment incredibly difficult to reproduce in culture. Beside the complex intertangling of neuronal axons and dendrites, there lies an intricate network of supporting glial cells. As outlined in simplified terms in the Background chapter, microglia rely on many signals to mediate a viable, homeostatic environment for neuronal health. Replicating these *in vitro* presents a great barrier for assaying the therapeutic efficacy of receptor antagonist peptides. To begin to address this issue, we first had to culture primary microglia *in vitro.*

Studies that characterize microglial response to fluctuations in the CNS typically use *in vivo* or tissue slice culture methods due to the highly motile processes that aid in the phenotypic characterization of microglia. However, for studies assaying individual cells and factors released from them under various conditions, a dense microglia culture *in vitro* is more useful.

Immortalized microglia cell lines are commercially available and have contrasting applications and benefits depending on their intended purpose. The popular N9 and BV2 lines are retrovirally immortalized mouse lines commonly used in neurodegenerative research. These lines are adherent and proliferate better than primary microglia but show alterations in the production and secretion of cytokines (Stansley et al., 2012). Our initial work with BV2 cells found them to grow well in culture well but concerns about their ability to respond to microglia-activating agents shifted our attention to primary microglia.

To better elucidate the effect of the receptor antagonist peptides, RAP310 and R103, on microglia secretion of proinflammatory cytokines, a culturing system is required that allows for the microglial exudate to be applied to neuronal cultures without any potentially confounding effects due to physical contact. Furthermore, microglia are most viable and proliferative in a serum-containing medium containing GM-CSF, whereas primary neurons grow best free of serum (Goshi et al., 2020; Guttenplan & Liddelow, 2019). Thus, the first aspect of work described in this chapter is the development of a culture method that allowed for the collection of microglia-conditioned medium before and after addition of microglia activating agents which could then be fractionated to remove the activating agents but allow for the reconstitution of a cell-free medium to add to neuronal cultures for testing cytotoxicity and rod-inducing activity.

After developing the methods for harvest, isolation, and culturing of primary mouse microglia and adaptation of the culture conditions to allow its transfer to cultured neurons and maintain their viability. We determined that microglia could be adapted to survive in the complete homemade neurobasal medium (HN+) by slowly transitioning them from LGDMEM/10% FBS/1% PenStrep & GM-CSF (1ng/mL) over 5 days of culturing. Slow transition to HN+ maintained viability and did not activate the microglia to a pro-inflammatory state as determined by proliferation rates over 7 days.

It was then necessary to establish a model system to study microglia-produced cytokines and chemokines in neuroinflammation. The microglia need to be activated to a pro-inflammatory state and secrete a sufficient amount of pro-inflammatory factors to study the potential neuroprotective effects of the peptides. In developing a system for microglia activation, we chose to use both hemin and alarmin as the primary activating agents based on published efficacy and their physiological relevance in neurodegeneration. Hemin is a major breakdown product of

hemoglobin that is released during ischemic injury (Chen-Roetling et al., 2014) and alarmin, also called S100B, is produced by astrocytes to activate microglia (Donato & Heizmann, 2010). We have already shown in previous studies that rodent hippocampal neurons are induced to form cofilin-actin rods by disease-associated substrates such as Aβ, αSynuclein fibers, TNFα, and gp120 (Maloney et al., 2005; Minamide et al., 2000; Oliveira da Silva et al, 2021; Walsh et al., 2014; Smith et al., 2018; Won et al., 2019). However, each of these molecules might also affect microglia which can contribute to the rod response. Thus, here we have focused studies on molecules that should work through microglia activation and not directly on neurons, but for which we need to confirm this hypothesis. Thus, we choose hemin and alarmin.

Although many studies on microglia activation utilize bacterial lipopolysaccharide (LPS), which is considered the gold standard for activation into a pro-inflammatory or disease-associated phenotype, LPS has no endogenous role in the brain's response to hemorrhage, TBI, ischemia, or degenerative disease. Therefore, its lack of relevance in pre-clinical therapeutic research outweighs its ability to function as a robust activator. Hemin, which has a molecular mass of 652 Da, presented a promising reagent for selectively activating the microglia since it could be removed from the secreted cytokines and chemokines, all of which have masses above 6 kDa. However, fully characterizing the direct effects of optimal hemin concentrations on neuronal viability and rod formation has yet to be established.

Methods are described for the fractionation of microglia-conditioned medium to remove low molecular weight activators, such as hemin, and reconstitute the higher molecular weight materials including secreted cytokines into a medium for use on cultured neurons. We determined that with post-column adjustments made to osmolarity, addition of low molecular weight N21Max components, and addition of insulin the fractionation protocol yielded relatively

healthy and viable cultures for assays using media from hemin-activated microglia. Alarmins present a different approach to microglial activation. Secreted after tissue injury, specific alarmins such as S100B have been observed in the CSF of patients suffering from neurological disorders (Hayakata et al., 2004). Additionally, S100B has strong effects on promoting prolonged microglia activation especially after TBI (Kabadi et al., 2015). Optimizing the concentration of S100B to be used for our experiments and determining its effect on microglia vs neurons will aid in its application for potentially co-culturing microglia with neurons. Based on published literature, the concentration of S100B should be around 2μg/mL (Xu *et al.,* 2016).

Most protocols for studying the *in vitro* effect of microglia in a neuropathology require the media to be conditioned on the microglia prior to addition to the neurons; because of the serum requirement and the secreted factors concentration this may be an unsuitable system to use for all applications. Secondly, given that the microglia secrete amount of signaling molecules that could be physiological, the dilution of these factors into the larger volume of culture medium necessary for their culture makes assaying for their presence and levels, difficult and expensive. Lastly, any membrane bound, or proximity-mediated effects would be loss in a separate culture model. Any effect seen in the neurons may be lessened due to these confounding factors. Successful efforts have been made to move to co-cultures and tri-cultures with astrocytes in neuroinflammation research (Goshi et al., 2020; Roqué & Costa, 2017); therefore, we decided to continue with co-cultures.

This co-culturing method is implemented here to assess the ability of RAPs in preventing rod formation and loss of neuronal viability. The proximity of the microglia and neurons in culture should help increase the local concentrations of secreted chemokines and cytokines and

their effect on nearby neurons, allowing us to eventually study the neuronal death process through time-lapse live cell imaging.

We identified the presence of the R5 and X4 receptors, the target of the RAP peptide antagonists, on our primary microglia. We then assessed the ability of neuronal cultures to retain the NeuO dye labeling for up to three days in culture and to follow viability under various chemically initiated neurotoxicity. The ability of the octapeptide RAP310 to protect against any hemin or S100B induced loss of neuronal viability on neuronal cultures directly treated with these agents or treated with microglia conditioned media was tested. Lastly, we co-cultured primary microglia with hippocampal neurons, and evaluated the effect of S100B to stimulate a microglia-mediated response, and the ability of RAP310 and R103 to mitigate effects on neuronal viability and/or rod formation.

The following chapter seeks to determine culturing methods for primary microglia cultures, microglia pro-inflammatory activator reagents, effect of activated microglia on neuronal viability and cofilin:actin rod formation, and the role of RAPs in preventing microglia activator-mediated effects.

Materials

Reagents

All chemical reagents ae analytical grade unless otherwise stated.

GM-CSF is obtained from BioLegend (San Diego, CA, USA). Low glucose (LG) DMEM
(Gibco, 31600083) and homemade Neurobasal media (HN) are used for cell culture. Homemade
neurobasal medium (HN+) (Smith et al., 2021) is supplemented with 1x penicillin/streptomycin
(Gibco), Glutamax I (Gibco), and N21max (R&D Systems, AR008) to generate complete HN+.
Fetal bovine serum (FBS) used in plating of primary neurons is obtained from Hyclone.
LGDMEM is supplemented with 10% FBS (VWR), 1% penicillin/streptomycin (Gibco).
Dissection medium (450mL 1x HBSS, 5mL 1M HEPES, 3g glucose, 5mL PenStrep was filter
sterilized and stored at 4°C). Freezing medium for microglia is 70% LGDMEM/10% FBS, 20%
FBS, 10% DMSO. Freezing medium Poly-D-lysine is obtained from Sigma (16634), and tissue-
culture grade plasticware is obtained from Thermofisher unless otherwise noted. MTT salt is
obtained from Sigma (M5655). Spin desalting columns (7 kDa MWCO) and protein
concentrators (3 kDa MWCO) media concentrators are obtained from ThermoScientific (CA,
USA). R103 and RAP310 peptides were obtained from Creative BioPeptides (Rockville, MA,
USA) and used at 10^{-8}M and 10^{-10}M respectively. These concentrations are 10^4 to 10^5 higher than
the effective concentration for a 50% reduction in the rod formation response (EC50). NeuO (cat.
01801) was obtained from StemCell Technologies (USA). Sodium azide was made up in water
(Sigma, S2002).

Buffers

Phosphate buffered saline (PBS) is a solution of NaCl (140mM), $NaH_2PO_4 \cdot H_2O$ (8mM), and KCl (2.7mM) in ultrapure water. 10N NaOH is used to bring the pH to 7.2. The buffer is autoclaved for sterility.

Tris buffered saline (TBS) is a solution of Tris pH 7.5 (10mM) and NaCl (150mM) in ultrapure water.

Antibodies

Primary antibodies: affinity purified rabbit 1439 antibody to ADF/Cofilin (2 ng/µL) (Shaw, A., et al., 2004), mouse monoclonal antibody to phosphorylated neurofilament heavy chain (1:1000) (BioLegend). Antibody dilution buffer: 1% BSA in 1x TBS.

Secondary antibodies: Alexa 488 labeled goat anti-rabbit IgG (1:500), Alexa 568 labeled goat anti-mouse IgG (1:500), Alexa 568 labeled goat anti-chicken IgY (1:500) (Invitrogen).

Blocking buffer: 2% normal goat serum in antibody dilution buffer.

Coverslips are mounted with ProLong Diamond Antifade (Invitrogen) for imaging.

Bradford Assay Dye Preparation

Coomassie Brilliant Blue G dye (Sigma-Aldrich B0770-25G) is made by dissolving 25 mg of dye in 25 mL of methanol at room temperature. Then 50 mL of H_3PO_4 is added to the solution on ice. 250 mL of ultrapure H_2O is added, and the solution is filter sterilized with 0.22 µm bottle filter to remove precipitates. An additional 175 mL of ultrapure water was added and filter sterilized, and the dye solution is stored at 4°C. It is allowed to sit for 24hrs before use in

the Bradford Assay. Absorbance readings are performed using a Nanodrop One/One[c] spectrophotometer (ThermoScientific).

Insulin

Insulin (Sigma, I6634) is made as a stock of 1.05 M in ultrapure water which is then filter sterilized by passage through a 0.22 µM syringe filter (Pall, Betcon, Dickinson and Company). Dilutions are always made fresh from the stock and added to the culture media to the final concentration listed at the time of a full media change.

Hemin Solution

Hemin (bovine, H9039, Sigma) is weighed and dissolved in 1 M NaOH and titrated to a neutral pH starting with 1 M and finishing with 0.1 M HCl. The solution is then filter sterilized by passage through a 0.2 µm syringe filter and stored in the dark (tinfoil wrapped) at 4°C.

Animals

All animal procedures are performed in accordance with protocols KP1023 and KP1412, approved by the Colorado State University Institutional Animal Care and Use Committee. Either Wistar Sprague-Dawley rats or C57BL/6 mice are utilized to obtain brain tissues for glia and microglia (P0-1), or neurons (E18 rat and E16.5 mice).

Methods

Microglial Isolation and Culture

Primary microglia are harvested from P0-P1 C57BL/6J mice to obtain the maximum pre-differentiated glial cells (Tan et al., 2018) and prepared using a procedure modified from Lian et al., 2016. Pups are euthanized, heads removed and washed with 70% ethanol and placed on ice in a 6 cm petri dish. All subsequent work is performed under sterile conditions in a laminar flow hood or biological safety cabinet. An incision is made along the midline of the scalp with forceps, with additional incisions made posterior to the eyes from the midline to the jaw. The skull is cut with forceps along the midline and posterior to the eyes, and the brain is removed. The olfactory bulbs, meninges, and brain stem are removed using forceps and discarded. The remaining tissue is finely chopped with a sharp razor blade in dissection medium and transferred to a 50 mL conical tube with additional medium to reach a final volume of 30 mL. Trypsin (1.5 mL of 2.5%) is added and the suspension incubated at 37°C for 15 min. Trypsin inhibitor (1.2 mL of 1 mg/mL) is then added, incubated for 1 min, and followed by addition of DNase I (750 µL of 1 mg/mL). After centrifugation at 400 x g for 5 min to pellet the cells/tissue, medium is aspirated, and the pellet resuspended in 5 mL of warm LGDMEM/10% FBS/1% pen/strep and triturated with a 1 mL pipette tip until cells are dissociated (no lumps of tissue remained). Cells are transferred to a 15 mL conical tube, centrifuged at 400 x g for 5min, medium aspirated, and the pellet resuspended in 5 mL of LGDMEM/10%FBS/1%pen/strep. Cells are counted with a hemocytometer and plated at a density of 50,000 cells/cm^2 into a poly-D-lysine (10 µg/mL in borate buffer for 1 hr at room temp or overnight at 4°C) coated T-75 flask with 15 mL (final volume) of culture medium supplemented with 1 ng/mL GM-CSF. Cultures are incubated in 5% CO_2, 100% humidity at 37° C for 10 days with full medium change on 1, 3, 5, and 7 DIV. By 10

DIV, microglia form a monolayer on top of an astrocyte layer. They are removed from the astrocyte layer by whacking the flask vigorously against your hand until the microglia are observed to be floating via microscopic inspection. A hemocytometer is used again to count the floating microglia, and these can be cultured directly or frozen. Dislodged cells could be further cultured in LGDMEM/10% FBS/1% Pen/Step to induce further differentiation (Lian et al., 2016) (Figure 3) or cells are frozen in cell cryo-sage storage vials at a density of 10^6/ml in 70% culture medium containing 20% FBS and 10% DMSO. Vials are placed in polystyrene tube holders and frozen overnight in a -80°C ultracold freezer. They are moved to liquid nitrogen the following day. All stocks are used within 6 months of their initial freezing date.

Microglia are plated at 125,000cells/well in tissue culture-grade plastic, 24 well-plates, unless otherwise noted (Sayeed et al., 2017) or 1,000 cells/well in a 96 microwell-plate with LGDMEM /10% FBS, 1% Pen/Strep (Lian et al., 2016) and incubated at 37°C in 5% CO_2. For microglia activation assays, microglial cultures are adapted to complete HN+ medium by gradually increasing the percentage of HN+ sequentially during media changes from 0% upon plating, 25% 1 DIV, 50% 3 DIV, and 100% 5 DIV. Activation agents were applied on 6 DIV and left in medium overnight.

E18 rat hippocampal neurons are obtained by dissection of the hippocampi of Sprague-Dawley rat embryos (Lian et al., 2016). Tissue is dissociated in HN+ media, transferred to freezing medium, and frozen by placing cryo-safe vials in polystyrene racks overnight at -80°C and then transferred to liquid nitrogen. Following rapid thawing, cells are plated at 55,000 cell per well onto poly-D-lysine-coated 12 mm German glass coverslips in 24 well plates with 1 mL of complete HN+, containing N21max, Glutamax I (Gibco), and Pen/Strep (Gibco) (Mi et al., 2013).

Microglia activation assays

Microglia cultures at 6 DIV are treated with 100 µM hemin (Sigma-Aldrich) made in LGDMEM/10%FBS. Medium is removed from the hemin-treated microglia at 24 hrs after hemin addition and fractionated as described below (Figure 2.4) to remove hemin and low molecular mass components (< 3kD) and then reconstituted for addition to neuronal cultures at 6 DIV. Fractionated media is added to neurons on 6DIV. Neurons are fixed at 7 DIV, and immunolabeled.

Microglia Proliferation Assays

MTT ((3-(4,5-Dimethylthiazol-2-yl)-2,5-diphenyltetrazolium bromide)) is metabolized by living cells into a formazan product and the amount of this product is an indicator of cellular metabolic activity. The protocol used here was adapted from (Mosmann, 1983). Microglia plated in 96 well microtiter plates at 1,000 cells/well, are grown in LGDMEM/10% FBS in the presence of GM-CSF (10 ng/mL) and treated analogously to microglia cultured in 24 well plates that are used to produce microglia-conditioned medium for testing on neurons. On 1 DIV, 3 DIV, 5 DIV, and 6 DIV medium is changed on the 96-well microtiter plate. At 7 DIV, 0.5 µg/µL of MTT reagent (MTT salt in PBS at 5 mg/mL) is added and after incubation at 37° C in 5% CO_2 for 4 hours the medium is discarded, and the formazan crystals solubilized with 100 µL of DMSO per well for 30-45min. The absorbance is measured at 600 nm using a microtiterplate reader and the relative viability indices calculated by taking the $Absorbance_{cells}/Absorbance_{empty\ wells\ with\ DMSO}$. Values are given out of 1, with a totally confluent well being 1.

Filter Paper Assay

Filter paper dye-binding assay is done according to the published procedure (Minamide and Bamburg, 1990). Whatman #1 filter paper is partitioned, protein standards (ovalbumin unless otherwise stated) and media samples are applied in 3 µL spots. Paper is allowed to dry, then fixed with methanol at room temperature for 30s and air dried. The paper is soaked in Coomassie Brilliant Blue G (0.5% in 7% acetic acid) for 10min, then 7% acetic acid (multiple changes) is used to destain until the paper background stain reaches allow constant level. Paper is air dried, squares of samples cut out and placed in 1.7 mL microfuge tubes, and dye is extracted with 1 mL of extraction buffer (66% methanol, 33% water, 1% ammonium hydroxide), by vortexing the tube until all bound dye is solubilized. A 300 µL aliquot of each sample is transferred into one well of a 96 well-plate and read at dual wavelengths of 405/600nm. Protein amount in each sample is determined after plotting values from a standard curve ranging from 0.5-10 mg/mL.

Osmolarity Measurement

Osmolarity is measured on Vapro Model 5600 Osmometer. Osmometer is calibrated with three standards: 290 mmol/kg, 1000 mmol/kg, and 100 mmol/kg respectively. Then media samples from the reconstitution of the spin column effluent are measured in triplicate on a filter disc. Media is adjusted by addition of sterile ultrapure water to obtain an osmolarity in the range of 300-310 to be consistent with that of the HN+ starting medium.

Live Imaging Assay

Cultures were plated in 24-well glass bottom plates. Hippocampal neurons were plated at a density of 33,000-42,000 cells/well. Microglia were plated at a density of 90,000-136,000

cells/well. Cultures were maintained for 5 days with a full media change every other day from 1DIV. For experiments requiring microglia-conditioned media for addition to neuronal cultures, the neurons were labeled 7 DIV with NeuO for 2 hrs followed by 2 washes with HN+ media. At 8 DIV the neurons were labeled again with NeuO and washed. The microglia-conditioned medium was added to neuronal cultures with or without RAPs after the washing and remained until the cells were fixed 10 DIV. Images were acquired at set locations on 8 DIV (0 hrs post treatment), 9 DIV (24 hrs post treatment), and 10 DIV (48hrs post treatment).

For co-culturing experiments, neurons were plated on PDL coated, 24-well glass bottom plates and cultured as previously described. Microglia were plated in a T-25 flask in LGDMEM/10% FBS/1% PenStrep, 1 ng/mL GM-CSF in the presence or absence of RAPs (pre-treatment) and converted to HN+. On 4 & 5 DIV neurons were labeled with NeuO for 2hrs and washed twice with HN+. Microglia were added to the neuronal cultures in the glass bottom dish at 5 DIV. On 6DIV activating agents and/or RAPs were added (co-treatment)Cultures were maintained for 48 hrs prior to fixation 7 DIV. Images were acquired at previously set locations 5 DIV (0 hrs post treatment), 6 DIV (24hrs post treatment), and 7 DIV (48hr post treatment).

Immunolabeling

Cells are fixed using 4% formaldehyde in PBS at 37° C for 30-45min, then washed 5x with PBS, followed by membrane permeabilization for 3 min with methanol chilled to -20°C and followed by 3 washes with PBS. Fixed cells are blocked with 2% goat serum in 1% BSA in TBS. Primary antibodies (neurofilament-H, mammalian cofilin-1/ADF) are applied overnight at 4º C. After 5 washes in PBS, secondary antibodies are applied for 1 h and then washed away 5x with PBS. ProLong Diamond Antifade is used to mount coverslips with cells onto glass slides or

mount a coverslip over cells cultured on a glass bottom 24 well plate. After overnight incubation in the dark at room temperature samples were imaged.

Microscopy and Image Analysis

Images are acquired on BZ-X710 Series Microscope (Keyence) fitted with filter cubes for DAPI, GFP, and TexasRed/RFP or NeuO as well as an open position for either brightfield or use of a 4th filter cube for fluorescence. Image arrays (ranging from 7x7 to 11x11) are collected using 20x or 40 x objectives and are processed and stitched with the BZ-X Analyzer software. Cell counts, morphologies, etc. were then analyzed using MetaMorph v 7.8 or Image J 1.53c. Data is transferred to Microsoft Excel for further analysis. Morphology parameters are determined in Image J. Plots and statistical evaluations of data are performed with Excel or GraphPad Prism.

Live imaging microscopy was conducted using a TokaiHit stage incubator set to a temperature of 48° C (to give readings on a thermocouple of 37º C in the medium) and 5% CO_2.

Images are opened in ImageJ. The color channels are split into separate 8-bit images, then a threshold is applied to fully highlight cells. Analyze particles tallies the cell count and collates the data.

Statistics

Averages, standard deviations, and data collation was done in Microsoft Excel. Statistical analysis was conducted by GraphPad Prism. A p-value of 0.05 was considered significant. Error bars represent 1 standard deviation in all charts. $* p < 0.05$, $** p < 0.005$, $*** p < 0.0005$, $**** p < 0.00005$.

Graphics created with BioRender.com
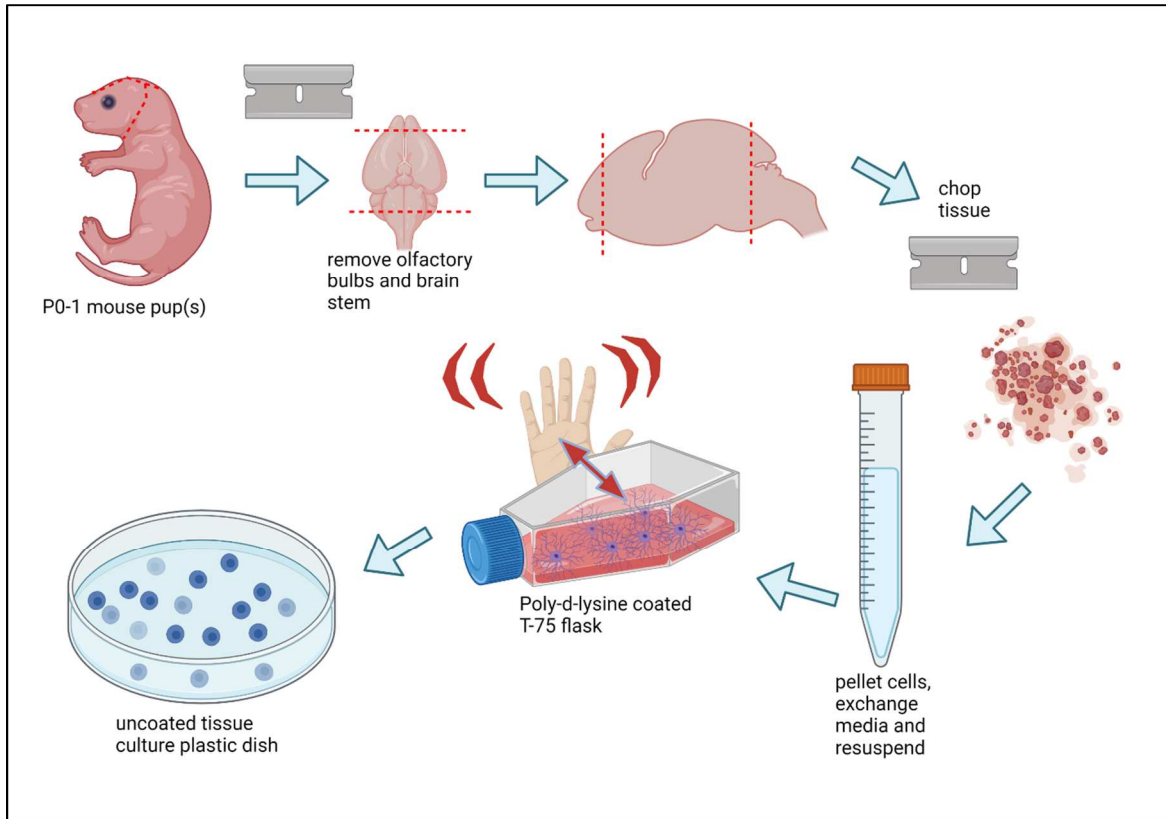
Figure 3: Mouse Pup Dissection and Microglia Isolation Protocol Overview

P0-1 mouse pups were euthanized, decapitated, and brains removed. The olfactory bulbs, brain stem, and meninges were removed, leaving the cortices and hippocampi. This tissue is then chopped, trypsinized, triturated, and plated into a poly-D-lysine coated T-75 flask. Following 10 days in culture the microglia are removed from the flask and plated for use in experiments.

Results

Microglia in culture demonstrated adherence and proliferative properties in a variety of plate conditions and with a minimum of 1 ng/mL GM-CSF based on the microglia isolation protocol modified from Lian et al., 2016. Quiescent microglia *in vitro* display a mixture of highly elongated cells, those with branched structures, a polar morphology, or a round or amoeboid morphology, each of which was observed in all growth conditions (Figure 4 A). These data indicate healthy cultures consistent with published images. Microglia also displayed adherence to tissue-culture grade plastic, but reduced adherence to Matrigel-coated plastic plates (not shown). Microglia cultured 7 DIV were fixed or subjected to a viability assay. Cell counts and viability (Figure 4 B & C) in response to increasing concentrations of GM-CSF were non-significantly different, indicating that 1 ng/ml of GM-CSF, the minimal amount used, might be sufficient to stimulate proliferation and survival. Thus, in future studies, 1ng/mL GM-CSF was used when culturing in LGDMEM/10% FBS/1% PenStrep.

48hrs after plating in HN+

A.
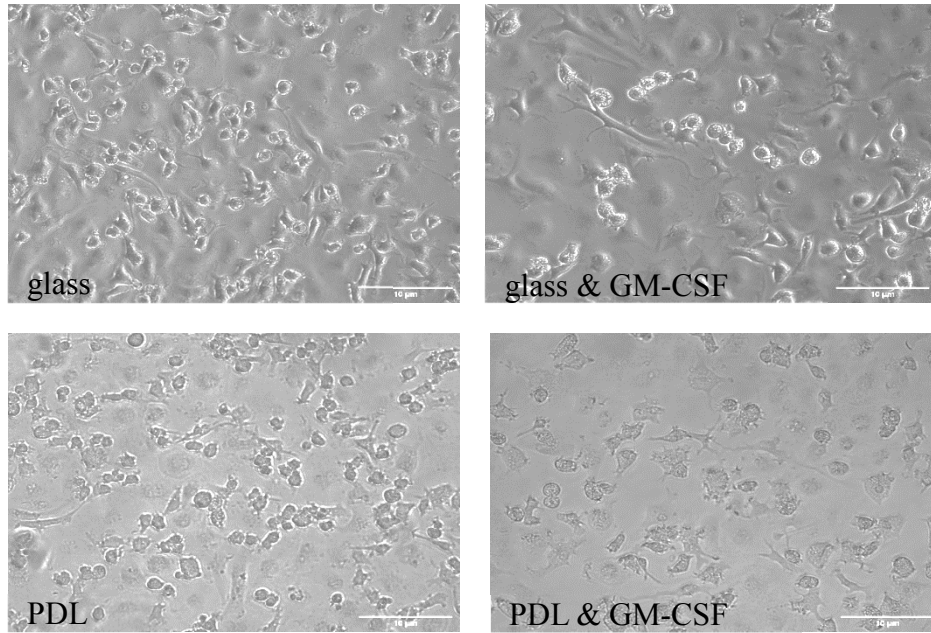
B.
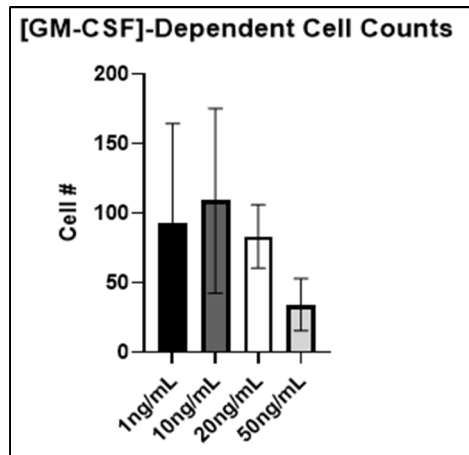
C.
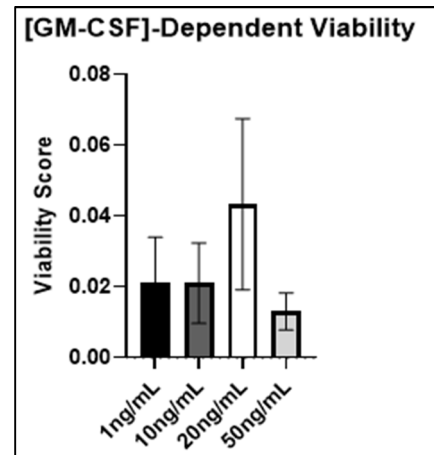
Figure 4: GM-CSF Dose Response of Microglial Proliferation and Viability

A.) Brightfield images of microglia plated on glass, or tissue-grade plastic, in the presence of GM-CSF 24hrs after plating in HN+ medium. Scale bars represent 10 µm. B.) Raw cell counts determined by Iba-1 immunolabeled coverslips of microglia cultures at 7 DIV. C.) MTT assay determined viability scores at 7 DIV. One way ANOVA determined no significance between groups in B or C (GraphPad Prism). Experiment conducted in triplicate. Error bars represent 1 standard deviation

The time in which microglia can survive in serum-free medium was determined by plating microglia in LGDMEM/10% FBS/1% PenStrep and converting the medium gradually to HN+ during media changes over 5 days: 1 DIV (25% HN+), 3 DIV (50% HN+), 5 DIV (100% HN+). Additional cultures were plated and maintained in LGDMEM/10% FBS/1% PenStrep and HN+ respectively for comparison (Figure 5 A-C). At 7 DIV, the cultures with differing media were fixed, permeabilized and immunolabeled for the microglia specific ionized calcium-binding adapter molecule I, Iba-1. There was no observable change in the morphologies or plating densities between media groups. Viability assays conducted on these cultures indicates that there was no difference in viability between media types (Figure 5 E). Use of cultures converted to a serum-free media is comparable to cultures maintained in serum-positive media, therefore we continued with cultures plated in LGDMEM/10% FBS/1% PenStrep and converted over 5 days to HN+.

Cultures plated in LGDMEM/10% FBS/1% PenStrep were converted to HN+ as outlined above. Starting at 5 DIV, cultures were maintained without media change for 24, 48, and 72 hrs in 100% HN+ and assayed for viability. There was no significant reduction in viability between 24, 48 and 72 hrs in HN+ media (Figure 5 D). However, in subsequent studies we utilized microglia and microglia conditioned medium within the first 24 hrs of their full conversion to HN+ medium.

39
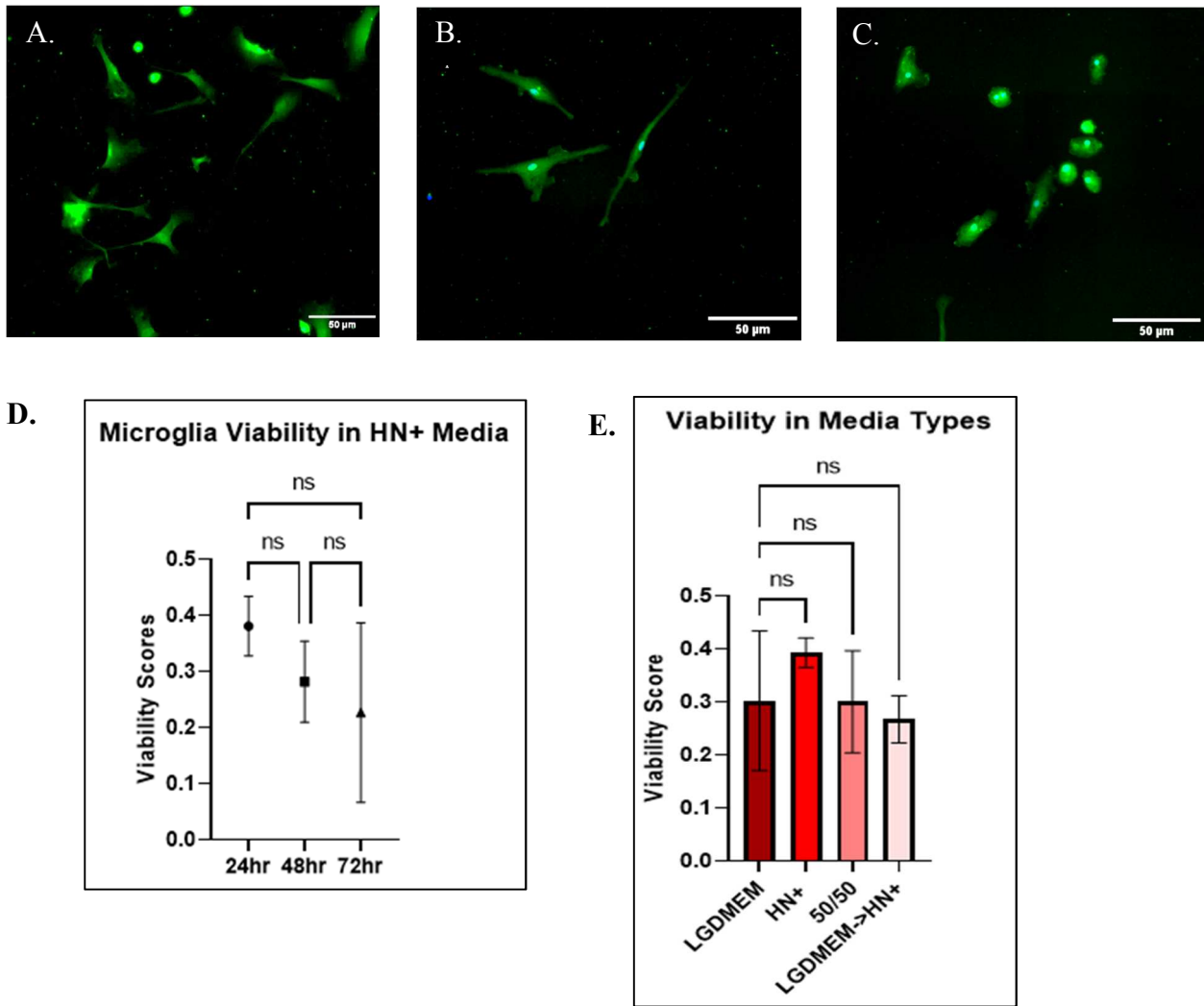
Figure 5: Microglia Viability in Serum-Free Medium Conditions
A-C) Microglia cultures immunolabeled with Iba-1 (green) A) Cultures maintained in LGDMEM/10% FBS/1% PenStrep. B) Cultures maintained in HN+. C) Cultures plated in LGDMEM/10% FBS/1% PenStrep and transitioned HN+ over 5 days. D) MTT assay results for microglia converted from LGDMEM/10% FBS/1% PenStrep to HN+ medium over 5 DIV. Cultures were maintained in HN+ for 24 (6 DIV), 48 (7 DIV), and 72 hrs (8 DIV) with viability assayed on each day. E) Viability assay results comparing microglia cultured in various media conditions. LGDMEM, HN+, and 50/50 columns were plated in indicated media and cultured for 24hrs prior to assay, LGDMEM-> HN+ was transitioned over 5 days and cultured in HN+ for 24hrs prior to assay. D-E.) One way ANOVA with Tukey's post hoc test determined significance between groups. *$p < 0.05$, was determined to be statistically significant. ***$p<0.001$.. Groups in E determined to be non-statistically different as determined by GraphPad Prism. Experiment conducted in triplicate.

Cultured microglia could now be treated with factors to activate them to a proinflammatory state. We first selected to test hemin, which we thought might be toxic to neurons at the high concentrations used for microglia activation and thus wanted to be able to remove it from the conditioned medium so that any effect in survival or rod formation in the treated neuronal cultures would come from microglia-secreted factors in response to the activating agent, and not the activating agent itself. The disparity between the molecular masses of the anticipated secreted chemokines and cytokines ((TNFα, 17 kDa; IL-1β, 17.5 kDa (proteolytically cleaved); IL-6, 23.7 kDa; IFNγ, 15-25 kDa).) and hemin (0.6 kDa) we selected desalting spin columns as an easy way to separate out the hemin. The concentration step would remove some hemin; however, the desalting would trap hemin along with other low molecular weight molecules.

The method for removing the hemin from microglia conditioned media is summarized in Figure 6. Microglia-conditioned medium was collected and processed individually from each well to be applied respectively to a single well of neurons (Figure 6 step 1). HN+ medium (1 mL) was added to microglia (activated with 100 mM hemin) for 24hrs and removed and concentrated on 3 kDa MWCO concentrators for 20 minutes at 10,000 x g at 4°C in a benchtop centrifuge (Figure 6 step 3). This resulted in about a 2x concentration of the components with higher mass. The concentrated medium of about 0.5 ml was then passed through a 7 kDa MWCO desalting column placed in a 15 ml conical sterile tube that was preequilibrated by 3 x 1 mL washes (1000 x g for 2 min) at 4º C with HN medium without N21 Max supplements Figure 6 step 5).

Desalting columns removed the majority of hemin and the same volume of medium that was loaded is collected in the flow-through which should contain the majority of starting protein

components of the HN+ medium but in a smaller volume of a 1X solution of HN medium low molecular weight components plus microglia secreted factors (chemokines and cytokines, all >8kDa) (Figure 7 A &B). To improve the protein recovery, two 100 µL washes (1000 g for 2 min) of the spin column using HN were performed in tandem (Figure 6 step 6). The flow-through plus washes was reconstituted back to the original medium volume by addition of the appropriate volume of the 50x stock of N21Max low molecular weight components (custom combination of 16 components from R&D Systems) and dilution to 1 ml with HN medium (Figure 6 step 7). The reconstituted medium is kept on ice and 20 µL is removed for measuring osmolarity, which is adjusted to the desired range with sterile water (Figure 6 step 10). The reconstituted medium is then added to neuronal cultures for 24 hrs at 37° C in 5% CO_2 until fixation.

A.
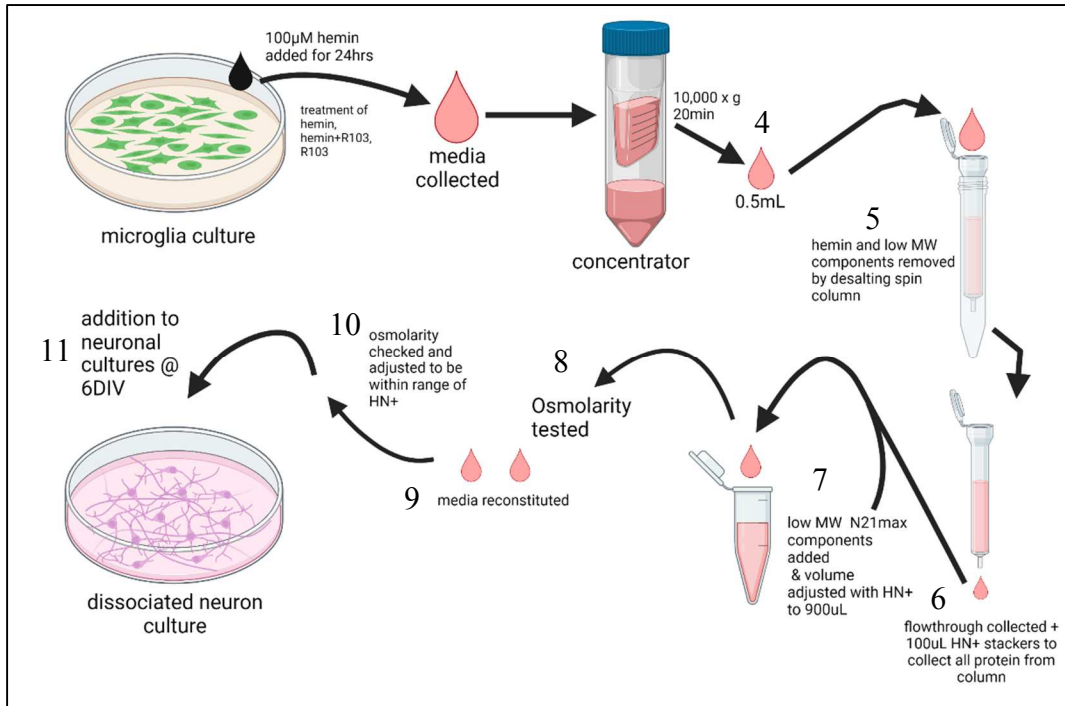
Figure 6: Media Fractionation of Low Molecular Weight Components

Outlined is the basic protocol used to culture, treat, and remove hemin from the media for the hemin activation experiments. Cultures are plated in LGDMEM, 10% FBS, 1 ng/mL GM-CSF and converted over 5 days to serum free HN+ media supplemented as outlined in methods. Microglia cultures are treated for 24 hrs with activating agents and RAP drugs. Media is concentrated via centrifugation, passed through a column, then diluted back to 1x for osmolarity testing and adjustment. Finally, the neuron-appropriate media can be added back to neuronal cultures for 24 hrs prior to the beginning of imaging or fixation. Graphic created with BioRender.

After flowing through the desalting column, the sample had an increased osmolarity compared to un-fractionated HN+. Additionally, repeated experiments determined that osmolarity may be causing substantial cell death before immunostaining could be done (data not shown). To combat this, we tested the osmolarity and adjusted it with sterile water to match un-fractionated HN+. This seemingly remedied some of the neuronal viability issues and was continued to be used as best practice for fractionation.

We verified that the sample volume before and after the desalting step was identical (Figure 7 B & C). Although there was a visible decline in the hemin content of the HN+ media before and after the spin column fractionation (Figure 7 C) not all of the hemin was removed (Figure 7 B).
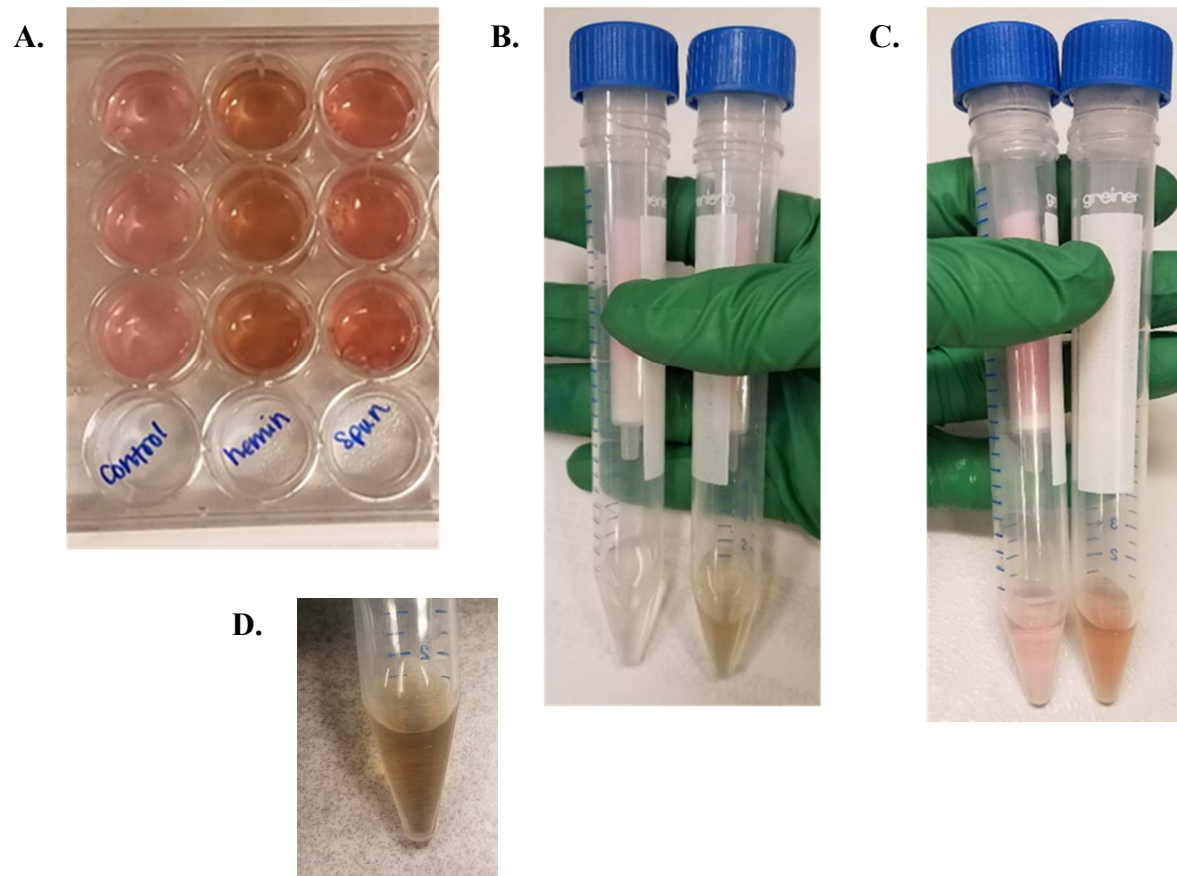
Figure 7: Removal of Hemin from Media via Fractionation

A) Hippocampal neuronal cultures on 24 well plate. Control: 3 wells containing HN+ media; hemin: 3 wells containing HN+ medium treated for 24 hrs with 100 μM hemin; Spin: 3 wells treated same as middle column but fractionated to remove hemin prior to addition to the neurons. B-C) Size-exclusion desalting columns with the flow-through to be tested for osmolarity. B) Left: water run through the column; Right: 100 μM hemin in water run through the column. C) Left: HN+ media run through a column equilibrated with HN media; Right: 100 μM hemin in HN+ media run through a column equilibrated with HN media. D) 100μM hemin in water before fractionation.

A small fraction of the neurons treated with reconstituted medium, prepared from hemin-containing died, but not enough to be significant when compared to the control/untreated group. (Figure 8 G), suggesting death was unrelated to hemin-induced toxicity. This was confirmed by finding that direct addition of the same concentration of hemin to the neurons without any fractionation had little if any toxicity resulting in cell death (Figure 8 G). Thus, some other imbalance in the medium fractionation/reconstitution protocol seemed to be at fault.
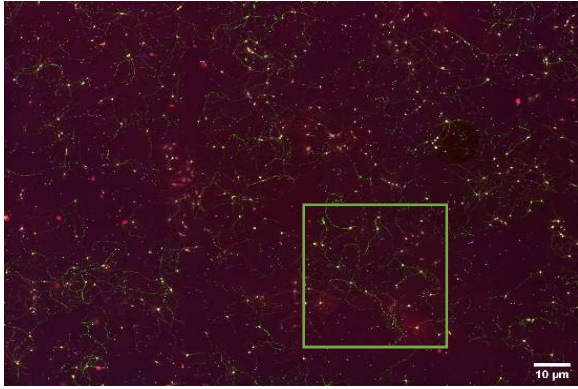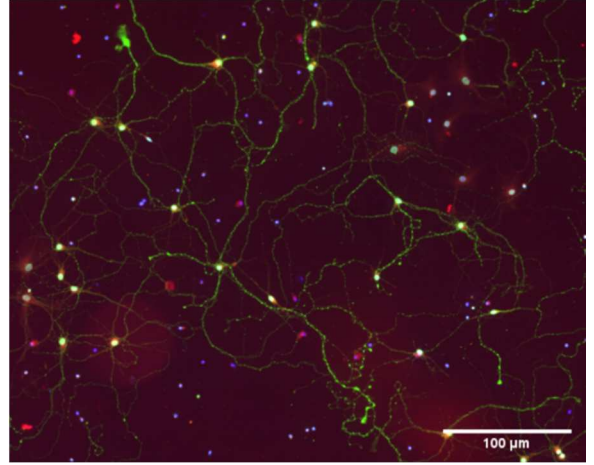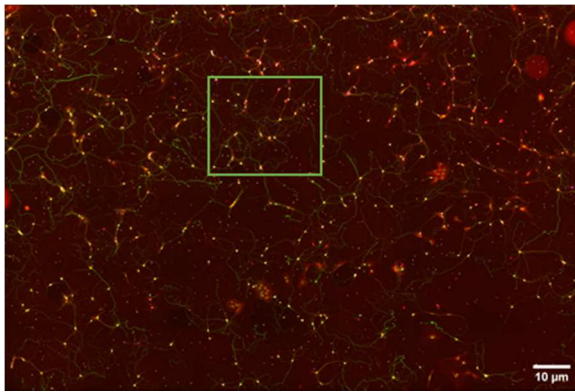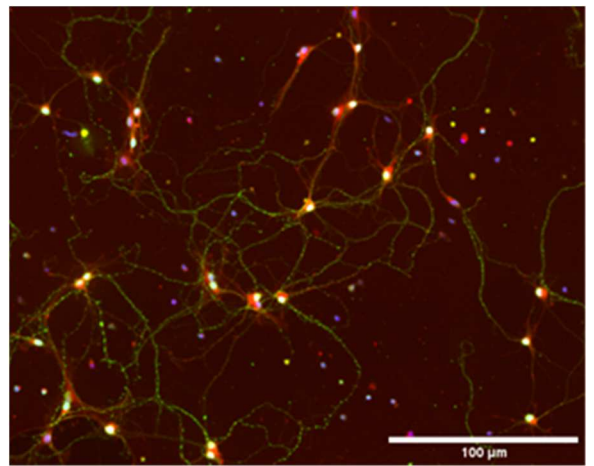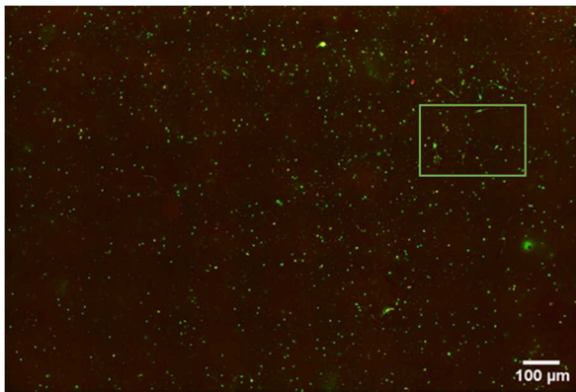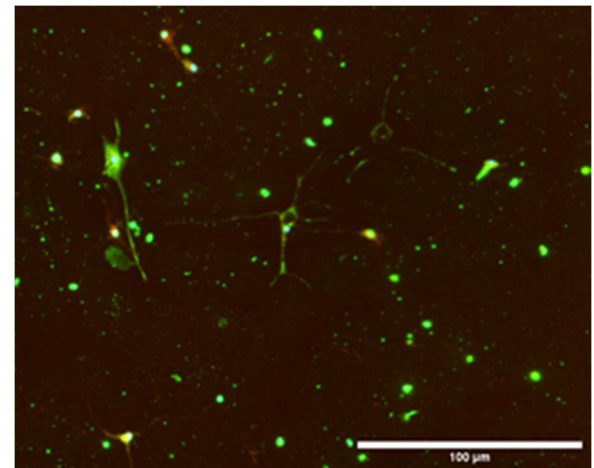
G.
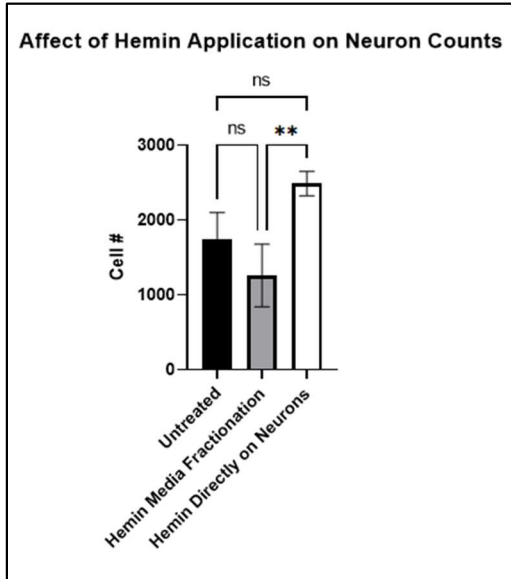
Figure 8: Neuronal Health following Direct Hemin Application or Fractionation

A-F) Representative immunolabeled images of hippocampal neurons obtained at 20x. DAPI (blue), immunolabeled cofilin (Alexa 488, green), immunolabeled neurofilament H (Alexa 564, red). **A)** Untreated 7 DIV hippocampal neurons. **B)** Blow up of green inset box from **A**. **C)** Hippocampal neurons treated on 6 DIV with 100 μM hemin and fixed on 7 DIV. **D)** Blow up of green inset box from **C**. **E)** Coverslip stained after media fractionation according to Figure 4. **F)** Blow up of green inset box from **E**. **G)** Comparison of cell counts for hippocampal cultures that were either untreated (**A**) or treated with microglia-conditioned media after the hemin removal protocol (Hemin Removed) (**E**) or with 100 μM hemin directly applied (**C**). Error bars represent 1 standard deviation. Experiments conducted in triplicate.

Although the columns' manufacturer claims >95% protein recovery of samples above 8.6kDa we measured this directly (Figure 9 A). There was about an 80% recovery of the protein when we assayed HN+ using a filter paper dye-binding assay that is not subjected to much interference by non-protein components which are washed away before dye binding. However, although there were some significant changes in protein content before and after fractionation of microglia conditioned medium with or without hemin, some of these shown an increased protein content after fractionation suggesting that on average, the protein recovery from the spin columns is quite high. This was confirmed by another comparison of hemin containing medium before and after fractionation along with fractionation of a BSA standard, the main carrier protein found in HN+ (Figure 9 C). These data indicate that there may be something vital for survival being removed from the media upon fractionating.

A.

B.

C.

Filter Paper Assay Standard Curve Media Fractions

$y = 0.087x + 0.0337$
$R^2 = 0.9857$

Absorbance

Protein (µg)

D.

Filter Paper Assay Standard Curve

$y = 0.075x + 0.0323$
$R^2 = 0.9926$
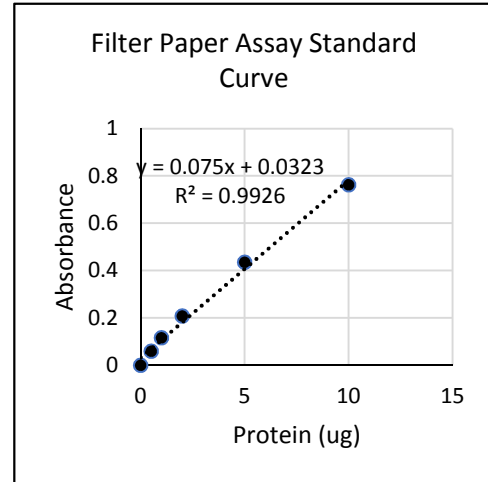
Absorbance
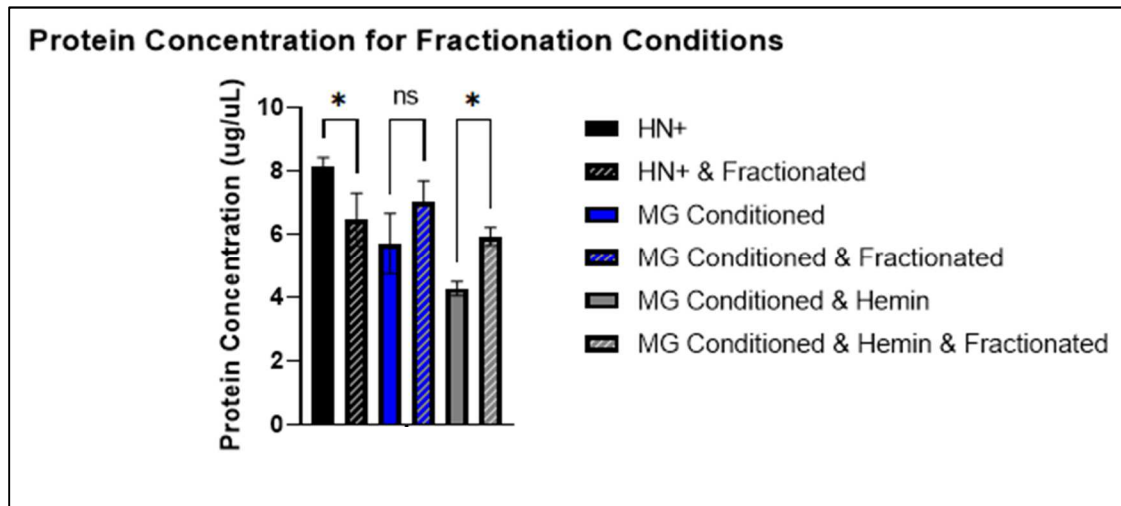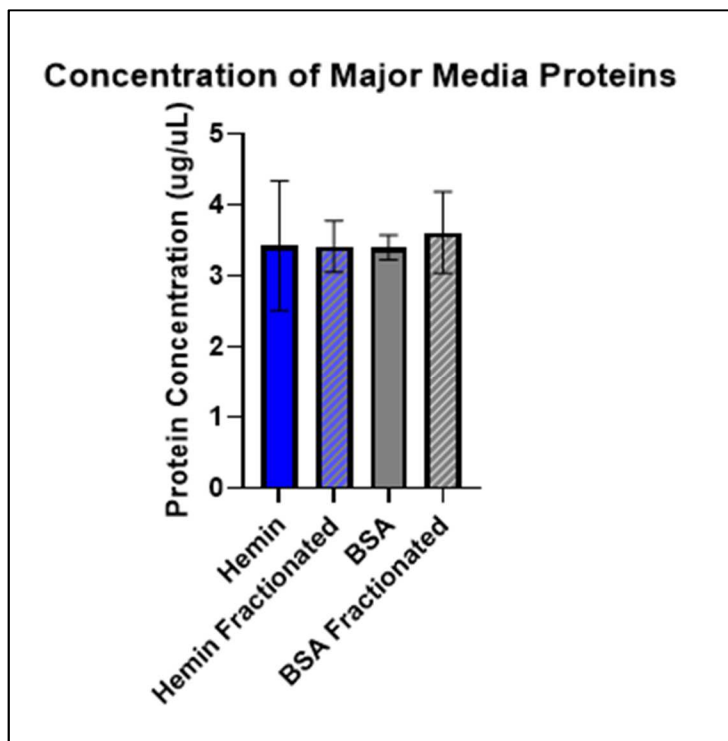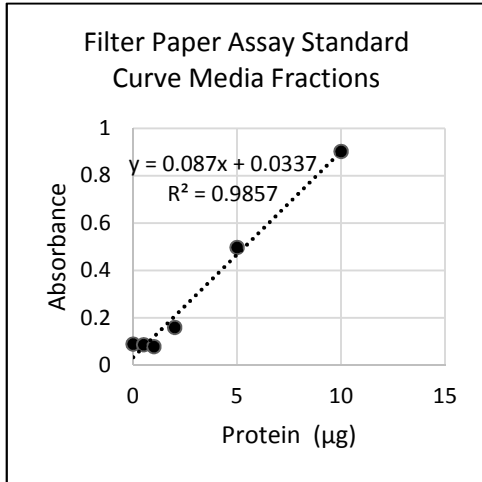
Protein (ug)

Figure 9: Protein Quantification of Medium Before and After Fractionation

A) Protein concentrations of medium at different steps of the hemin-conditioning, removal, and reconstitution protocols as measured with the filter paper dye-binding assay, whose standard curve is shown in C. MG: microglia B) Comparison of protein recovery of hemin-containing medium before and after fractionation on desalting column and between a BSA solution before and after desalting column fractionation using filter paper protein assay whose standard curve is shown in D. Results in A and B analyzed by one way ANOVA with Tukey's post hoc test. Experiment conducted in triplicate. No significance between groups in B.

The N21Max supplement supplies insulin for neuronal cultures, and since it has a molecular mass of <6 kDa it below the cut off for gel exclusion on the desalting column. Thus, re-addition of insulin to the samples post-fractionation might be beneficial for neuronal survival; however, due to the proprietary nature of component concentrations in N21Max, we needed to test a range of added back insulin concentrations (Figure 10). Adding insulin from 5 nM to 1 mM to neurons cultured in HB+ medium had no statistically significant effect on survival although 1 μM re-addition provided a higher viability than the control medium. Neurons cultured in fractionated/reconstituted medium show a modest decline in neuronal viability and the add back of 5 nM insulin was too little to correct the significant ($p < 0.05$) viability loss. However, re-addition of insulin to 1 μM to 1 mM restored viability such that it was not significantly lower than pre-fractionated control medium. These data suggest that there may be a lower limit for insulin levels in media for maintenance of healthy neuronal cultures but that up to 1 mM, insulin is not toxic.
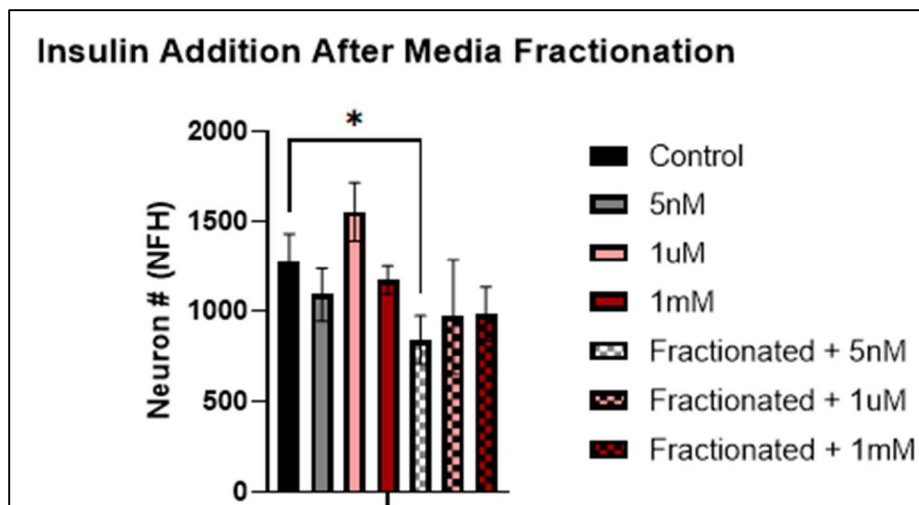
Figure 10: Insulin Addition Before or After Media Fractionation

Quantification of cell numbers before and after the hemin removal protocol was performed and insulin was added to cultures. Cells on coverslips were quantified 24 hrs after the media fractionation and insulin add back Cell counts were performed on cells after immunolabeling for neurofilament-H (red). One-way ANOVA followed by Tukey's post hoc was performed using GraphPad Prism. Experiment conducted in triplicate.

In summary, these studies suggest that with careful fractionation and readjustments, it is possible to utilize small molecules to modify microglia behavior and then to remove them from the medium when assaying the effects of microglia-produced factors on neurons. One of our goals is to be able to look at the effects of small molecule antagonists of the CXCR4 and CCR5 receptors on microglia activation and separate these from the microglia released protein factors that stimulate the neuroinflammatory response (Figure 6) . This system for fractionation should allow us to carry forward that work.

Although hemin activation of microglia is well established in the literature, the optimal concentration for activation varies between studies. We tested the effects at 24, 48 and 72 hrs of hemin at concentrations between 12.5-200 μM on microglia viability and spreading. Coverslips were immunolabeled with Iba-1 a microglial specific-ionized calcium binding adapter molecule frequently used in general staining of microglia (Davies et al., 2017). The optimal concentration of hemin for maintaining the highest microglia number and the percentage of coverslip area covered by the cells occurred at 100 μM and was significant in both measures over untreated cultures (Figure 11). The less than 2-fold increase in cell number coupled with a 3-fold increase in coverslip area, strongly suggests a large increase in cell spreading, which accompanies microglia activation to a pro-inflammatory, proliferative state. Thus, 100 μM was selected for continuing with this work. studies. The decline in area and cell number following treatment with 200 μM hemin suggests toxicity at this higher concentration.
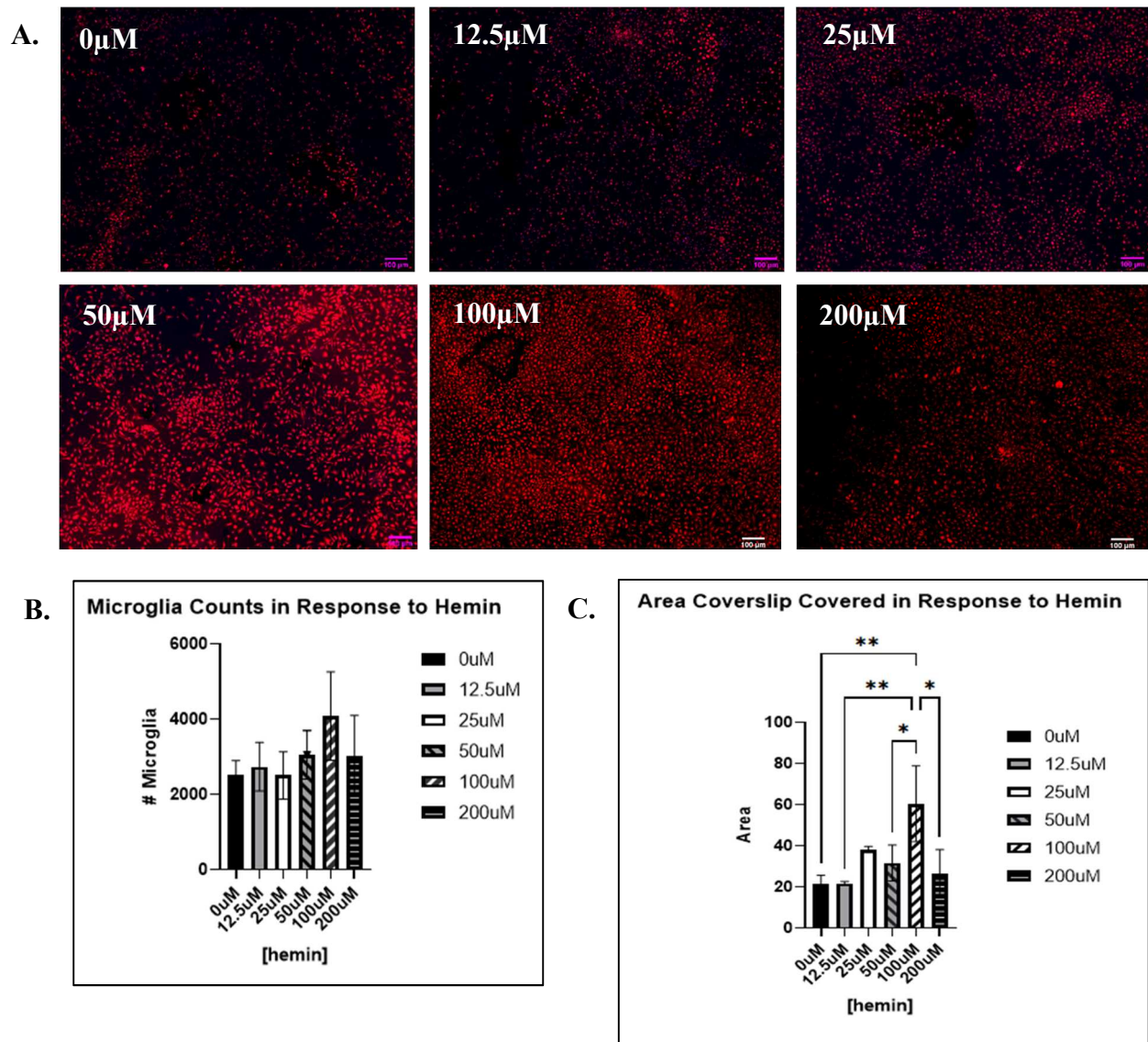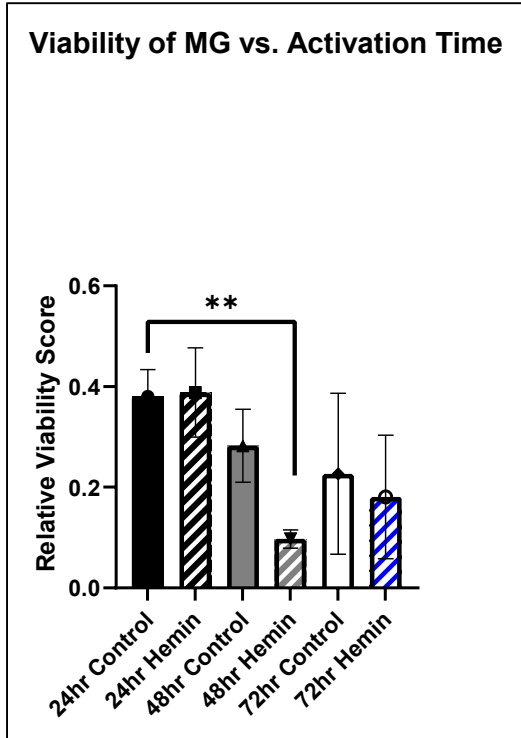
Figure 11: 100μM Hemin Stimulates Microglia Proliferation and Spreading, Parameters Associated with their M1 Activation State

A) P0-1 mouse microglia cultures 5 DIV were untreated or hemin-treated (upper left to lower right) and were fixed and immunolabeled on DIV 6. DAPI (blue), Iba-1 (Alexa 564, red). Scale bar: 100 μm. B) Cell counts based on Iba-1 immunolabeling of microglia. Error bars represent 1 standard deviation. C) Average percentage of the coverslip covered by microglia immunolabeled for Iba-1 positive cells. Error bars represent 1 standard deviation from control. 3-4 coverslips/condition.

There is also disparity in the literature on the length and persistence of microglia activation after initial exposure to activating agents (Goshi, *et al.,* 2020) To test these parameters for hemin, we applied 100 μM hemin to cultures for 24, 48, and 72 hrs and assayed for microglia viability with a MTT (Figure 12). The results confirm those in Figure 5, indicating that hemin lose viability over time in HN+ medium, but the loss is not due to hemin addition per se (Figure 12). We did see a significant reduction in viability at the 48hrs timepoint, but when compared to the 24hrs control value, this was non-significant (Figure 12 A). To minimize effects of neurotoxic factors released from dying microglia, we opted for a maximal activation period of 24 hrs.

A.

Viability of MG vs. Activation Time

B.

MTT Assay 24hr Activation

MTT Assay 48hr Activation
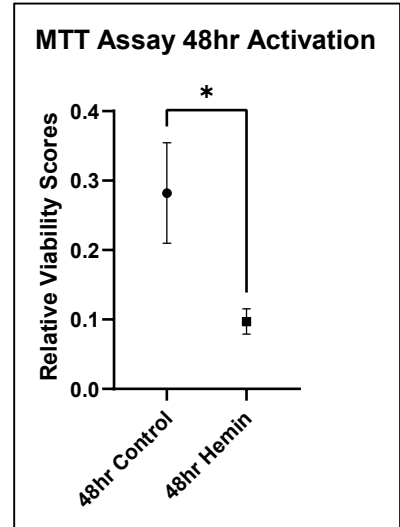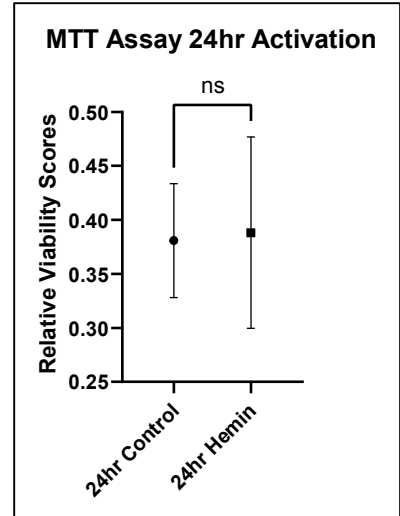
MTT Assay After 72hr Activation
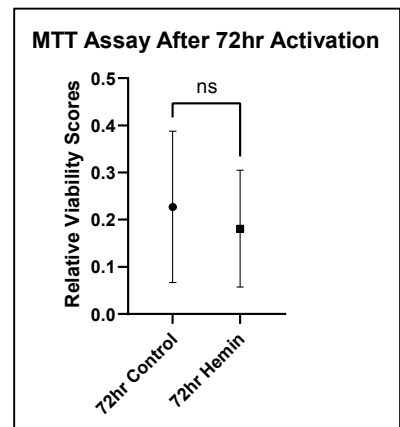
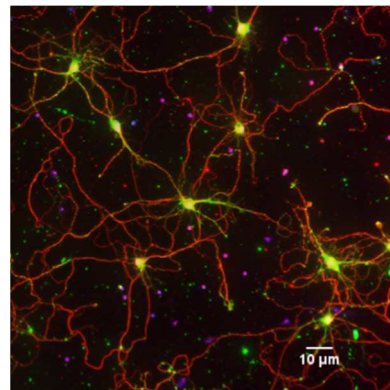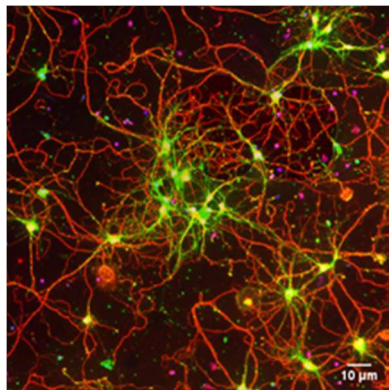**Figure 12: Microglia Viability in Response to Hemin Stimulation**

A) MTT assay of microglia cultures treated with 100 μM hemin for 24 hours (24 hrs Treated), 48 hours (48 hrs Treated), or 72 hours (72 hrs Treated) compared with timepoint matched control applications of saline. Data shown in terms of raw viability scores. Error bars represent 1 standard deviation from respective control. B) Individual comparisons at each activation time point (24, 48, and 72hrs) compared with saline-treated matched control. Replotting of the data in A. Unpaired T test was performed and the asterisk (*) indicates statistically significant differences. Experiments conducted in triplicate.

Neurons directly treated with hemin showed no visible neurite blebbing which is often

seen in dying neurons. There was also no segmentation of processes or discontinuous staining of

neurofilament-H along neurites exposed to 12.5-100 µM hemin (Figure 13 A-E), but in one

experiment (Figure 13 F) there was a dose-dependent loss of neurons of about 50% at 100 µM

hemin. However, this result is not consistent between different hemin preparations and may

depend on batch-to-batch variability in hemin solubilization by titration of the hemin suspension

using HCl. For example, in comparing the neurotoxicity of hemin by direct addition to neurons

versus its removal from microglia conditioned medium of hemin (Figure 2.6 G), direct addition

of 100 µM hemin appears to result in greater survival than in controls (although not significant)

whereas applying the hemin removal protocol significantly decreased the neuronal viability.
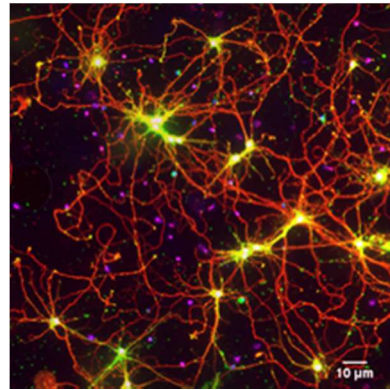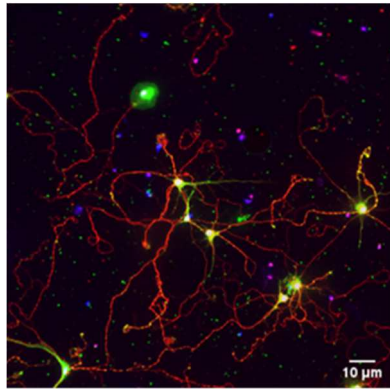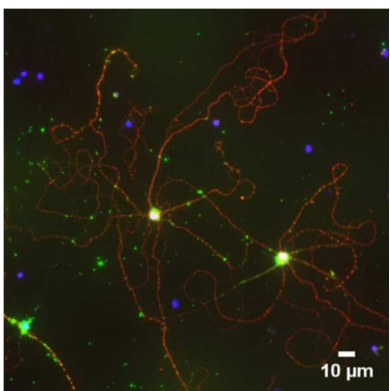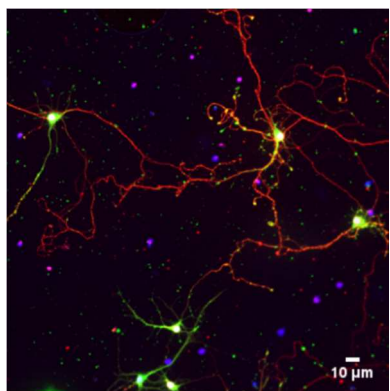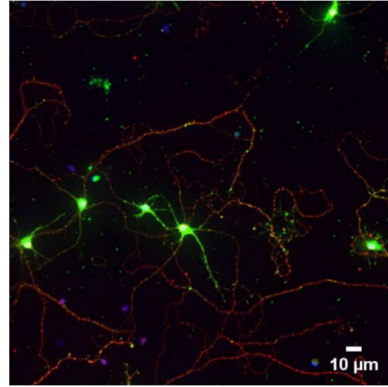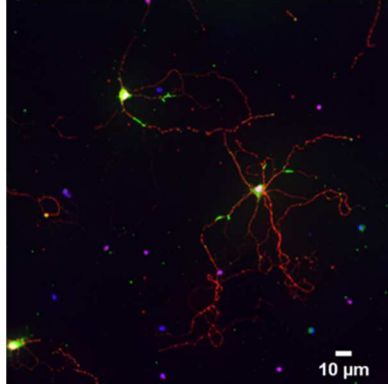
D.

E.
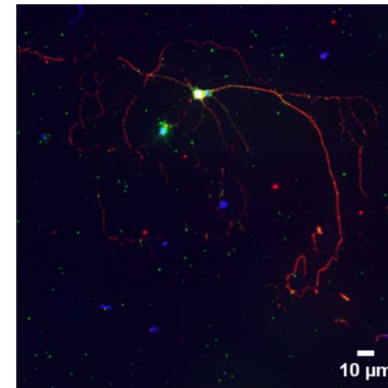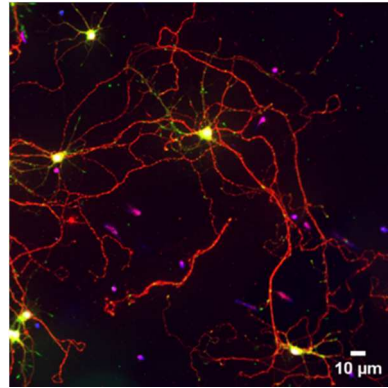
F.
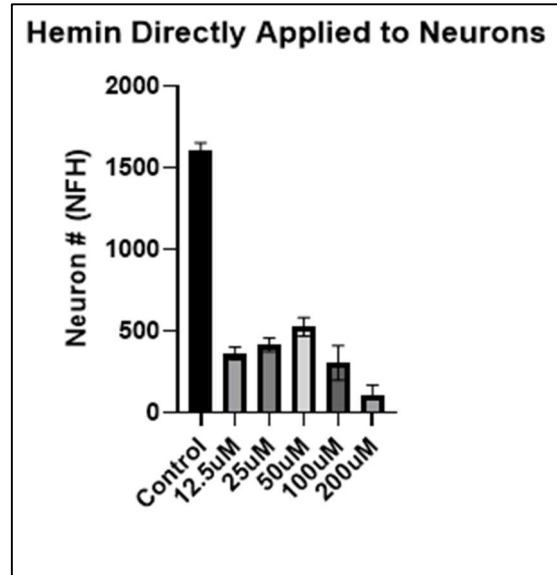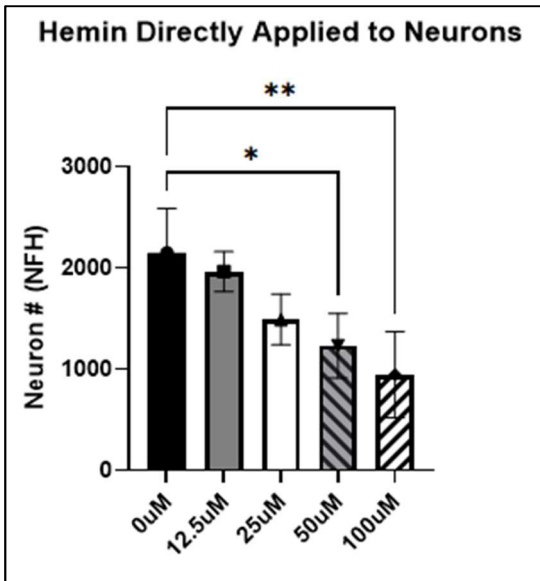
Figure 13: Neuronal Viability in Response to Hemin Stimulation

Immunolabeled images of rat hippocampal neurons fixed on 7 DIV. No visible blebbing, discontinuous staining, or other visual indicators of stress are observed. A) 0 µM hemin, B) 12.5 µM hemin, C) 25 µM hemin, D) 50 µM hemin, E) 100 µM hemin. Scale bar: 10 µm. Neurons were stained with DAPI (blue), and immunolabeled for cofilin (Alexa 488. green), and neurofilament H (Alexa 564, red). F) Neuronal viability to various amount of hemin when applied directly to neurons for 24 h. Left: trial with hemin stock 1. Right: trial with hemin stock 2. Error bars represent 1 standard deviation. Experiments conducted in triplicate.

Because we observed reasonable neuronal survival after 24 hrs of direct exposure to 100 μM hemin, we quantified the effects of various concentrations of hemin on cofilin-actin rod induction (Figure 14). Again, the variability of neuronal survival to hemin is evident in the large loss of neurons at and above 25 μM hemin (Figure 14 E). Although some spontaneously formed rods are observed in neurons cultured under control conditions, hemin at 100 μM appears to have an elevated number of rod-like inclusions when rod index is calculated by dividing the rod numbers by the neuron numbers (Figure 14 G). Although interpreting results from an experiment in which 95% of cells are lost is not very meaningful, the higher percentage of rods in surviving neurons could be interpreted to mean that rod formation might be initially neuroprotective, as was suggested by a previous study (Bernstein et al., 2006).

A.

B.

10 µm

C.

D.

10 µm

E.

Neuronal Count in Response to Hemin

***

***

***

ns

Neuron Counts (NFH)

1000
800
600
400
200
0

0uM 12.5uM 25uM 50uM 100uM

[hemin]

F.

Neuronal Rod Count in Response to Hemin

*

**

**

Rod Count

80

60

40

20

0

0uM 12.5uM 25uM 50uM 100uM
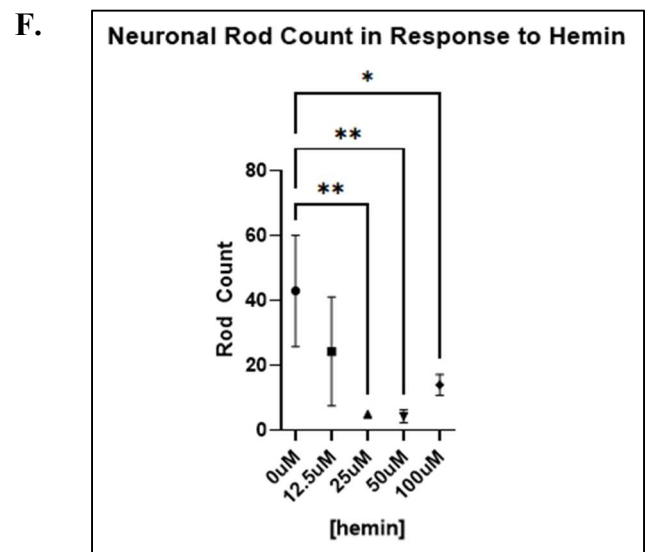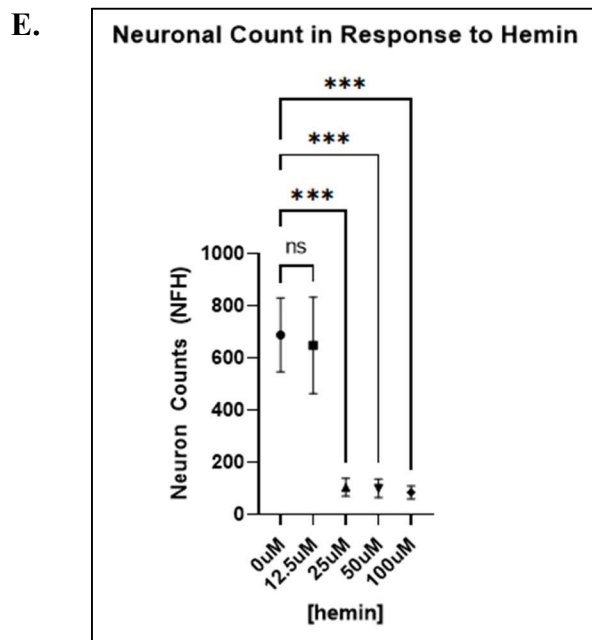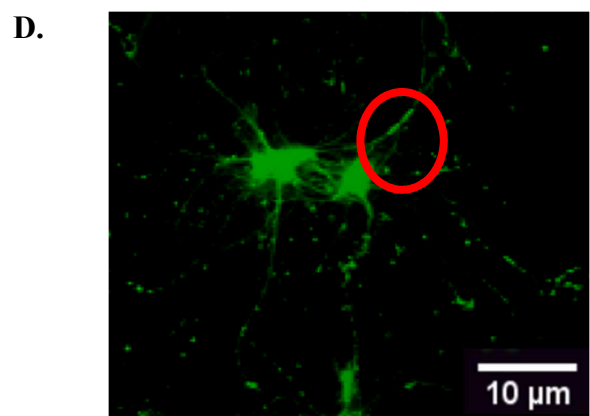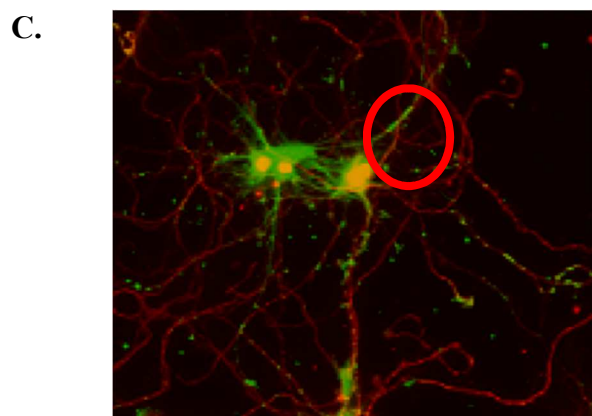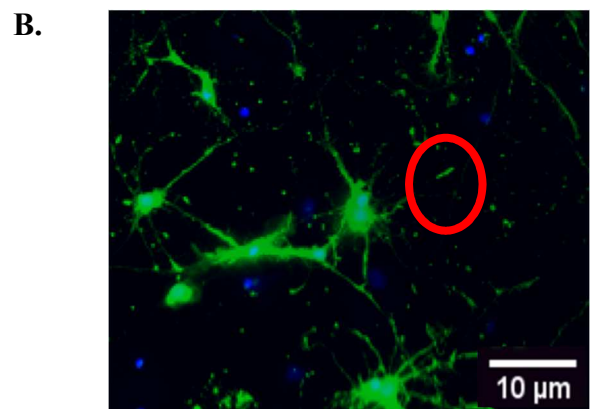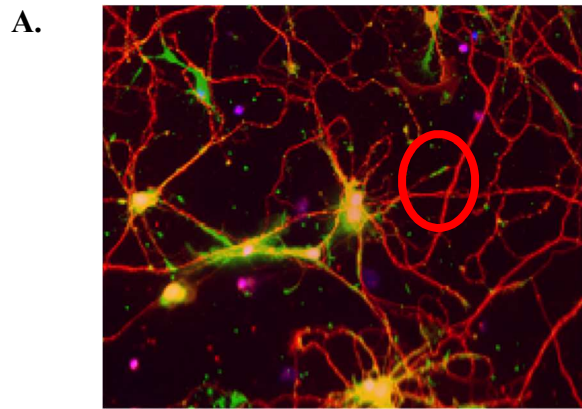
[hemin]

G.
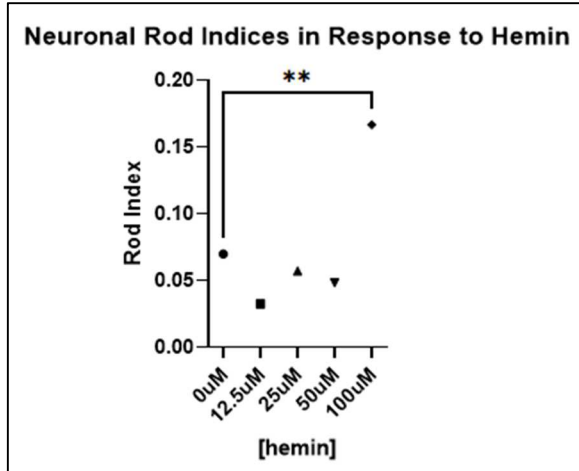
Figure 14: Hemin Application to Neurons Increases the Rod Index Score

A-D) E16.5 hippocampal rat neurons, treated with hemin on 6 DIV, and fixed and immunolabeled/stained on 7 DIV. DAPI (blue), immunolabeled cofilin (Alexa 488, green), immunolabeled Neurofilament H (Alexa 564, red). Red circles outline cofilin:actin rods. A) Cofilin immunolabeled rod in neuron treated with 12.5 μM hemin. B) Same field as A. but in green/blue channel. C) Cofilin immunolabeled rod in neuron treated with 50 μM hemin. D) Same field as C. but in green/blue channel. E) Raw neuronal cell counts for each concentration of hemin applied to neurons directly F) Raw data of rod numbers for each concentration of hemin applied to neurons directly. G) Rod index score for same coverslips as E-G. Error bars represent 1 standard deviation. Experiment conducted in triplicate.

S100B is a physiological activator of microglia that is secreted by astrocytes to initiate microglia activation. Studies with S100B applied to microglia generally use 0.2 ug/ml or less for prevention of proinflammatory activation and 2 ug/ml for full activation without toxicity (Xu et al., 2016). We tested both 0.2 and 2 µg/ml for effects on microglia proliferation over 48 hrs (Figure 15). There were no significant differences between the untreated control and the S100B-treated groups; however, observable morphological changes towards the M1 phenotype were observed in brightfield images of the 2 µg/ml-treated cultures at 48 hrs (Figure 16 B). Upon direct application to neuronal cultures there was no significant cell death observed in the cultures treated with 2 µg/mL S100B for up to 48 hrs and observed with NeuO labeling (Figure 15 B). After 48 hrs of direct exposure to S100B, neurons still displayed healthy branching and no signs of blebbing. Our results therefore indicate that S100B is a less neurotoxic microglia-activating agent than hemin at the concentrations outlined in this chapter.

A. Viability of Microglia in Response to S100B

B. Neuronal Viability in Response to S100B

C. Neuronal Rod Index in Response to S100B
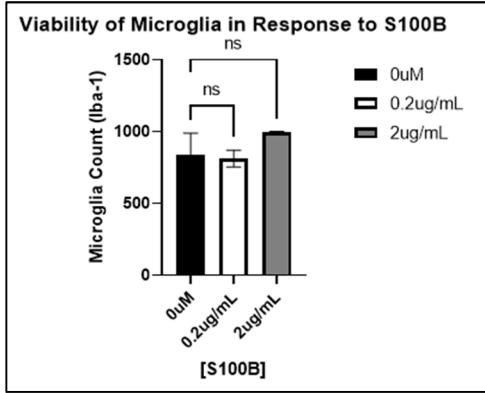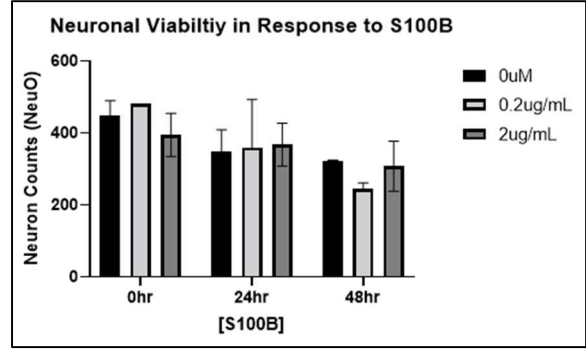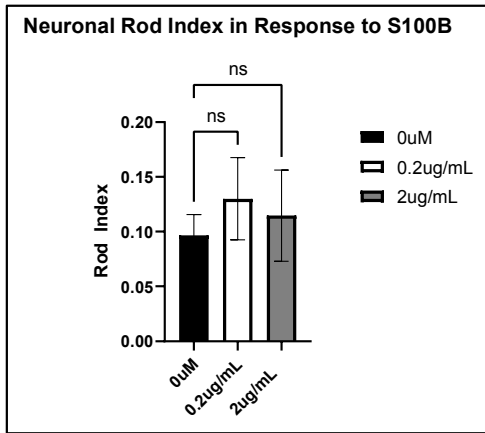
D.
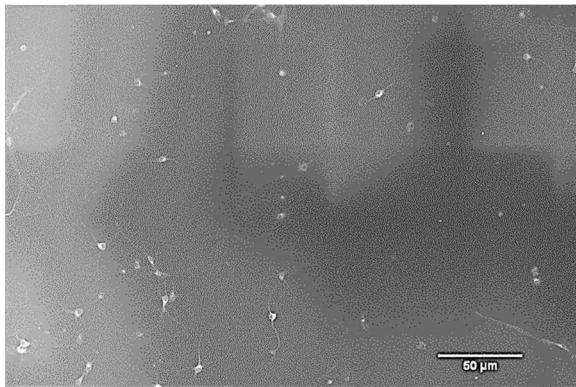
E.
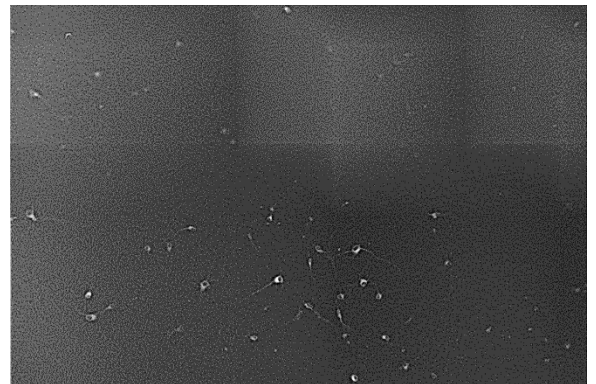
F.
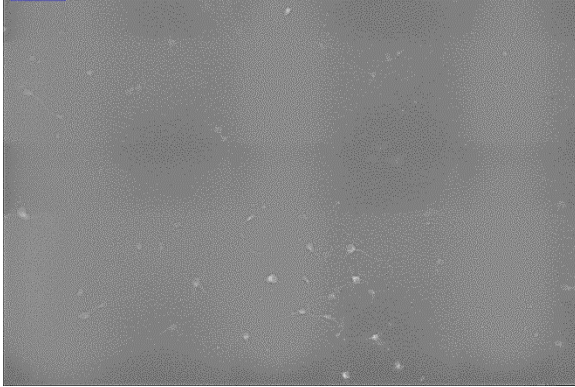
Figure 15: Effects of direct application of S100B on neuronal and microglia viability

A) Microglia response to S100B after a 24 hrs exposure as quantified by Iba-1 positive immunolabeling. B) Neuronal response to S100B over 48 hrs tracked with NeuO dye. C) Rod index score of neurons treated with S100B for 24 hrs prior to fixation and scoring. D) 0 hrs image of NeuO positive cells. E) Same NeuO-labeled field of neuronal culture as (D) after 24 hrs exposure to 2 µg/mL S100B. F) Same NeuO-labeled field of neuronal culture as (D) after 48 hrs exposure to 2 µg/mL S100B. 20x magnification. Error bars represent 1 standard deviation. Groups determined to be non-significant (A-C) by one-way ANOVA followed by a Tukey's post-hoc test. Repeated in triplicate.

A.

0min   10min

0min inset

Untreated

1hr   2hr

2hr inset

B.

0min   10min

0min inset

S100B (2μg/mL)

1hr   2hr

2hr inset

C.

RAP310
$(1\times10^{-10}M)$

0min　　　　　10min

1hr　　　　　2hr

0min inset

1hr inset

D.

S100B
&
RAP31

0min　　　　　10min

1hr　　　　　2hr

0min inset

1hr inset
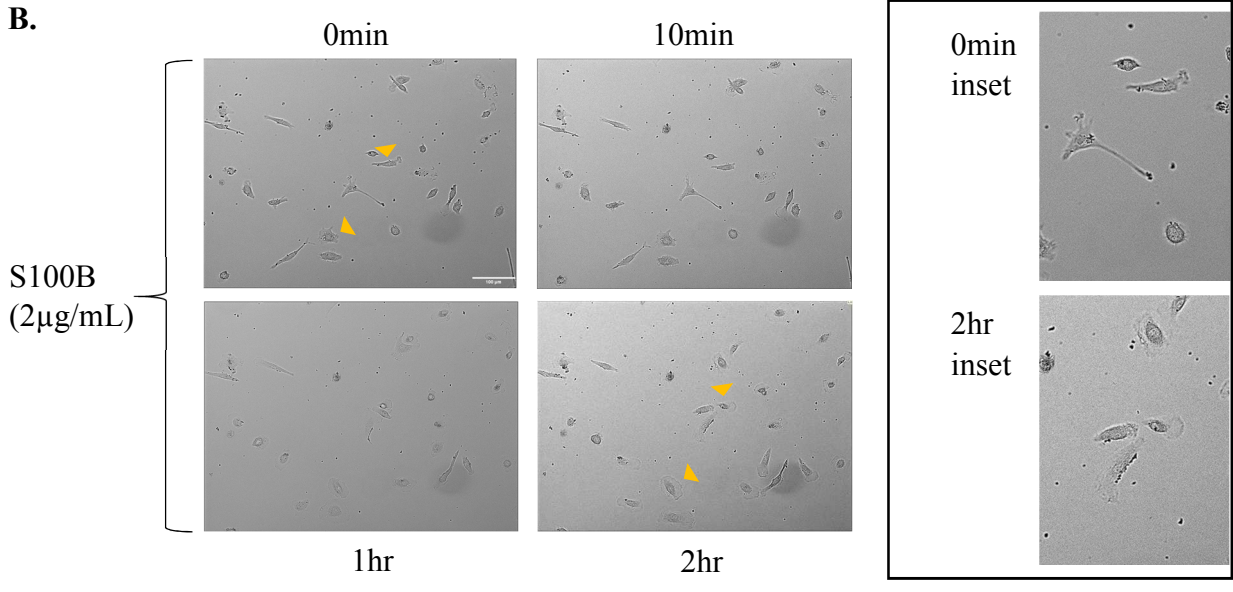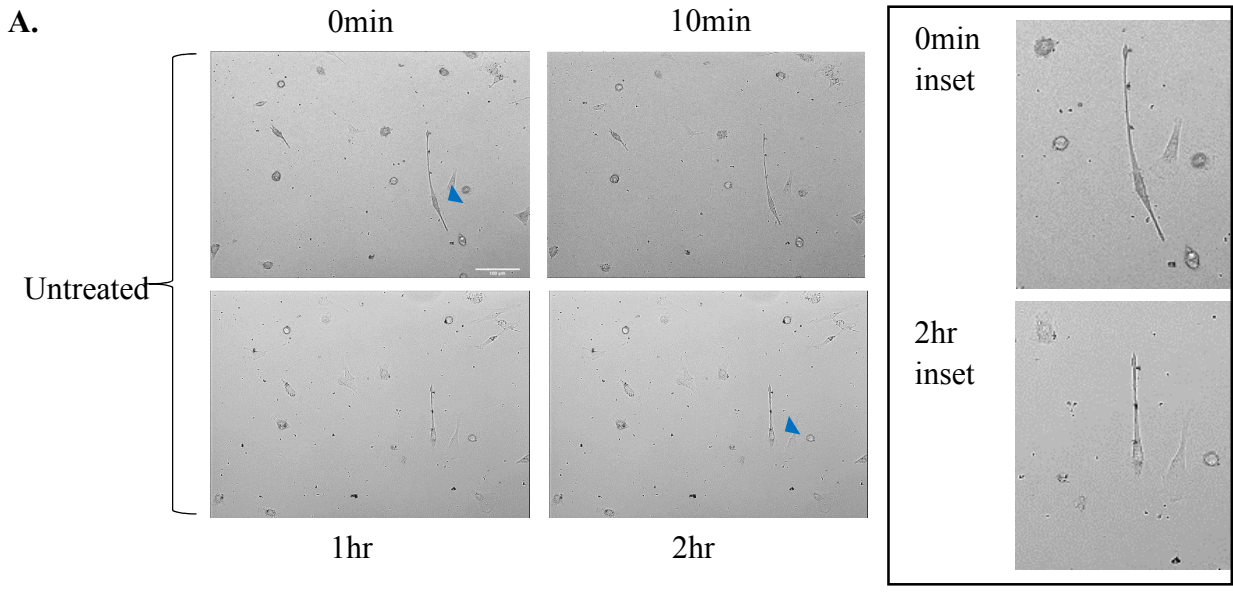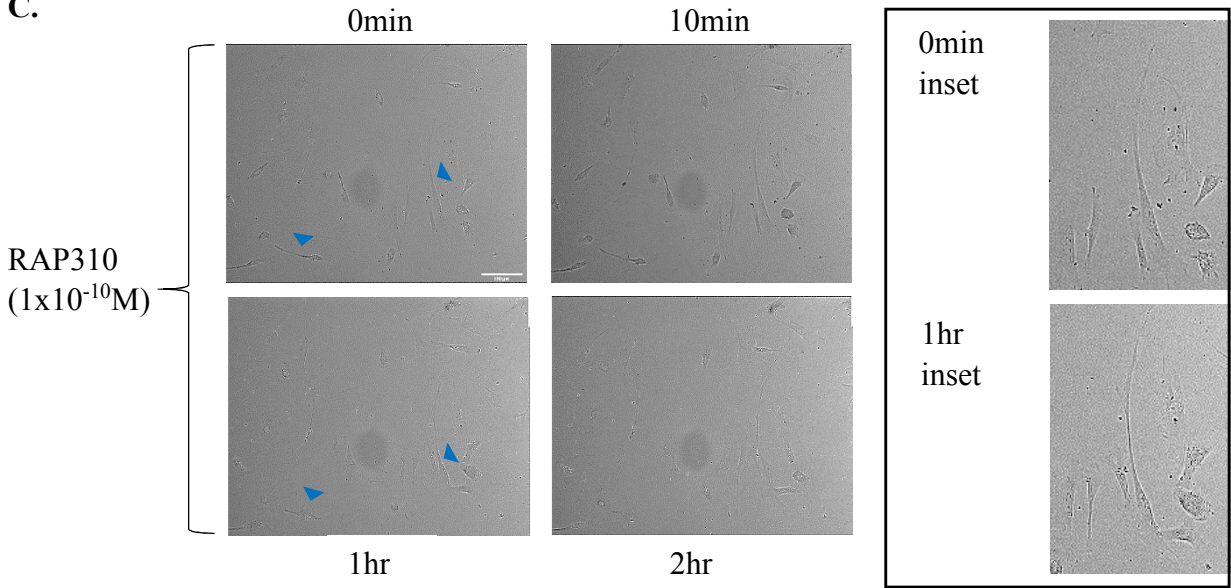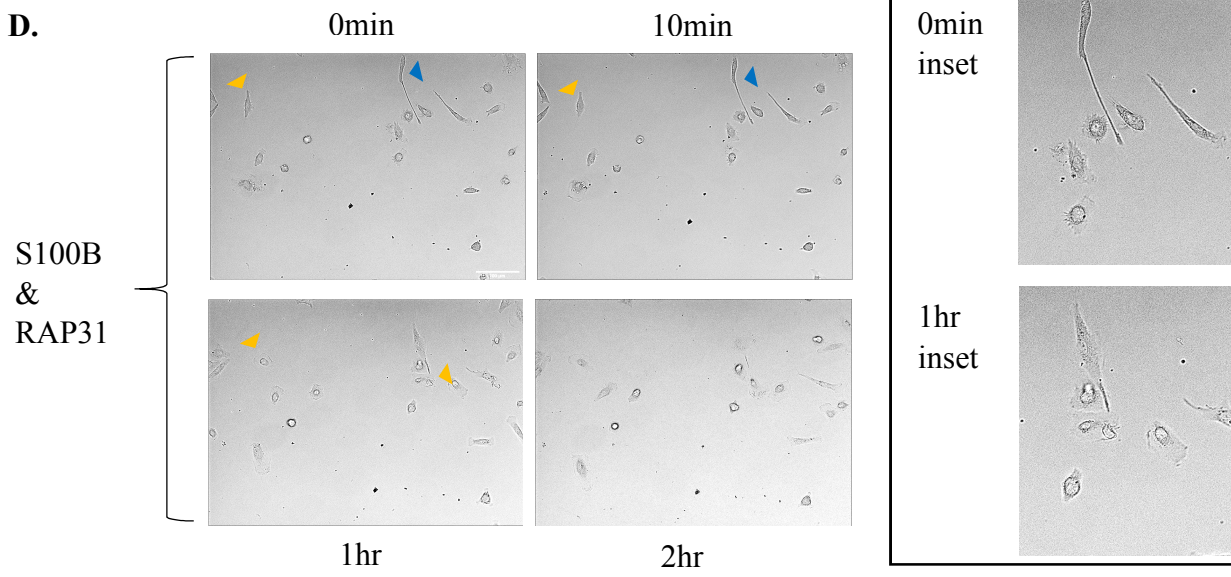
Figure 16: Brightfield Images of Morphological Changes in Microglia treated with S100B

A-D) Microglia cultures were imaged in brightfield at 20x and followed for 4 hrs. Left-most images: insets of 0min and 1hr microglia indicated by colored triangles. A) Untreated. B) Treated with S100B (2μg/mL) C) Treated with RAP310 ($1x10^{-10}$M) D) Treated with RAP310 and S100B. Scale bars = 100 μm. Orange triangles follow cells that undergo a morphological change associated with the M1 phenotype. Blue triangles follow a cell that remains ramified (M0).

To begin the testing of RAP inhibition of microglia-mediated neurotoxicity, we treated microglia with 2 µg/mL S100B in the presence or absence of RAP310 and observed morphological changes over 4 hrs via brightfield. More amoeboid, M1, microglia were observed in the S100B and S100B + RAP310 treated wells. Minimal amoeboid cells were observed in the RAP310 treated wells alone. Further studies will continue to investigate the effects of the RAPs. Prior to looking at the effect of RAPs, we wanted to ensure that the RAP-targeted chemokine receptors are present on the microglia in our cultures. To do so microglia converted to HN+ media and cultured for 7 DIV were immunolabeled to show X4 and R5 distribution. Cells were permeabilized, therefore, staining shows that both receptors are present based on immunolabeling. Cultures treated with only the secondary antibodies showed only background fluroescence, indicating any immunolabeling is fairly specific (Figure 17).
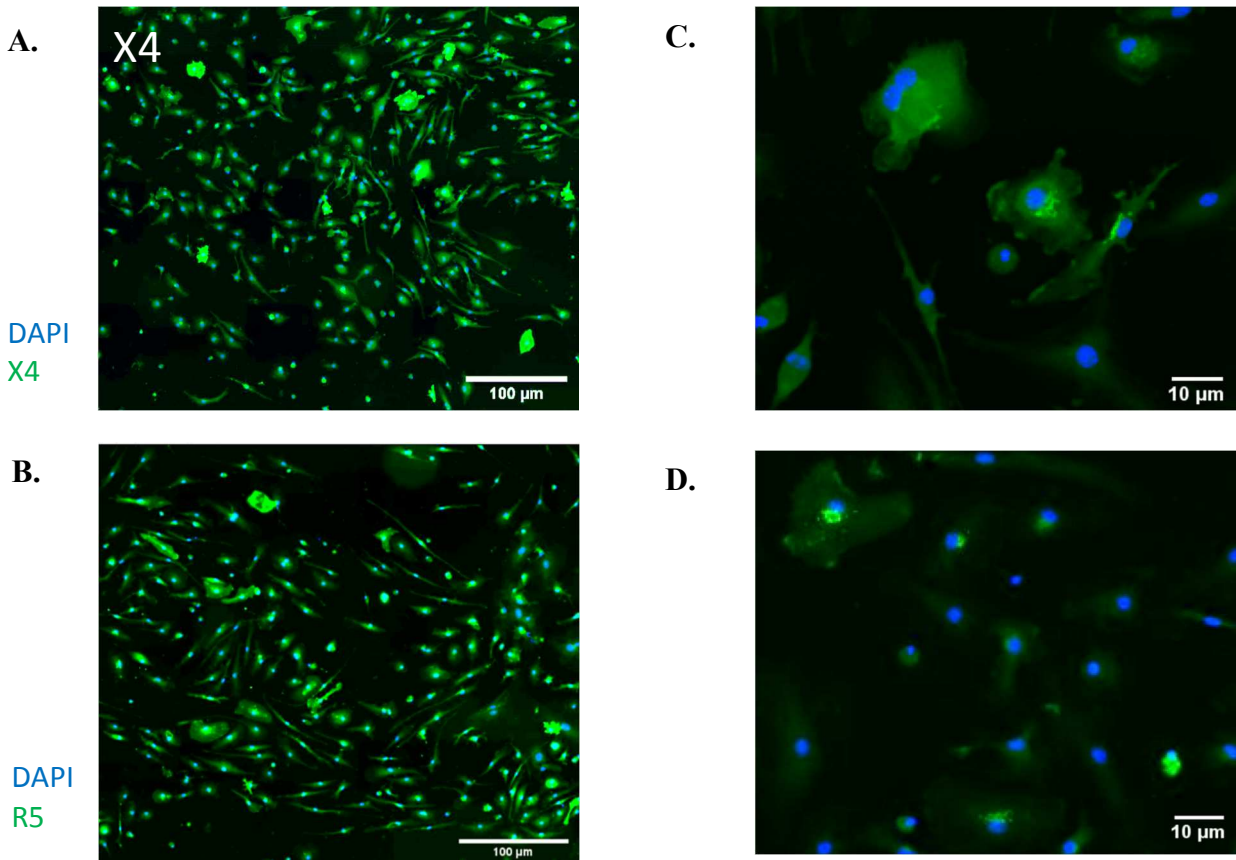
Figure 17: Staining of X4 and R5 Receptors in Primary Mouse Microglia

A-D.) 7DIV microglia imaged at 20x, in a 7x7 stitched array and immunolabeled A) Magnified image of a stitched array showing CXCR4 (green) and DAPI (blue). B) Inset image from A. C) Magnified image of a stitched array showing CCR5 (green) and DAPI (blue). D) Inset image from C.

In preparation of the co-culturing assays performed later in this chapter, primary neuronal cultures were cultured for 7 days and treated with sodium azide at 10mM in either PBS or HN+ medium to elicit cell death, or untreated and followed for 48 hrs using the neuronal specific dye, NeuO (Figure 18). Cultures were treated with NeuO 24 hrs and 2 hrs prior to introduction of the sodium azide. As observed by fluorescent images, there was reduction in the intensity of the NeuO labeling by 24 hrs with the sodium azide treated cells. The untreated wells retained higher amounts of dye for longer, but also exhibited a decrease in fluroescence intensity over the 48 hrs observation (Figure 18 D). These data assure that use of NeuO in live imaging assays aimed at determining neuronal viability in a 24 hrs window are feasible and dying neuronal cells display reduced fluroescence by this time point. Therefore, dying cells are less likely to be counted in the automated analysis pipeline used for obtaining cell counts from live imaging captures. We believe that use of NeuO will yield a valid indication of neuronal viability for the experiments outlined in the remainder of this chapter.

A. Untreated

| 0min | 1hr | 2hr |
| 6hr | 24hr | 48hr |

B. Sodium Azide in PBS (10mM)

| 0min (in HN+) | 1hr | 2hr |
| 6hr | 24hr | 48hr |

C.

Sodium
Azide
in HN+
(10mM)

0min   1hr   2hr

6hr   24hr   48hr

D.

NeuO Intensity Over Time

NeuO Intensity (0-255)

— Untreated
— 10mM Sodium Azide in PBS
— 10mM Sodium Azide in HN+

0hr   24hr   48hr
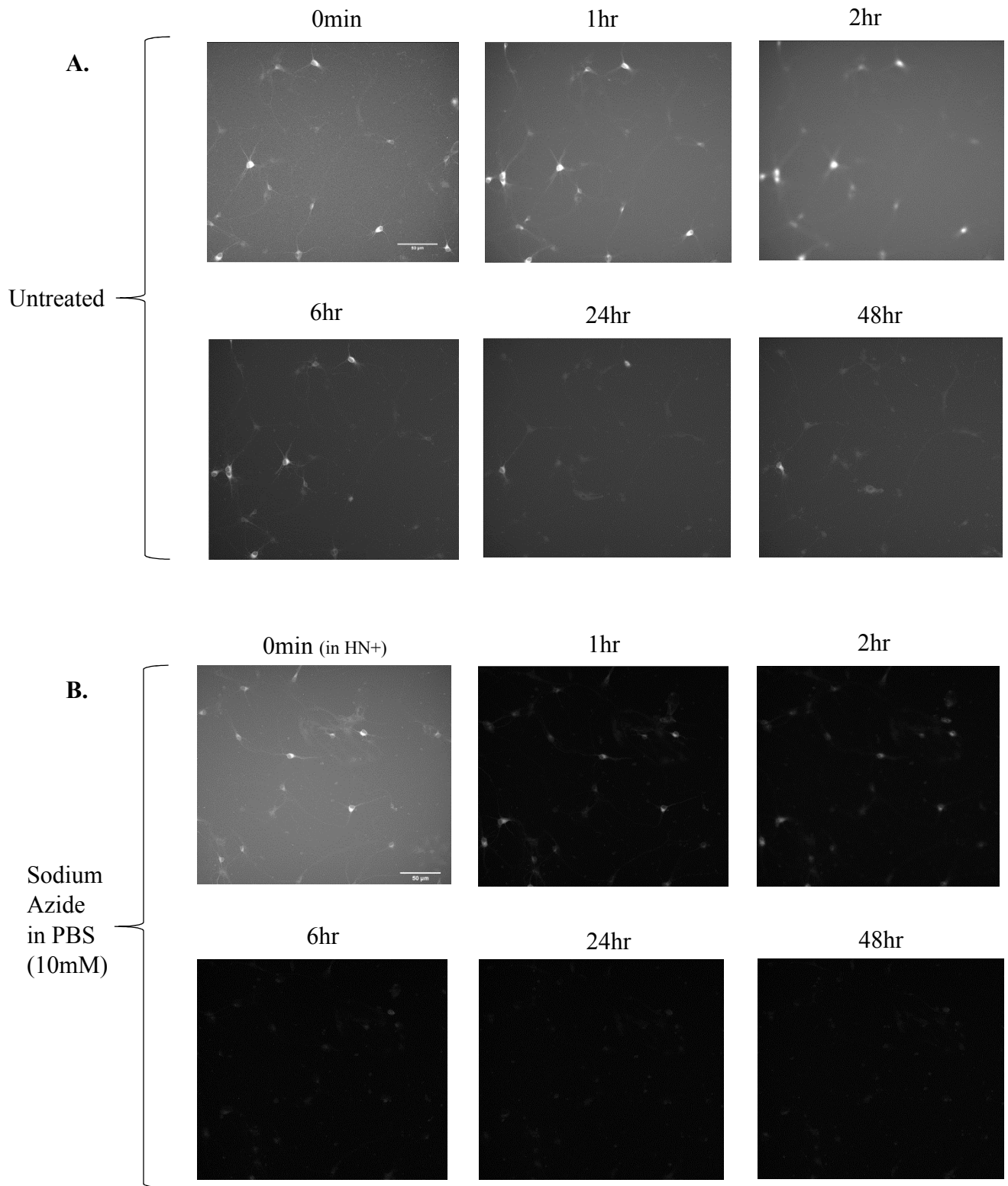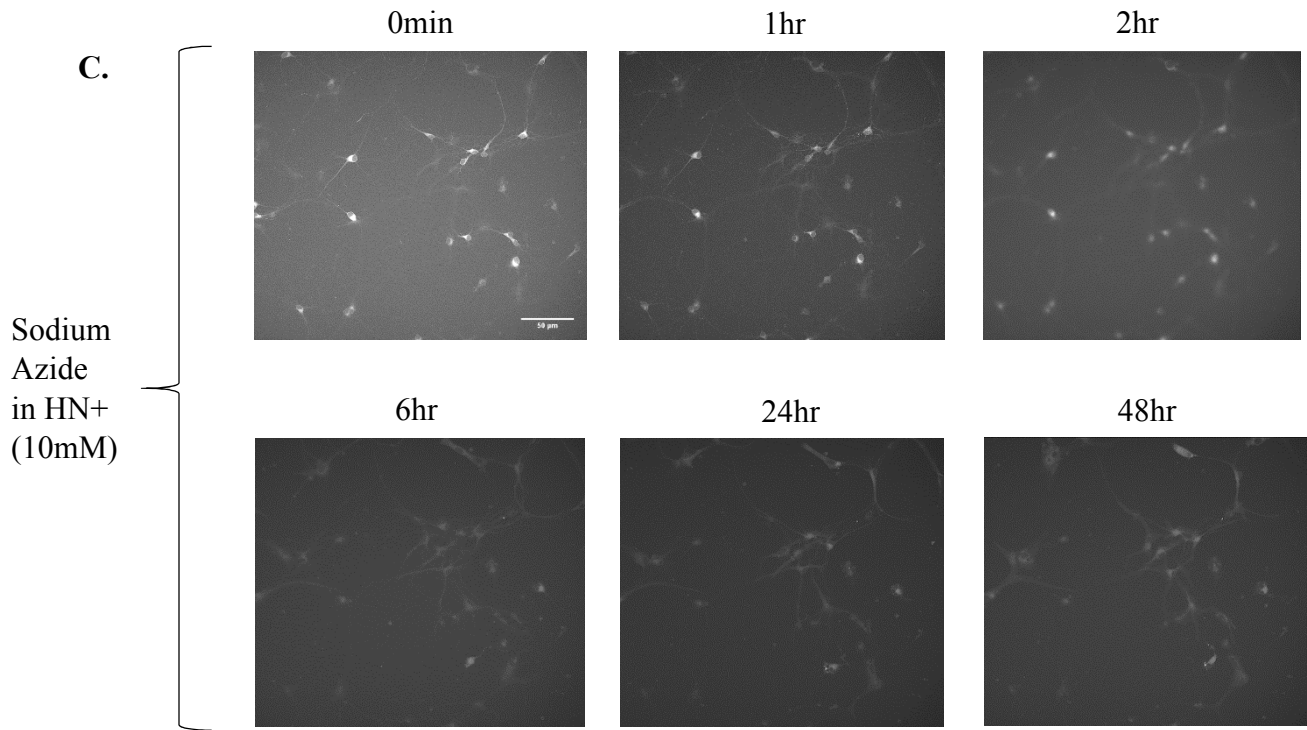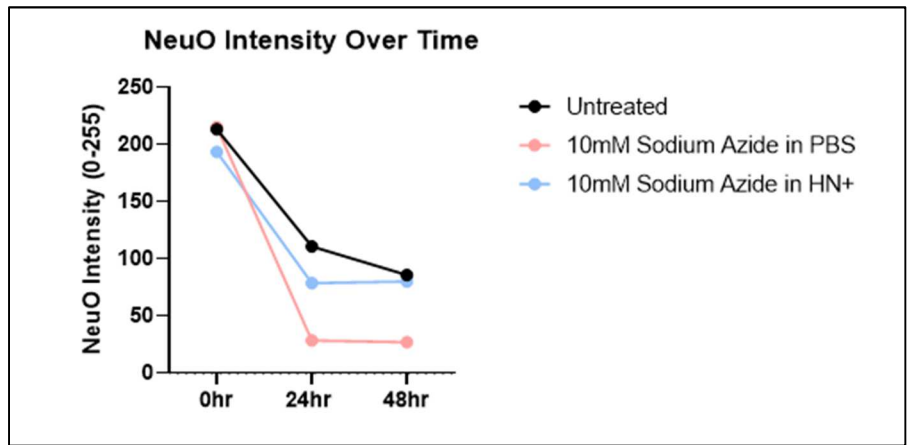
Figure 18: NeuO Intensity of Neuronal Cultures Over 24hrs with Sodium Azide to Induce Death

A-C) Neuronal cultures labeled twice with NeuO 24 & 2 hrs prior to image acquisition A) Untreated neuronal cultures B) Sodium azide (10mM in PBS) treated neuronal cultures C) Sodium azide (10mM in HN+ media) treated neuronal cultures. Images acquired at 20x of a single field in NeuO. Scale bars represent 50µm. D) Relative intensity of NeuO staining over 24 hrs. Experiments done in triplicate.

Our next experiment aimed to better understand the effect of microglia-secreted factors, and potentially neurotoxic factors, stimulated by hemin on neurons over time. Secondly, we sought to determine if the treatment of neurons with RAP310 simultaneously with the addition of hemin-activated microglia-conditioned medium changed the outlook on neuronal viability. To do so, we cultured 3 plates of neurons and 3 plates of microglia for 7 days. The microglia were converted to HN+ media (Figure 5), and treated with hemin for 24, 48, or 72 hrs. The media from the microglia (untreated, hemin) was then applied to neuronal cultures with or without the addition of RAP310 at time of media application (Figure 19). Hemin was not fractionated out of the microglia conditioned media and therefore was applied to the neurons with the conditioned media. The viability of the neuronal cultures was followed for 48 hrs post microglia-conditioned media application via live imaging with NeuO. Experimental setup detailed in Table 1.

With 24 hrs microglia conditioned media there was no significant difference between the treatments (untreated, hemin, RAP310, hemin & RAP310) at each timepoint. However, there was a significant decrease in viable neurons treated with hemin-containing microglia-conditioned media and RAP310 at the 48 hrs point (Figure 19 A).

Data with 48-72 hrs microglia conditioning in HN+ media likely recapitulate what was observed in Figure 5, effects of the microglia on neuronal viability were minimal as determined by viability tracking with NeuO over 72 hrs. The 48 hrs microglia conditioned media demonstrated no difference between treatments at each timepoint; but a significant reduction in viable neurons at 24 and 48 hrs when compared to 0-2 hrs. Wells treated with RAP310 and RAP310 with hemin were non-significantly different from untreated controls (Figure 19 B).Wells treated with 72 hrs microglia conditioned media showed no change in NeuO labeled

cells over time or in response to hemin activated microglia conditioned medium, or addition of

RAP310 at day 8.

We then sought to determine if S100B had similar effects when used in place of hemin in the same experimental design as Figure 19. Again, 3 plates of microglia and 3 plates of neurons were set up and cultured for 7 days. Microglia were converted to HN+ media and exposed to S100B (2 µg/mL) for 24 (7 DIV) or 48 hrs (6 DIV). Following the S100B-microglia incubation, 8 DIV the microglia-conditioned medium (untreated, S100B) was added to NeuO labeled cultures with or without R103 (Figure 20). Experimental setup detailed in Table 2.

Microglia Treatment	Length of Microglia Treatment (hrs)	Neuronal Treatment	Length of Neuronal Treatment (hrs)	Label in Figure 19
Untreated	24hrs	Untreated	48hrs	Control
Untreated	24hrs	RAP310	48hrs	RAP310
Hemin	24hrs	Untreated (hemin added with media change)	48hrs	Hemin
Hemin	24hrs	RAP310 (hemin added with media change)	48hrs	Hemin & RAP310
Untreated	48hrs	Untreated	48hrs	Control
Untreated	48hrs	RAP310	48hrs	RAP310
Hemin	48hrs	Untreated (hemin added with media change)	48hrs	Hemin
Hemin	48hrs	RAP310 (hemin added with media change)	48hrs	Hemin & RAP310
Untreated	72hrs	Untreated	48hrs	Control
Untreated	72hrs	RAP310	48hrs	RAP310
Hemin	72hrs	Untreated (hemin added with media change)	48hrs	Hemin
Hemin	72hrs	RAP310 (hemin added with media change)	48hrs	Hemin & RAP310

Table 1: Experimental Setup for Figure 19

(Green rows) Microglia treated with activating agent, hemin, for 24 hrs prior to addition to neuronal cultures. NeuO labeled-neuron cultures were or were not treated at time of media change with microglia-conditioned media with RAP310. (Red rows) Same as green rows but microglia were treated with activating agent, hemin, for 48 hrs prior to addition to neuronal cultures (with or without RAP310). (Blue rows) Same as green rows but microglia were treated with activating agent, hemin, for 72 hrs prior to addition to neuronal cultures (with or without RAP310).
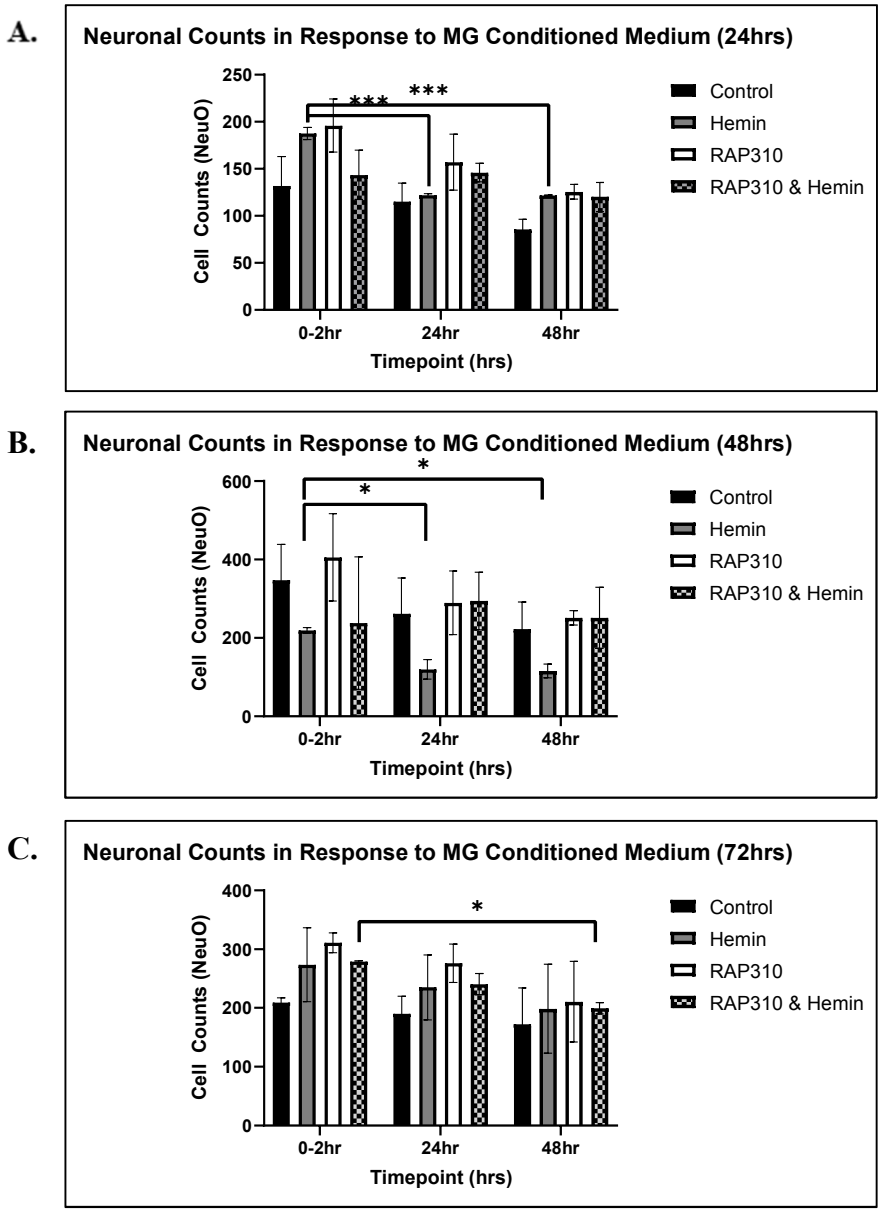
Figure 19: Neuronal Response to Media Conditioned by Microglia Exposed to Hemin & RAP310

A-C) Neuronal cultures were maintained for 7 days, with addition of RAP310 and hemin-activated microglia-secreted medium at 8 DIV. A) Live imaging over 72 hrs of neuronal cultures labeled with NeuO and treated with microglia conditioned media where the microglia were incubated with nothing, hemin, RAP310, or hemin and RAP310 for 24 hrs (A), same as A where microglia were incubated with agents for 48 hrs. B), same as A, where microglia were incubated with agents for 72 hrs. C). Error bars indicated 1 standard deviation. Non-significance values are not indicated. Treatments conducted in duplicate. MG: microglia.

S100B had a greater effect on the ability of microglia to produce neurotoxic substances than did hemin (Figure 20 A). The RAP310-treated neurons showed a significantly increased survival at in the 24 hrs conditioned medium than any of the other treatments which led to an almost complete toxicity of the neurons, and by 48 hrs virtually all neurons were dead in every treatment group, including controls, which confounds the interpretation of the results. Potential reasons for the cell death are addressed in the discussion. Better survival of neurons occurred in all groups that received the 48 hrs microglia conditioned medium, again perhaps suggesting the loss of the neurotoxic cytokines/chemokines following death of the microglia (Figure 20 B).For every treatment there was a progressive decline in viability over time except for the 48 hrs time point with RAP310 addition, which showed no significant change from 24 hrs and indeed was at or above neuronal survival in the control cultures (48 hrs Control bar) (Figure 20 B). There appeared to be neurotoxicity with the S100B treated cultures at 48 hrs of neuronal exposure (Figure 20 B); however, in the group treated with RAP310 and the S100B-microgila conditioned media there was a distinct protective effect. Additionally, the RAP310 treated wells were comparable to control. Finally, there was a reduction in viable cells between RAP310 and S100B & RAP310 treated cells, but the S100B & RAP310-treated wells were significantly increased compared to just S100B-treated wells, and non-significantly different from control. Therefore, RAP310 may have a beneficial effect on neuron viability after 48 hrs-exposure to microglia-conditioned media activated with S100B.Although the neurotoxicity of the microglia conditioned medium seen in Figure 20 A was disappointing, the possible neuronal protection by RAP310 was intriguing and we wanted to determine if this would show up in experiments in which microglia were cultured directly with neurons.

Microglia Treatment	Length of Microglia Treatment (hrs)	Neuronal Treatment	Length of Neuronal Treatment (hrs)	Label in Figure 20
Untreated	24hrs	Untreated	48hrs	Control
Untreated	24hrs	RAP310	48hrs	RAP310
S100B	24hrs	Untreated (S100B added with media change)	48hrs	S100B
S100B	24hrs	RAP310 (S100Badded with media change)	48hrs	S100B & RAP310
Untreated	48hrs	Untreated	48hrs	Control
Untreated	48hrs	RAP310	48hrs	RAP310
S100B	48hrs	Untreated (S100Badded with media change)	48hrs	S100B
S100B	48hrs	RAP310 (S100Badded with media change)	48hrs	S100B & RAP310

Table 2: Experimental Setup for Figure 20

(Green rows) Microglia treated with activating agent, S100B, for 24 hrs prior to addition to neuronal cultures. NeuO labeled-neuron cultures were or weren't treated at time of media change with microglia-conditioned media with RAP310. (Red rows) Same as green rows but microglia were treated with activating agent, S100B, for 48 hrs prior to addition to neuronal cultures (with or without RAP310).
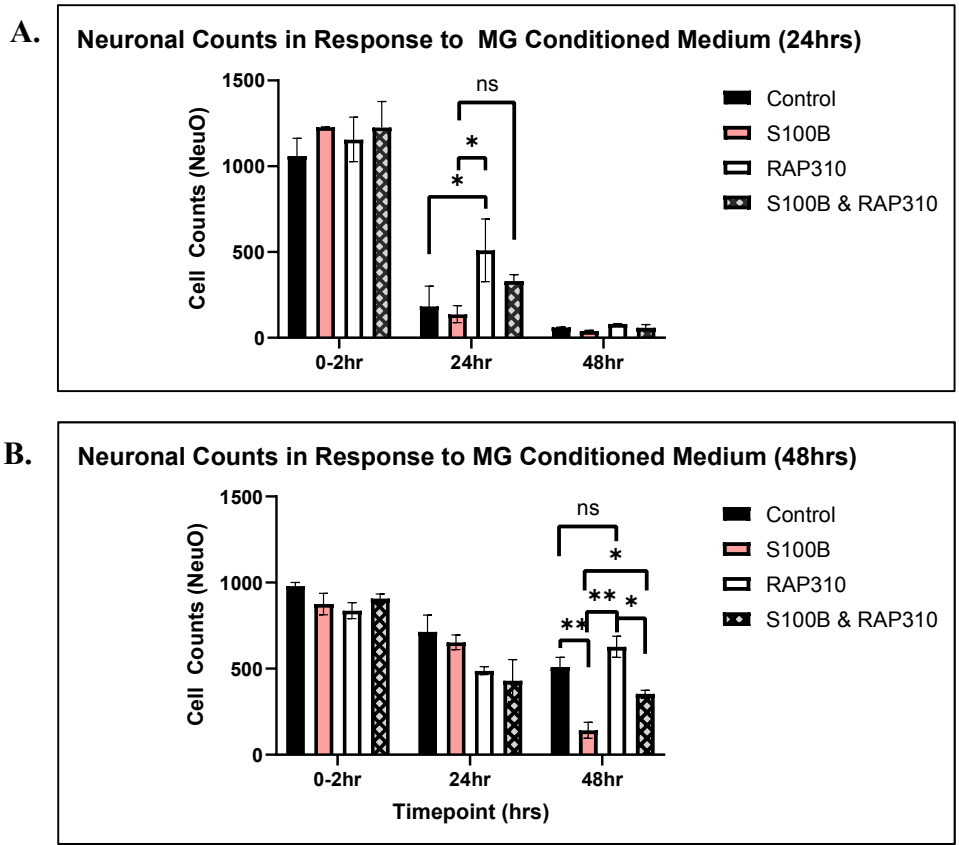
Figure 20: Neuronal Response to Direct Addition of RAPs and S100B or Microglia Conditioned Media + S100B and R103

A) Live imaging over 72 hrs of neuronal cultures labeled with NeuO and treated with microglia conditioned media where the microglia were incubated with nothing, S100B, RAP310, or S100B and RAP310 for 24 hrs (A), and 48 hrs (B). Error bars indicated 1 standard deviation. * indicates $p < 0.05$, ** indicates $p < 0.005$ Comparison between treatments at same timepoint for A & B were non-significantly different. Non-significant differences between treatments at each timepoint not shown for A-B. Experiment conducted in triplicate.

Neurons were plated on 24-well glass-bottom dishes coated with PDL. Microglia were separately plated in LGDMEM in T-25 flasks with or without RAPs as a pre-treatment. Microglia were then converted to HN+ media from LGDMEM/ 10% FBS/1% PenStrep 1 ng/mL GM-CSF over 5 days. Neurons were labeled with NeuO on DIV 5 and 6 and imaged as a baseline for cell counts following the second labeling on DIV 6 (0 hrs on Figure 21 B). 2 hrs after NeuO labeling of neurons, microglia were added in co-culture and allowed to settle for 24 hrs. At 6 DIV co-cultures were treated with activating agents and/or RAPs as a co-treatment. Images were taken again at 24 and 48 hrs, followed with fixation and immunostaining. There was no difference between groups of S100B treated neurons with or without RAP pre- or co-treatment. Some wells were treated with the known neurotoxic dimer/trimer species of Aβ as a positive control; however, these cultures behaved comparable to the control and S100B-treated cultures with regard to viable neuronal counts.
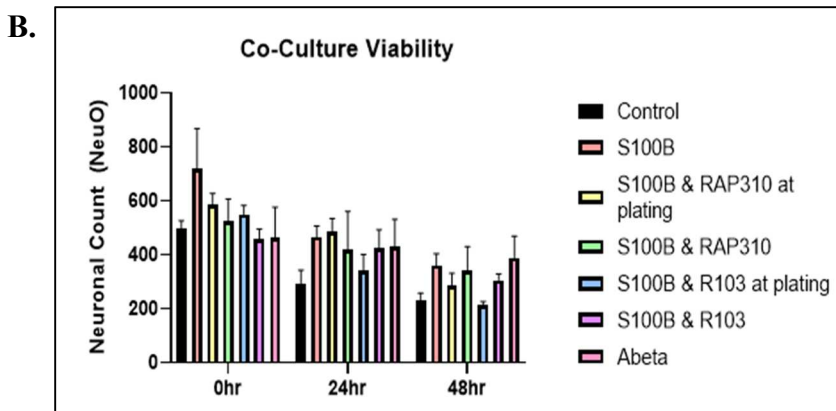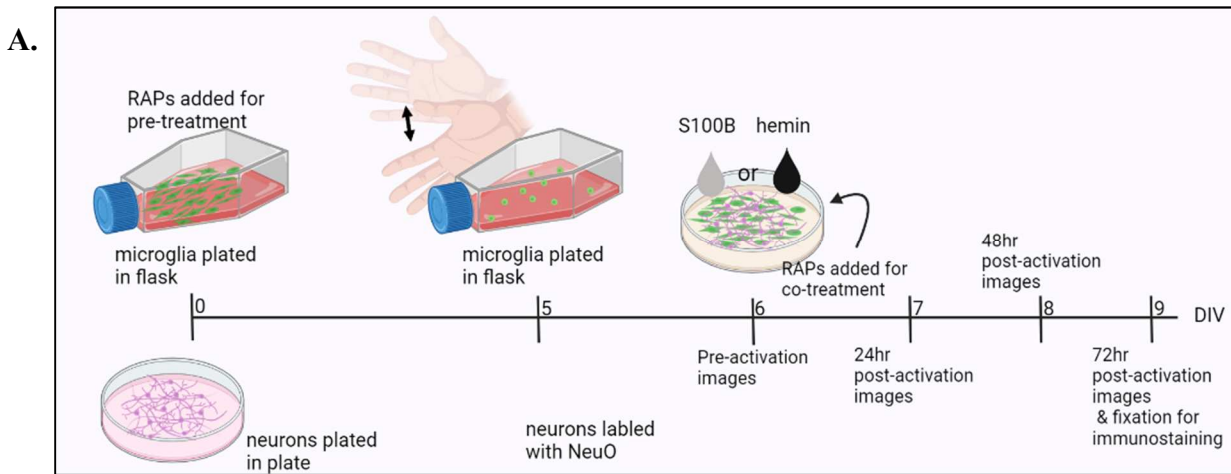
Figure 21: Co-culture Response to S100B and Pre-treatment or Co-Treatment with RAPs

A) Experimental timeline for co-culturing of microglia and neurons. RAPs are added either to the microglia at time of plating or to the neurons with the treatment of microglia conditioned media on 6 DIV. Neurons are labeled with NeuO on 5 DIV, and 6 DIV immediately before the treatment with conditioned media and/or RAPs. B)Neuronal counts determined by NeuO labeling of neurons and treatment with/without S100B and RAP310 or R103 as a pre-treatment or co-treatment followed for 48 hrs. Error bars represent 1 standard deviation. No significant difference between groups. Experiment conducted in triplicate. Graphic created by BioRender.

Discussion

Although our laboratory has extensive experience in neuronal culture, microglia culture was not previously performed. We utilized a modified version of a published method to harvest and culture primary microglia from mouse pups. We further established a method for making frozen stocks of these cells which could be used for up to 6 months and thus supplied the cells for the majority of work contained in this thesis. Conditions for culturing were shown to be versatile, as microglia can adhere, proliferate, and maintain a resting state as determined by morphology when plated on glass, glass coated with PDL, tissue culture plastic, and tissue culture plastic coated with PDL. Microglia did not grow well on Matrigel. To stimulate proliferation in culture, GM-CSF was added (Bhattacharya et a., 2015) and we explored the potential cytotoxicity as well as the minimal concentration needed for this cytokine. There was no significant difference on culture growth or microglial viability between 1 and 50 ng/ml of GM-CSF, although there was a trend toward poorer survival at the highest level (50 ng/ml) (Figure 4 B & C). For this reason, the lowest concentration tested, 1ng/mL, was chosen for future assays.

Like many proliferative, mitotic cells, microglia require serum in medium especially at time of plating. However, rodent neuronal cultures are generally performed in the absence of serum or with very low (e.g. 2%) FBS whereas microglia prefer growth in 10% FBS. Thus, finding a method that allowed us to culture microglia in which the medium could be transferred directly to neurons to deduce effects of cytokine and chemokine secretion was a major goal of our initial research. Our primary microglia cultures demonstrated remarkable ability to retain viability in the several medium types tested (Figure 5 D). Studies requiring microglia-conditioned media were limited to 24 and 48hrs for microglia conditioning to combat the effects

87

on viability seen in Figure 5 D. We did not test whether use of 2% serum will prolong microglia

viability as well as support neuronal health, but this is something that should be pursued since

microglial responses to activation factors might be declining during the first 24 hrs in serum-free

medium.

The media fractionation protocol outlined here is a relatively quick, and effective way to

remove specific agents below a certain molecular weight threshold. With modifications after

fractionation to the osmolarity and insulin concentrations (Figure 6 A & 10), minimal reductions

are observed in viability when this medium is reconstituted and applied to neurons in culture.

Although methods such as buffer exchange, dialysis, chelating columns, etc. could be another

avenue to purify samples or remove iron-centered proteins from solution, the associated time

investments for each were too extensive to explore here. Additionally, the desire to maintain a

1:1 well to well transfer between microglia and neurons limited the volumes for which we

wanted to fractionate to 1 mL. Such a low volume is not feasible for many fractionation methods.

Other commercially available desalting columns did not offer molecular weight cut offs in the

desired range for our sample volumes.

Although we have successfully established a method for hemin removal from the

microglia-conditioned medium and medium reconstitution in a manner that is viable for neuronal

survival, along the way we also discovered that hemin addition directly to neurons is not toxic.

Promising preliminary data (Figure 8 G) suggests that the effect of hemin on neurons might be

mostly microglia mediated. Hemin is produced in vivo during traumatic brain injury or

intracerebral brain hemorrhaging and tagged-hemin release/uptake profiles (Chen-Roetling et al.,

2014) suggest that neurons, while expressing the correct receptors for hemin uptake, may not do

so (Robinson et al., 2009). This may be why we saw very little cell-death with hemin directly

applied to neurons, as they do not have the means to produce the ROS necessary to mediate cytotoxicity. The mechanism for hemin uptake by microglia remains largely unknown. It has been suggested that serum albumin may complex with hemin to prevent its uptake by neurons or astrocytes, however this was not directly tested by our experiments (Robinson et al., 2009).

Although the results presented here suggest that this fractionation method could be applied to removal of low molecular weight medium components from microglia conditioned medium, a desire to be able to skip the fractionation procedure has changed our focus.

We tested the ability of our selected microglia-activating agents to stimulate proliferation and alter morphology in vitro associated with activated microglia. We determined 100 μM hemin and 2 μg/mL S100B to be suitable working concentrations for microglia activation in cell culture (Figure 13 & Figure 15 A).

To determine if hemin itself influenced neuronal viability or rod formation, we performed direct addition of hemin to neurons (Figure 13). In addition, we also tested for direct neurotoxicity with one well established potent microglia activator of higher molecular mass (14.5 kDa), S100B (alarmin), which would not be removed by the spin column method. Direct addition of hemin appeared to induce a dose-dependent decline in neuronal survival as determined from neurofilament positive immunolabeled cultures. However, there was no observed blebbing, discontinuous staining, or other indications of neuronal toxicity and death in the cultures treated directly with hemin (Figure 13). Furthermore, some variability in response to hemin can be attributed to the difficulty in solubilizing and adjusting the pH of hemin solutions and thus results in different neuronal responses to different preparations. Since some direct addition of 100 μM hemin to neurons gave no decrease in survival, we feel that hemin is non-toxic to neurons at this concentration. Thus, we felt confident that we can treat co-cultures of

89

neurons and microglia with hemin and toxic effects will most likely be from microglia produced factors.

S100B demonstrated an ability to adequately activate microglia to a proliferative state, and minimal neurotoxicity when applied to neuronal cultures (Figure 15). Given these data, we continued with S100B as a less toxic and physiologically relevant microglia-activating agent in our co-culturing assays. Although it did not yield the same increase in proliferation of microglia that was observed with hemin, there was a noticeable morphological change in brightfield images of S100B-treated microglia consistent with literature identification of M1 activation.

We aimed to determine the effects of RAPs on neuronal cultures treated with microglia-secreted factors. Rather than relying on the fractionation method for isolating the effect of these secreted factors, we sought to more co-culture microglia with neurons as a means for directly facilitating this interaction. Immunolabeling revealed the existence in generous quantities the X4 and R5 receptors on our microglia, indicating that treating the microglia with the RAPs prior or following activation may be a feasible route for neuroinflammation intervention.

Our co-culturing assays depend upon the use of NeuO, when observing the effect of known poison and mitochondrial ATPase inhibitor, sodium azide, on our neurons we saw a decrease in fluoescence of dying cells primarily in the first 24hrs. The ability of dying neurons to retain NeuO labeling may present a source for unexplainably high neuronal cell counts when compared to alternative methods for quantifying cell death such as immunolabeling for a neuron-specific marker such as NFH. However, we feel that given these data the NeuO viable neurons counts are fairly accurate to actual cell numbers.

When following neuronal cultures with NeuO that were treated with hemin-activated microglia-conditioned media over 48 hrs, there seemed to be little effect of hemin overall on cell viability. The mild effect seen with media that was conditioned by microglia for 24 hrs may have been due to the inability of the microglia to produce cytokines and chemokines in such a quantity as to elicit an effect in the neuronal cultures. Therefore, any effect of the RAPs protective against cell death would be unobservable. Optimal response for induced cell death/reduction in viability was observed with media conditioned by microglia treated with hemin for 48 hrs. Likely, this was ample time to produce signaling molecules in high enough amounts to be effective on neurons when applied to cultures. However, previous results indicated that microglia begin to die in HN+ medium past 24 hrs, driving us to consider co-cultures as a future direction. Although Figure 11 demonstrates microglia can be activated after 24 hrs hemin exposure, the cells may have not been able to secrete *in vitro* relevant amounts until the 48 hrs mark. Alternatively, the mild effect seen with the 72 hrs microglia conditioned media group may have been exposed to hemin for too long. These cells may have experience activation, and secretion by 48 hrs then when hemin levels lowered, and the microglia had proliferated in response to stimulation the relative activator concentrations were too low to sustain prolonged activation and the glia likely returned to a more quiescent state prior to addition to the neuronal cultures.

When applied to microglia for 48 hrs, S100B conditioned media caused significant neuronal death after just 48 hrs, an effect which was mitigated by the introduction of RAP310. We are led to believe that perhaps RAP310 has a protective effect on neurons which was demonstrated with the more toxic activator, S100B. This finding in conjunction with the data presented in Figure 15, pinpoint the microglia-neuronal signaling axis as a target for RAPs because S100B had no significant effect on either cell type when monocultured. The results for

24 hrs neuronal treatment with conditioned medium from S100B treated microglia demonstrated catastrophic cell death. We believe these data more reflect experimental set up errors than cellular responses. It is possible that these cells were poorly incubated with the stage adapter during live imaging, resulting in them cooling and dying. Replicates of these experiment are required to determine the effect of RAPs on neurons treated with S100B conditioned medium.

Co-cultures of neurons and microglia present a means to test the effects of RAPs where microglia secreted factors would be more locally concentrated on neurons and any proximal cell mediated signaling would be intact. Our aspirations for this assay are high, although our first round of testing shown in Figure 21 showed a lack of any effect of either the S100B conditioned medium or the RAPs. This assay warrants replicates to attempt to determine these effects in a more stream-lined manner than separate culturing methods. Rod indexes may determine if co-culturing is a more suitable system for testing RAPs protective effects against rod formation in microglia.

Future directions for this work include replicating and recapitulating much of the work here. S100B presents a more robust activating agent than hemin and will likely be the focus of future work. We aim to determine if microglia could live past 24 hrs in HN+ with 2% serum to better test the timeline and secretion effects on neuronal cultures with longer microglia-activating agent incubation periods. Additionally, our lab possesses knockout mouse lines of the NOX subunit, p47. Previous work has identified NOX activity as essential to cofilin:actin rod formation, so we seek to determine if it is important in any elicited effects of the RAPs in this microglia-neuron system.

REFERENCES

Alhadidi, Q., & Shah, Z. A. (2018). Cofilin Mediates LPS-Induced Microglial Cell Activation and Associated Neurotoxicity Through Activation of NF-κB and JAK–STAT Pathway. Molecular Neurobiology, 55(2), 1676–1691. https://doi.org/10.1007/s12035-017-0432-7

Alkhatib, G. (2009). The biology of CCR5 and CXCR4. In Current Opinion in HIV and AIDS (Vol. 4, Issue 2, pp. 96–103). https://doi.org/10.1097/COH.0b013e328324bbec

Alliot, F., Godin, I., Pessac, B., & Francé, F. (n.d.). Microglia derive from progenitors, originating from the yolk sac, and which proliferate in the brain. In Developmental Brain Research (Vol. 117). www.elsevier.comrlocaterbres

Alsegiani, A. S., & Shah, Z. A. (2020). The role of cofilin in age-related neuroinflammation. Neural Regeneration Research, 15(8), 1451–1459. https://doi.org/10.4103/1673-5374.274330

Andrianantoandro, E., & Pollard, T. D. (2006). Mechanism of Actin Filament Turnover by Severing and Nucleation at Different Concentrations of ADF/Cofilin. Molecular Cell, 24(1), 13–23. https://doi.org/10.1016/j.molcel.2006.08.006

Bachstetter, A. D., Morganti, J. M., Jernberg, J., Schlunk, A., Mitchell, S. H., Brewster, K. W., Hudson, C. E., Cole, M. J., Harrison, J. K., Bickford, P. C., & Gemma, C. (2011). Fractalkine and CX 3CR1 regulate hippocampal neurogenesis in adult and aged rats. Neurobiology of Aging, 32(11), 2030–2044. https://doi.org/10.1016/j.neurobiolaging.2009.11.022

Balcer, H. I., Goodman, A. L., Rodal, A. A., Smith, E., Kugler, J., Heuser, J. E., & Goode, B. L. (2003). Coordinated Regulation of Actin Filament Turnover by a High-Molecular-Weight Srv2/CAP Complex, Cofilin, Profilin, and Aip1. Current Biology, 13(24), 2159–2169. https://doi.org/10.1016/j.cub.2003.11.051

Bamburg, J., Bernstein, B., Davis, R., Flynn, K., Goldsbury, C., Jensen, J., Maloney, M., Marsden, I., Minamide, L., Pak, C., Shaw, A., Whiteman, I., Wiggan, O., Author, C., Bamburg, J. R., & Alzheimer Res, C. (2010). ADF/cofilin-actin rods in neurodegenerative diseases. In Curr Alzheimer Res (Vol. 7, Issue 3).

Bamburg, J. R., & Bernstein, B. W. (2016). Actin dynamics and cofilin-actin rods in Alzheimer disease. In Cytoskeleton (Vol. 73, Issue 9, pp. 477–497). John Wiley and Sons Inc. https://doi.org/10.1002/cm.21282

Bamburg, J. R., Minamide, L. S., Wiggan, O., Tahtamouni, L. H., & Kuhn, T. B. (2021). Cofilin and actin dynamics: Multiple modes of regulation and their impacts in neuronal development and degeneration. In Cells (Vol. 10, Issue 10). MDPI. https://doi.org/10.3390/cells10102726

Bernier, L. P., Bohlen, C. J., York, E. M., Choi, H. B., Kamyabi, A., Dissing-Olesen, L., Hefendehl, J. K., Collins, H. Y., Stevens, B., Barres, B. A., & MacVicar, B. A. (2019). Nanoscale Surveillance of the Brain by Microglia via cAMP-Regulated Filopodia. Cell Reports, 27(10), 2895-2908.e4. https://doi.org/10.1016/j.celrep.2019.05.010

Bernstein, B. W., & Bamburg, J. R. (2002). Actin-ATP Hydrolysis Is a Major Energy Drain for Neurons.

Bernstein, B. W., Chen, H., Boyle, J. A., Bamburg, J. R., & Bernstein, B. W. (2006). Formation of actin-ADF/cofilin rods transiently retards decline of mitochondrial potential and ATP in stressed neurons. Am J Physiol Cell Physiol, 291, 828–839. https://doi.org/10.1152/ajpcell.00066.2006.-When

Bhattacharya, P., Thiruppathi, M., Elshabrawy, H. A., Alharshawi, K., Kumar, P., & Prabhakar, B. S. (2015). GM-CSF: An immune modulatory cytokine that can suppress autoimmunity. Cytokine, 75(2). https://doi.org/10.1016/j.cyto.2015.05.030

Block, M. L., Zecca, L., & Hong, J. S. (2007). Microglia-mediated neurotoxicity: Uncovering the molecular mechanisms. In Nature Reviews Neuroscience (Vol. 8, Issue 1, pp. 57–69). https://doi.org/10.1038/nrn2038

Boche, D., Perry, V. H., & Nicoll, J. A. R. (2013). Review: Activation patterns of microglia and their identification in the human brain. In Neuropathology and Applied Neurobiology (Vol. 39, Issue 1, pp. 3–18). https://doi.org/10.1111/nan.12011

Bohlen, C. J., Bennett, F. C., Tucker, A. F., Collins, H. Y., Mulinyawe, S. B., & Barres, B. A. (2017). Diverse Requirements for Microglial Survival, Specification, and Function Revealed by Defined-Medium Cultures. Neuron, 94(4), 759-773.e8. https://doi.org/10.1016/j.neuron.2017.04.043

Bolós, M., Llorens-Martín, M., Perea, J. R., Jurado-Arjona, J., Rábano, A., Hernández, F., & Avila, J. (2017). Absence of CX3CR1 impairs the internalization of Tau by microglia. Molecular Neurodegeneration, 12(1). https://doi.org/10.1186/s13024-017-0200-1

Bongarzone, S., Savickas V., Luzi F., Gee A., (2017). Targeting the Receptor for Advanced Glycation Endproducts (RAGE): A Medicinal Chemistry. Journal of Medicinal Chemistry, 60(17), 7213-7232. https://doi.org/ 10.1021/acs.jmedchem.7b00058

Bonham, L. W., Karch, C. M., Fan, C. C., Tan, C., Geier, E. G., Wang, Y., Wen, N., Broce, I. J., Li, Y., Barkovich, M. J., Ferrari, R., Hardy, J., Momeni, P., Höglinger, G., Müller, U., Hess, C. P., Sugrue, L. P., Dillon, W. P., Schellenberg, G. D., … Singleton, A. B. (2018). CXCR4 involvement in neurodegenerative diseases. Translational Psychiatry, 8(1). https://doi.org/10.1038/s41398-017-0049-7

Boutajangout, A., & Wisniewski, T. (2013). The innate immune system in Alzheimer's disease. In International Journal of Cell Biology. https://doi.org/10.1155/2013/576383

Brody, A. H., & Strittmatter, S. M. (2018). Synaptotoxic Signaling by Amyloid Beta Oligomers in Alzheimer's Disease Through Prion Protein and mGluR5. In Advances in

Pharmacology (Vol. 82, pp. 293–323). Academic Press Inc. https://doi.org/10.1016/bs.apha.2017.09.007

Chamera, K., Trojan, E., Szuster-Głuszczak, M., & Basta-Kaim, A. (2019). The Potential Role of Dysfunctions in Neuron-Microglia Communication in the Pathogenesis of Brain Disorders. Current Neuropharmacology, 18(5), 408–430. https://doi.org/10.2174/1570159x17666191113101629

Chan, C., Beltzner, C. C., & Pollard, T. D. (2009). Cofilin Dissociates Arp2/3 Complex and Branches from Actin Filaments. Current Biology, 19(7), 537–545. https://doi.org/10.1016/j.cub.2009.02.060

Chen-Roetling, J., Cai, Y., Lu, X., & Regan, R. F. (2014). Hemin uptake and release by neurons and glia. Free Radical Research, 48(2), 200–205. https://doi.org/10.3109/10715762.2013.859386

Chhor, V., le Charpentier, T., Lebon, S., Oré, M. V., Celador, I. L., Josserand, J., Degos, V., Jacotot, E., Hagberg, H., Sävman, K., Mallard, C., Gressens, P., & Fleiss, B. (2013). Characterization of phenotype markers and neuronotoxic potential of polarised primary microglia In vitro. Brain, Behavior, and Immunity, 32, 70–85. https://doi.org/10.1016/j.bbi.2013.02.005

Chinta S., Anderson J. Dopaminergic neurons. (2005). International Journal of Biochemistry and Cell Biology, 37 (5), 945-946.

Cichon, J., Sun, C., Chen, B., Jiang, M., Chen, X. A., Sun, Y., Wang, Y., & Chen, G. (2012). Cofilin aggregation blocks intracellular trafficking and induces synaptic loss in hippocampal neurons. Journal of Biological Chemistry, 287(6), 3919–3929. https://doi.org/10.1074/jbc.M111.301911

Davies, D. S., Ma, J., Jegathees, T., & Goldsbury, C. (2017). Microglia show altered morphology and reduced arborization in human brain during aging and Alzheimer's disease. Brain Pathology, 27(6), 795–808. https://doi.org/10.1111/bpa.12456

Donato R., Heizmann C. (2010). S100B Protein in the Nervous System and Cardiovascular Apparatus in Normal and Pathological Conditions. Cardiovascular Psychiatry and Neurology. https://doi.org/10.1155/2010/929712

Ferreira, D. G., Temido-Ferreira, M., Miranda, H. V., Batalha, V. L., Coelho, J. E., Szegö, É. M., Marques-Morgado, I., Vaz, S. H., Rhee, J. S., Schmitz, M., Zerr, I., Lopes, L. v., & Outeiro, T. F. (2017). α-synuclein interacts with PrPC to induce cognitive impairment through mGluR5 and NMDAR2B. Nature Neuroscience, 20(11), 1569–1579. https://doi.org/10.1038/nn.4648

Filipello, F., Morini, R., Corradini, I., Zerbi, V., Canzi, A., Michalski, B., Erreni, M., Markicevic, M., Starvaggi-Cucuzza, C., Otero, K., Piccio, L., Cignarella, F., Perrucci, F., Tamborini, M., Genua, M., Rajendran, L., Menna, E., Vetrano, S., Fahnestock, M., … Matteoli, M. (2018). The Microglial Innate Immune Receptor TREM2 Is Required for Synapse Elimination and Normal Brain Connectivity. Immunity, 48(5), 979-991.e8. https://doi.org/10.1016/j.immuni.2018.04.016

Galkin V., Orlova A., Lukoyanova N., Wriggers W., Egelmen E. (2001). Actin Depolymerizing Factor Stabilizes and Existing State of F-Actin and Can Change the Tilt of F-Actin Subunits. Journal of Cell Biology. 153(1), 75-86.

Ginhoux, F., Greter, M., Leboeuf, M., Nandi, S., See, P., Gokhan, S., Mehler, M., Conway, S. J., Guan Ng, L., Stanley, R., Samokhvalov, I., & Merad, M. (2010). Fate Mapping Analysis Reveals That Adult Microglia Derive From Primitive Macrophages. Science, 330(6005), 841–845. https://doi.org/10.1126/science.1194554

Gireud, M., Sirisaengtaksin, N., & Bean, A. J. (2014). Molecular Mechanisms of Neurological Disease. In From Molecules to Networks: An Introduction to Cellular and Molecular Neuroscience: Third Edition (pp. 639–661). Elsevier Inc. https://doi.org/10.1016/B978-0-12-397179-1.00021-X

Gohla A., Bokoch G., (2002). 4-3-3 Regulates Actin Dynamics by Stabilizing Phosphorylated Cofilin. Current Biology 12, 1704-1710.

Goshi, N., Morgan, R., Lein, P., Seker, E. (2020) A primary neural cell culture model to study neuron, astrocyte, and microglai interactions in neuroinflammation. Journal of Neuroinflammation 17(155). https://doi.org/10.1186/s12974-020-01819-z

Gu J., Lee C., Fan Y., Komlos D., Tang X., Sun C., Yu K., Hartzell C., Chen G., Bamburg J. (2010). ADF/cofilin-mediated actin dynamics regulate AMPA receptor trafficking during synaptic plasticity. Nature Neuroscience 13(10), 1208-1216. https://doi.org/10.1038/nn.2634.

Guerreiro, R., Wojtas, A., Bras, J., Carrasquillo, M., Rogaeva, E., Majounie, E., Cruchaga, C., Sassi, C., Kauwe, J. S. K., Younkin, S., Hazrati, L., Collinge, J., Pocock, J., Lashley, T., Williams, J., Lambert, J.-C., Amouyel, P., Goate, A., Rademakers, R., … Hardy, J. (2013). TREM2 Variants in Alzheimer's Disease . New England Journal of Medicine, 368(2), 117–127. https://doi.org/10.1056/nejmoa1211851

Guttenplan, K., Liddelow, S. (2019) Astrocytes and microglia: Models and tools. Journal of Experimental Medicine 216(1), 71-83. https://doi.org/10.1084/jem.20180200

Haigh, C. L., Edwards, K., & Brown, D. R. (2005). Copper binding is the governing determinant of prion protein turnover. Molecular and Cellular Neuroscience, 30(2), 186–196. https://doi.org/10.1016/j.mcn.2005.07.001

Hanafy, K. A. (2013). The role of microglia and the TLR4 pathway in neuronal apoptosis and vasospasm after subarachnoid hemorrhage. Journal of Neuroinflammation, 10. https://doi.org/10.1186/1742-2094-10-83

Hayakata, T., Shiozaki, T., Tasaki, O., Ikegawa, H., Inoue, Y., Toshiyuki, F., Hosotubo, H., Kieko, F., Yamashita, T., Tanaka, H., Shimazu, T., & Sugimoto, H. (2004). Changes in CSF S100B and cytokine concentrations in early-phase severe traumatic brain injury. Shock, 22(2), 102–107. https://doi.org/10.1097/01.shk.0000131193.80038.fl

Heizmann C., Schafer B., Fritz G. (2003). The Family of S100 Cell Signaling Proteins. Handbook of Cell Signaling (2), 83-93.

Heneka, M. T., Kummer, M. P., Stutz, A., Delekate, A., Schwartz, S., Vieira-Saecker, A., Griep, A., Axt, D., Remus, A., Tzeng, T. C., Gelpi, E., Halle, A., Korte, M., Latz, E., & Golenbock, D. T. (2013). NLRP3 is activated in Alzheimer's disease and contributes to pathology in APP/PS1 mice. Nature, 493(7434), 674–678. https://doi.org/10.1038/nature11729

Kabadi, S. v., Stoica, B. A., Zimmer, D. B., Afanador, L., Duffy, K. B., Loane, D. J., & Faden, A. I. (2015). S100B inhibition reduces behavioral and pathologic changes in experimental traumatic brain injury. Journal of Cerebral Blood Flow and Metabolism, 35(12), 2010–2020. https://doi.org/10.1038/jcbfm.2015.165

Kang, D. E., & Woo, J. A. (2019). Cofilin, a Master Node Regulating Cytoskeletal Pathogenesis in Alzheimer's Disease. In Journal of Alzheimer's Disease (Vol. 72, Issue s1, pp. S131–S144). IOS Press. https://doi.org/10.3233/JAD-190585

Laudati, E., Currò, D., Navarra, P., & Lisi, L. (2017). Blockade of CCR5 receptor prevents M2 microglia phenotype in a microglia-glioma paradigm. Neurochemistry International, 108, 100–108. https://doi.org/10.1016/j.neuint.2017.03.002

Lee, C. Y. D., & Landreth, G. E. (2010). The role of microglia in amyloid clearance from the AD brain. In Journal of Neural Transmission (Vol. 117, Issue 8, pp. 949–960). https://doi.org/10.1007/s00702-010-0433-4

Lian, H., Roy, E., & Zheng, H. (2016). Protocol for Primary Microglial Culture Preparation. BIO-PROTOCOL, 6(21). https://doi.org/10.21769/bioprotoc.1989

Liu, C., Cui, G., Zhu, M., Kang, X., & Guo, H. (2014). neuroinflammation in Alzheimer's disease chemokines produced by astrocytes and chemokine receptors (Liu). International Journal of Clinical Experimental Pathology, 7(12), 8342–8355.

López-Coral A, Striz AC, Tuma PL. A Serine/Threonine Kinase 16-Based Phospho-Proteomics Screen Identifies WD Repeat Protein-1 As A Regulator Of Constitutive Secretion. Sci Rep. 2018 Aug 29;8(1):13049. doi: 10.1038/s41598-018-31426-1.

Maloney, M. T., & Bamburg, J. R. (2007). Cofilin-Mediated Neurodegeneration in Alzheimer's Disease and Other Amyloidopathies. Molecular Neurobiology, 21.

Marinelli, S., Basilico, B., Marrone, M. C., & Ragozzino, D. (2019). Microglia-neuron crosstalk: Signaling mechanism and control of synaptic transmission. In Seminars in Cell and Developmental Biology (Vol. 94, pp. 138–151). Elsevier Ltd. https://doi.org/10.1016/j.semcdb.2019.05.017

Mcgeer, P. L., Itagaki, S., Tago, H., & Mcgeer, E. G. (n.d.). Reactive microglia in patients with senile dementia of the Alzheimer type are positive for the histocompatibility glycoprotein HLA-DR. In Neuroscience Letters (Vol. 79).

McGough A., Pope B., Chiu W., Weeds A., McLean M. (1997). Cofilin Changers the Twist of F-Actin: Implications for Actin Filament Dyanmics and Cellular Function. Journal of Cell Biology 138(4), 771-781.

Mi, J., Shaw, A. E., Pak, C. W., Walsh, K. P., Minamide, L. S., Bernstein, B. W., Kuhn, T. B., & Bamburg, J. R. (2013). A genetically encoded reporter for real-time imaging of cofilin-

actin rods in living neurons. PLoS ONE, 8(12). https://doi.org/10.1371/journal.pone.0083609

Minamide, L. S., Striegl, A. M., Boyle, J. A., Meberg, P. J., & Bamburg, J. R. (2000). Neurodegenerative stimuli induce persistent ADF/cofilin-actin rods that disrupt distal neurite function. In NATURE CELL BIOLOGY (Vol. 2). http://cellbio.nature.com628

Mosman T. (1983) Rapid Colorimetric Assay for Cellular Growth and Survival: Application to Proliferation and Cytotoxicity Assays. Journal of Immunological Methods 65, 55-63.

Mu, Y., & Gage, F. H. (2011). Adult hippocampal neurogenesis and its role in Alzheimer's disease. In Molecular Neurodegeneration (Vol. 6, Issue 1). https://doi.org/10.1186/1750-1326-6-85

Munsie, L., Caron, N., Atwal, R. S., Marsden, I., Wild, E. J., Bamburg, J. R., Tabrizi, S. J., & Truant, R. (2011). Mutant huntingtin causes defective actin remodeling during stress: Defining a new role for transglutaminase 2 in neurodegenerative disease. Human Molecular Genetics, 20(10), 1937–1951. https://doi.org/10.1093/hmg/ddr075

Nimmerjahn, A., Kirchhoff, F., & Helmchen, F. (2005). Resting Microglial Cells AreHighly Dynamic Surveillantsof Brain Parenchyma in Vivo. Science, 308(5726), 1314–1318. https://doi.org/10.1126/science.1107891

Niwa, R., Nagata-Ohashi, K., Takeichi, M., Mizuno, K., & Uemura, T. (2002). Control of actin reorganization by Slingshot, a family of phosphatases that dephosphorylate ADF/cofilin. In Cell (Vol. 108). Amano.

Oliveira da Silva, M.I., Santejo, M., Babcock, I.W., Magalhaes, A., Minamide, L. S., Castillo, E., Gerhardt, E., Fahlbusch, C., Swanson, R.A., Outerio, T.F., Bamburg, J.R & Liz, M.A. (2021) Cofilin pathology is a new player on α-synuclein-induced spine impairment in models of hippocampal synucleinopathy. bioRxiv https://doi.org/10.1101/2021.02.02425931

Ono, S. (2003). Regulation of Actin Filament Dynamics by Actin Depolymerizing Factor/Cofilin and Actin-Interacting Protein 1: New Blades for Twisted Filaments. In Biochemistry (Vol. 42, Issue 46, pp. 13363–13370). https://doi.org/10.1021/bi034600x

Padi, S. S. V., Shi, X. Q., Zhao, Y. Q., Ruff, M. R., Baichoo, N., Pert, C. B., & Zhang, J. (2012). Attenuation of rodent neuropathic pain by an orally active peptide, RAP-103, which potently blocks CCR2- and CCR5-mediated monocyte chemotaxis and inflammation. Pain, 153(1), 95–106. https://doi.org/10.1016/j.pain.2011.09.022

Paolicelli, R. C., Bolasco, G., Pagani, F., Maggi, L., Scianni, M., Panzanelli, P., Giustetto, M., Ferreira, T. A., Guiducci, E., Dumas, L., Ragozzino, D., & Gross, C. T. (2011). Synaptic pruning by microglia is necessary for normal brain development. Science, 333(6048), 1456–1458. https://doi.org/10.1126/science.1202529

Parhizkar, S., Arzberger, T., Brendel, M., Kleinberger, G., Deussing, M., Focke, C., Nuscher, B., Xiong, M., Ghasemigharagoz, A., Katzmarski, N., Krasemann, S., Lichtenthaler, S. F., Müller, S. A., Colombo, A., Monasor, L. S., Tahirovic, S., Herms, J., Willem, M., Pettkus, N., … Haass, C. (2019). Loss of TREM2 function increases amyloid seeding but

reduces plaque-associated ApoE. Nature Neuroscience, 22(2), 191–204. https://doi.org/10.1038/s41593-018-0296-9

Park, J., Min, J. S., Kim, B., Chae, U. bin, Yun, J. W., Choi, M. S., Kong, I. K., Chang, K. T., & Lee, D. S. (2015). Mitochondrial ROS govern the LPS-induced pro-inflammatory response in microglia cells by regulating MAPK and NF-κB pathways. Neuroscience Letters, 584, 191–196. https://doi.org/10.1016/j.neulet.2014.10.016

Rahman, T., Davies, D. S., Tannenberg, R. K., Fok, S., Shepherd, C., Dodd, P. R., Cullen, K. M., & Goldsbury, C. (2014). Cofilin rods and aggregates concur with tau pathology and the development of alzheimer's disease. Journal of Alzheimer's Disease, 42(4), 1443–1460. https://doi.org/10.3233/JAD-140393

Ransohoff, R. M. (2016). A polarizing question: Do M1 and M2 microglia exist. In Nature Neuroscience (Vol. 19, Issue 8, pp. 987–991). Nature Publishing Group. https://doi.org/10.1038/nn.4338

Robinson, S. R., Dang, T. N., Dringen, R., & Bishop, G. M. (2009). Hemin toxicity: A preventable source of brain damage following hemorrhagic stroke. In Redox Report (Vol. 14, Issue 6, pp. 228–235). https://doi.org/10.1179/135100009X12525712409931

Roqué, P., Costa, L. (2017). Co-Culture of Neurons and Microglia. Current Protocols in Toxicology 74(1). doi:10.1002/cptx.32

Rosi, S., Pert, C. B., Ruff, M. R., McGann-Gramling, K., & Wenk, G. L. (2005). Chemokine receptor 5 antagonist D-Ala-peptide T-amide reduces microglia and astrocyte activation within the hippocampus in a neuroinflammatory rat model of Alzheimer's disease. Neuroscience, 134(2), 671–676. https://doi.org/10.1016/j.neuroscience.2005.04.029

Ruff, M. R., Polianova, M., Yang, Q.-E., Leoung, G. S., Ruscetti, F. W., & Pert, C. B. (2003). Update on D-Ala-Peptide T-Amide (DAPTA): A Viral Entry Inhibitor that Blocks CCR5 Chemokine Receptors.

Rust, M. B., Gurniak, C. B., Renner, M., Vara, H., Morando, L., Görlich, A., Sassoè-Pognetto, M., Banchaabouchi, M. al, Giustetto, M., Triller, A., Choquet, D., & Witke, W. (2010). Learning, AMPA receptor mobility and synaptic plasticity depend on n-cofilin-mediated actin dynamics. EMBO Journal, 29(11), 1889–1902. https://doi.org/10.1038/emboj.2010.72

Sayeed, M. S. bin, Alhadidi, Q., & Shah, Z. A. (2017). Cofilin signaling in hemin-induced microglial activation and inflammation. Journal of Neuroimmunology, 313, 46–55. https://doi.org/10.1016/j.jneuroim.2017.10.007

Schlachetzki, J. C. M., & Hüll, M. (2009). Microglial Activation in Alzheimer's Disease. In Current Alzheimer Research (Vol. 6).

Schmitz M., Lullmann K., Zafar S., Ebert E., Wohlhage M., Oikonomou P., Schlomm M., Mitrova E., Beekes M., Zerr I. (2014). Association of prion protein genotype and scrapie prion protein type with cellular prion protein charge isoform profile sin cerebrospinal fluid of humans with sporadic or familial prion diseases. Neurobiology of Aging 35(5),

1177-1188. http://dx.doi.org/10.1016/j.neurobiolaging.2013.11.010Neurobiology of Aging 35 (2014) 1177e1188

Sellner, S., Paricio-Montesinos, R., Spieß, A., Masuch, A., Erny, D., Harsan, L. A., Elverfeldt, D. v., Schwabenland, M., Biber, K., Staszewski, O., Lira, S., Jung, S., Prinz, M., & Blank, T. (2016). Microglial CX3CR1 promotes adult neurogenesis by inhibiting Sirt 1/p65 signaling independent of CX3CL1. Acta Neuropathologica Communications, 4(1). https://doi.org/10.1186/s40478-016-0374-8

Shi, Y., & Holtzman, D. M. (2018). Interplay between innate immunity and Alzheimer disease: APOE and TREM2 in the spotlight. In Nature Reviews Immunology (Vol. 18, Issue 12, pp. 759–772). Nature Publishing Group. https://doi.org/10.1038/s41577-018-0051-1

Sierra, A., Encinas, J. M., Deudero, J. J. P., Chancey, J. H., Enikolopov, G., Overstreet-Wadiche, L. S., Tsirka, S. E., & Maletic-Savatic, M. (2010). Microglia shape adult hippocampal neurogenesis through apoptosis-coupled phagocytosis. Cell Stem Cell, 7(4), 483–495. https://doi.org/10.1016/j.stem.2010.08.014

Smith, L. K., Kuhn, T. B., Chen, J., & Bamburg, J. R. (2018). HIV Associated Neurodegenerative Disorders: A New Perspective on the Role of Lipid Rafts in Gp120-Mediated Neurotoxicity. Current HIV Research, 16(4), 258–269. https://doi.org/10.2174/1570162x16666181003144740

Smith LK, Babcock IW, Minamide LS, Shaw AE, Bamburg JR, Kuhn TB. [2021] Direct interaction of HIV gp120 with neuronal CXCR4 and CCR5 receptors induces cofilin-actin rod pathology via a cellular prion protein- and NOX-dependent mechanism. PLoS One. 16(3):e0248309. doi: 10.1371/journal.pone.0248309.

Stansley, B., Post, J., & Hensley, K. (2012). A comparative review of cell culture systems for the study of microglial biology in Alzheimer's disease. http://www.jneuroinflammation.com/content/9/1/115

Stevens, B., Allen, N. J., Vazquez, L. E., Howell, G. R., Christopherson, K. S., Nouri, N., Micheva, K. D., Mehalow, A. K., Huberman, A. D., Stafford, B., Sher, A., Litke, A. M. M., Lambris, J. D., Smith, S. J., John, S. W. M., & Barres, B. A. (2007). The Classical Complement Cascade Mediates CNS Synapse Elimination. Cell, 131(6), 1164–1178. https://doi.org/10.1016/j.cell.2007.10.036

Süß, P., & Schlachetzki, J. C. M. (2020). Microglia in Alzheimer's Disease. In Current Alzheimer Research (Vol. 17).

Tahtamouni, L. H., Shaw, A. E., Hasan, M. H., Yasin, S. R., & Bamburg, J. R. (2013). Non-overlapping activities of ADF and cofilin-1 during the migration of metastatic breast tumor cells. BMC Cell Biology, 14(1). https://doi.org/10.1186/1471-2121-14-45

Tan, Y., Tan, S.-W., Fan, B.-Y., Li, L., & Zhou, Y.-G. (2018). Hemin Induces the Activation of NLRP3 Inflammasome in N9 Microglial Cells. In Iran.J.Immunol (Vol. 15, Issue 2).

Taylor, R. A., & Sansing, L. H. (2013). Microglial responses after ischemic stroke and intracerebral hemorrhage. In Clinical and Developmental Immunology (Vol. 2013). https://doi.org/10.1155/2013/746068

Tremblay, M. È., Stevens, B., Sierra, A., Wake, H., Bessis, A., & Nimmerjahn, A. (2011). The role of microglia in the healthy brain. Journal of Neuroscience, 31(45), 16064–16069. https://doi.org/10.1523/JNEUROSCI.4158-11.2011

van Troys, M., Huyck, L., Leyman, S., Dhaese, S., Vandekerkhove, J., & Ampe, C. (2008). Ins and outs of ADF/cofilin activity and regulation. In European Journal of Cell Biology (Vol. 87, Issues 8–9, pp. 649–667). https://doi.org/10.1016/j.ejcb.2008.04.001

Tudorica V., Balseanu T., Albu V., Bondari S., Bumbea A., Pirscoveanu M. (2017). Tau Protein in Neurodegenerative Diseases – A Review. Rom J Morphol Embryol, 58(4), 1141-1150.

Varnum, M. M., & Ikezu, T. (2012). The classification of microglial activation phenotypes on neurodegeneration and regeneration in alzheimer's disease brain. In Archivum Immunologiae et Therapiae Experimentalis (Vol. 60, Issue 4, pp. 251–266). https://doi.org/10.1007/s00005-012-0181-2

Walsh, K. P., Kuhn, T. B., & Bamburg, J. R. (2014). Cellular prion protein: A co-receptor mediating neuronal cofilin-actin rod formation induced by β-amyloid and proinflammatory cytokines. In Prion (Vol. 8, Issue 6, pp. 375–380). Landes Bioscience. https://doi.org/10.4161/pri.35504

Walsh, K. P., Minamide, L. S., Kane, S. J., Shaw, A. E., Brown, D. R., Pulford, B., Zabel, M. D., Lambeth, J. D., Kuhn, T. B., & Bamburg, J. R. (2014). Amyloid-β and proinflammatory cytokines utilize a prion protein-dependent pathway to activate NADPH oxidase and induce cofilin-actin rods in hippocampal neurons. PLoS ONE, 9(4). https://doi.org/10.1371/journal.pone.0095995

Wang, M., Ye, X., Hu, J., Zhao, Q., Lv, B., Ma, W., Wang, W., Yin, H., Hao, Q., Zhou, C., Zhang, T., Wu, W., Wang, Y., Zhou, M., Zhang, C. hui, & Cui, G. (2020). NOD1/RIP2 signalling enhances the microglia-driven inflammatory response and undergoes crosstalk with inflammatory cytokines to exacerbate brain damage following intracerebral haemorrhage in mice. Journal of Neuroinflammation, 17(1). https://doi.org/10.1186/s12974-020-02015-9

Wang, W. Y., Tan, M. S., Yu, J. T., & Tan, L. (2015). Role of pro-inflammatory cytokines released from microglia in Alzheimer's disease. In Annals of Translational Medicine (Vol. 3, Issue 10). AME Publishing Company. https://doi.org/10.3978/j.issn.2305-5839.2015.03.49

Weinstein, J. R., Koerner, I. P., & Mller, T. (2010). Microglia in ischemic brain injury. In Future Neurology (Vol. 5, Issue 2, pp. 227–246). https://doi.org/10.2217/fnl.10.1

Wirths, O., Breyhan, H., Marcello, A., Cotel, M. C., Brück, W., & Bayer, T. A. (2010). Inflammatory changes are tightly associated with neurodegeneration in the brain and spinal cord of the APP/PS1KI mouse model of Alzheimer's disease. Neurobiology of Aging, 31(5), 747–757. https://doi.org/10.1016/j.neurobiolaging.2008.06.011

Wu, Y., Dissing-Olesen, L., MacVicar, B. A., & Stevens, B. (2015). Microglia: Dynamic Mediators of Synapse Development and Plasticity. In Trends in Immunology (Vol. 36, Issue 10, pp. 605–613). Elsevier Ltd. https://doi.org/10.1016/j.it.2015.08.008

Xu, L., He, D., & Bai, Y. (2016). Microglia-Mediated Inflammation and Neurodegenerative Disease. In Molecular Neurobiology (Vol. 53, Issue 10, pp. 6709–6715). Humana Press Inc. https://doi.org/10.1007/s12035-015-9593-4

Yonezawa N., Nishida E., Lida K., Yahara I., Sakai H. (1990). Inhibition of the Interactions of cofilin, destrin, and deoxyribonuclease I with actin by phosphoinositides. Journal of Biological Chemistry 265(15), 8382-8386.

Zhang L., Jiang Y., Deng S., Mo Y., Huang Y., Li W., Ge C., Ren X., Zhang H., Zhang X. (2021). S100B/RAGE/Ceramide signaling pathway is involved in sepsis-associated encephalopathy. Life Sciences 277. https://doi.org/10.1016/j.lfs.2021.119490

LIST OF ABBREVIATIONS

αsyn: alpha synuclein

Aβ (0/42): amyloid beta (oligomers/monomers)

AD: Alzheimer's Disease

ADF: actin depolymerizing factor

AMPA: α-amino-3-hydroxy-5-methyl-4-isoxazolepropionic acid

APP: amyloid precursor protein

BBB: blood brain barrier

CNS: central nervous system

CSF: cerebrospinal fluid

DAPTA: D-Ala-peptide T-amide

DIV: days in vitro

DMSO: Dimethyl Sulfoxide

ER: endoplasmic reticulum

FBS: fetal bovine serum

GM-CSF: granulocyte-monocyte colony stimulating factor

GPI: glycosylphosphatidylinositol

GWAS: genome wide association study

HAND: HIV associated neurocognitive disorder

HD: Huntington's Disease

HN+: homemade neurobasal (+: supplemented)

HO1: hemeoxygenase 1

ICH: intracerebral hemorrhage

LGDMEM: low glucose Dulbecco's Modified Eagle's Media

MG: microglia

NFH: neurofilament heavy chains

NO: nitric oxide

NOX: NADPH oxidase

PAMP: pathogen associated molecular pattern

PBS: phosphate buffered saline

PD: Parkinson's disease

PDL: poly-D-lysine

PrPC: cellular prion precursor protein

RAPs: receptor antagonist peptides

ROS: reactive oxygen species

TBI: traumatic brain injury

TBS: tris buffered saline

TLR: toll like receptor

TREM2: triggering receptor expressed on myeloid cells 2

RAGE: receptor for glycation end-products